

**Exploring a “Nature-Inspired” Strategy for Enhancing  
the Pharmacology of Small Molecules:  
Towards the Development of Next Generation Anti-Infectives**

by

Paul Stephen Marinec

A dissertation submitted in partial fulfillment  
of the requirements for the degree of  
Doctor of Philosophy  
(Molecular and Cellular Pathology)  
in The University of Michigan  
2011

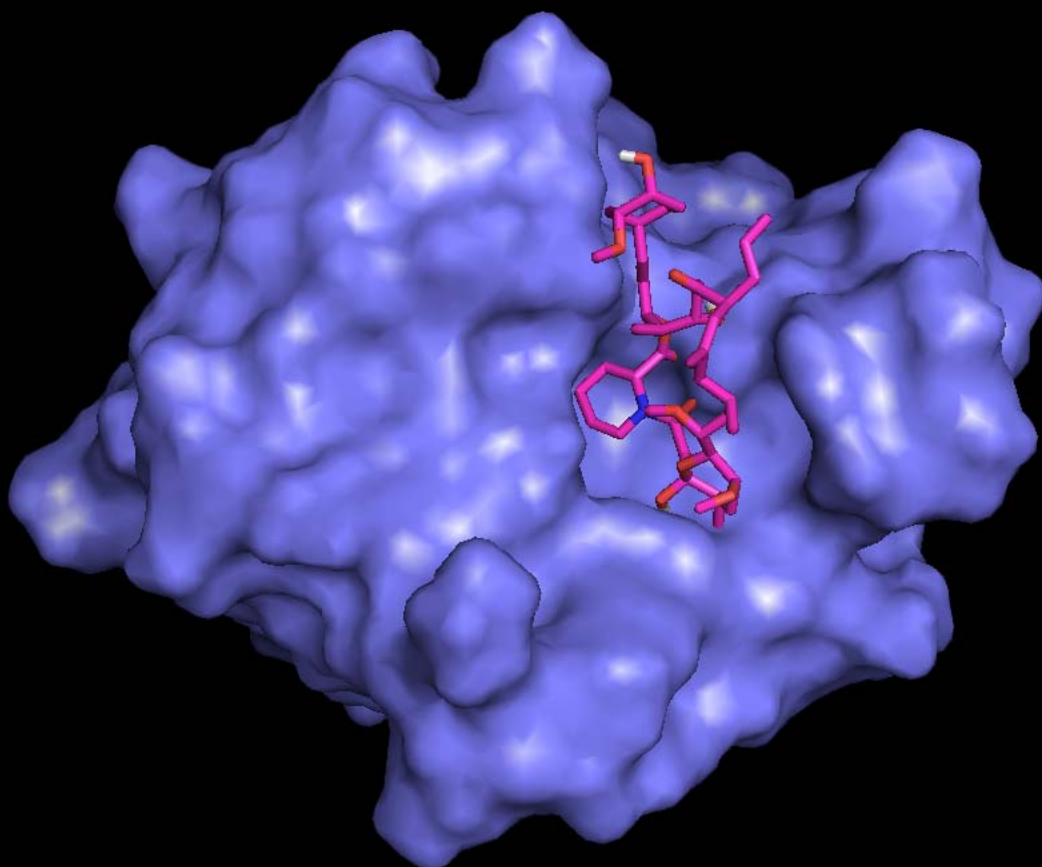
Doctoral Committee:

Assistant Professor Jason E. Gestwicki, Chair  
Professor Colin S. Duckett  
Professor Nicholas W. Lukacs  
Professor Roger K. Sunahara  
Assistant Professor Zaneta Nikolovska-Coleska

© Paul Stephen Marinec

---

2011



**“The best way to predict the future is to invent it.”**

**-Alan Kay**

To Mom & Dad,  
you made this dream possible  
and never, ever stopped believing in me

## **Acknowledgements**

I am forever indebted to my mentor, Dr. Jason Gestwicki. It was during a pharmacology seminar early on in my graduate pursuits that I first encountered Jason who initially captivated me with his awe-inspiring accounts of thwarting Alzheimer's progression with chimeric textile dyes, and later, with his epic chronicles of collegiate chemistry where I learned that liquid nitrogen is what legends are made of. In Jason's lab, I fell in love with the chemistry behind the pharmacology of drugs and with the ability to manipulate protein-protein interactions using rational design. He profoundly revolutionized the way I think about small molecules and gave me the opportunity to truly believe in my work. Jason had me at "bifunctional molecules" and I have never looked back.

A fundamental element of my success during this doctoral endeavor has been my best friend and wife, Nicolle. Her perfect stoichiometry of unfailing love and steadfast support over the last five years was essential to my maturation as a scientist, evermore strengthening the bond between us. I cannot wait to embark on the next stage of our lifelong adventure together as a perfect pair.

Finally, I would not be anything today if it wasn't for my mother and father. They worked tirelessly and sacrificed absolutely for as long as I can remember to ensure that my brother and I had every possible opportunity to become great, hoping only that we would someday have a better life than they had. I can only pray that they are as proud of me as I am of them. Mom and Dad, this is for you. Picture me rollin'.

## Preface

This dissertation is a compilation of both published and unpublished work on the synthesis of bifunctional drugs and the pharmacological consequences of appending FKBP-binding group onto small molecules. Chapter 1 is primarily based on a review article published in *Combinatorial Chemistry & High Throughput Screening* that provides a comprehensive overview of chemical inducers of dimerization (CIDs) and their utility in modern chemical biology. The citation for this article is Gestwicki, J.E. and Marinec, P.S., “Chemical Control Over Protein-Protein Interactions: Beyond Inhibitors”, *Comb. Chem. High Throughput Screen*, **2007**, *10*, 667-675. Chapter 2 is derived from a manuscript where we explored the protective effects of adding recombinant FK506-Binding Protein (FKBP) to small molecules functionalized with FKBP binding groups and FK506 itself. This citation is Marinec, P.S., Lancia, J.K., and Gestwicki, J.E., “Bifunctional Molecules Evade Cytochrome P450 Metabolism by Forming Protective Complexes with FK506-Binding Protein”, *Mol. Biosyst.*, **2008**, *4*, 571-578. Chapter 3 stems from our *Proceedings of the National Academy of Sciences* manuscript that investigates the *in vivo* effects of appending an FKBP binding group onto the HIV-1 protease inhibitor Amprenavir. The citation for this paper is Marinec, P.S., Chen, L., Barr, K.J., Mutz, M.W., and Gestwicki, J.E., “FK506-Binding Protein (FKBP) Partitions a Modified HIV Protease Inhibitor into

Blood Cells and Prolongs its Lifetime *in vivo*", *Proc. Natl. Acad. Sci. USA*, **2009**, *106*, 1336-1341. Chapter 4 is based on our recent *Bioorganic Medicinal Chemistry* manuscript where we developed a method for the high throughput synthesis of bifunctional molecules using a microwave-assisted cross metathesis reaction. The citation for this paper is Marinec, P.S., Evans, C.G., Gibbons, G.S., Tarnowski, M.A., Overbeek, D.L., and Gestwicki, J.E., "Synthesis of Orthogonally Reactive FK506 Derivatives via Olefin Cross Metathesis", *Bioorg. Med. Chem.*, **2009**, *17*, 5763-5768. Finally, Chapter 5 presents our conclusions and future directions.

## Table of Contents

<b>Dedication</b>	ii
<b>Acknowledgements</b>	iii
<b>Preface</b>	iv
<b>List of Figures</b>	xiii
<b>List of Tables</b>	xvi
<b>List of Abbreviations</b>	xvii
<b>Abstract</b>	xxiii
<b>Chapter</b>	
<b>I. Prologue</b>	
1.1 Introduction to Protein-Protein Interactions	1
1.1.1 Inhibitors of Protein-Protein Interactions	1
1.1.2 Promoters of Protein-Protein Interactions	2
1.2 Chemical Inducers of Dimerization	3
1.2.1 Inspirations from Nature	3
1.2.2 A Synthetic Homodimerizer	4
1.2.3 Agonist-Independent Internalization of GPCRs	6
1.2.4 Inducible Inactivation of Neurotransmission	9
1.2.5 Conditional Control of Chromosomal Cohesion	12
1.3 Creating New Protein Functions	14
1.3.1 A Bifunctional Inhibitor of Amyloid Beta Aggregation	15



1.3.2	Targeting Based on Dual Protein Availability	16
1.4	Outlook for the Future	19
1.4.1	Creating Orthogonal Binding Pairs to Expand the Toolbox	20
1.4.2	Protein Mislocalization	21
1.4.3	Inducible Stabilization	22
1.4.4	Integration of Bifunctional Molecules with –Omics	23
1.5	Prospectus	24
1.6	References	26
<b>II.</b>	<b>Bifunctional Molecules Evade Cytochrome P450 Metabolism by Forming Protective Complexes with FK506-Binding Protein</b>	
2.1	Abstract	37
2.1.1	The Interesting Pharmacology Behind Rapamycin and FK506	38
2.1.2	Protein Binding as a Protective Mechanism	38
2.1.3	Synthetic Chemical Inducers of Dimerization	39
2.2	Results	41
2.2.1	FK506 is Protected from CYP3A4 Metabolism by FKBP <i>in vitro</i>	41
2.2.2	Synthesis of FKBP-binding Bifunctional Molecules	42
2.2.3	Bifunctional Molecules are Protected from Binding to CYP3A4 <i>in vitro</i>	44
2.2.4	Some Bifunctional Molecules are Membrane Permeable	48
2.2.5	FKBP Alters the Partitioning of a Bifunctional Compound	48

2.2.6	Cells Protect a Bifunctional Molecule	49
2.3	Discussion	50
2.3.1	Binding to FKBP Augments the Pharmacology of FK506	50
2.3.2	Synthetic Considerations with Bifunctional Molecules	51
2.3.3	Dual Mechanisms for Metabolic Protection	53
2.3.4	Looking Forward	53
2.4	Experimental Procedures	54
2.4.1	Synthesis of Bifunctional Molecules	54
2.4.2	CYP3A4 Metabolism Assays	56
2.4.3	Fluorescence Assay for Cellular Uptake	56
2.4.4	Equilibrium Dialysis	57
2.5	References	59
<b>III.</b>	<b>FKBP Partitions a Modified Protease Inhibitor into Blood Cells and Prolongs its Lifetime <i>in vivo</i></b>	
3.1	Abstract	64
3.1.1	The Human Immunodeficiency Virus	65
3.1.2	The Protein-Protein Interactions Mediating HIV Infection	65
3.1.3	Current State of HIV-1 Therapeutics	67
3.1.4	Prodrug Approaches to Antivirals	68
3.1.5	Our “Nature-Inspired” Strategy	68
3.2	Results	70
3.2.1	Design and Synthesis of a Bifunctional Protease Inhibitor, SLFavir	70

3.2.2	SLFavir Retains Anti-HIV-1 Protease Activity <i>in vitro</i>	71
3.2.3	Binding of SLFavir to Purified FKBP does not Block its Anti-Protease Activity <i>in vitro</i>	73
3.2.4	SLFavir is Preferentially Localized within the Cellular Component of Whole Blood <i>ex vivo</i>	73
3.2.5	SLFavir is a Prodrug that Prolongs Anti-Protease Activity <i>ex vivo</i>	74
3.2.6	SLFavir is Sequestered into Blood Cells <i>in vivo</i>	76
3.2.7	SLFavir Exhibits a Dramatically Enhanced Lifetime <i>in vivo</i>	77
3.2.8	Anti-HIV Protease Activity is Stably Maintained in SLFavir-Treated Mice	78
3.2.9	Partitioning of a Fluorescent Bifunctional Molecule is Reliant on the Availability of FKBP	79
3.2.10	A Bifunctional Protease Inhibitor has Superior Anti-HIV Activity in a Cultured Cell Model	80
3.3	Discussion	82
3.3.1	A Substantial Room for Improvement in Current Antiviral Treatment Paradigms	82
3.3.2	A Dramatic Shift in Pharmacology	83
3.3.3	Why is FK506 Bifunctional?	85
3.3.4	Outlook for the Future	86
3.4	Experimental Procedures	87
3.4.1	Synthesis of a Bifunctional Protease Inhibitor	87
3.4.2	HIV Protease Inhibition Assay	90
3.4.3	Animal Care	90
3.4.4	<i>Ex vivo</i> Pharmacokinetic Studies in Whole Blood	90

3.4.5	<i>In vivo</i> Pharmacokinetic Studies in Mice	91
3.4.6	Determination of Inhibitor Concentrations in Plasma and Blood	91
3.4.7	Cell Culture	92
3.4.8	Confocal Microscopy	92
3.4.9	HIV-1 Infectivity Assay	93
3.5	References	95
<b>IV.</b>	<b>Synthesis of Orthogonally Reactive FK506 Derivatives via Olefin Cross Metathesis</b>	
4.1	Abstract	100
4.1.1	Selection of the FKBP Ligand in CID Systems	101
4.1.2	Cross Metathesis as a Synthetic Route to Functionalizing FK506	102
4.2	Results	103
4.2.1	Optimization of Reaction Time and Temperature	103
4.2.2	Selection of Solvent	104
4.2.3	Evaluation of Target Alkenes	105
4.2.4	Scaling the Synthesis of Reactive FK506 Derivatives	107
4.2.5	A Novel Method for the Facile Removal of Ruthenium	107
4.2.6	Design and Synthesis of an FK506-Bearing HIV Protease Inhibitor	109
4.2.7	FK506-Functionalization Dramatically Alters Cellular Partitioning	111
4.2.8	FKBP is Required for Partitioning <i>ex vivo</i>	112
4.2.9	Appending Drugs to the C39 Position of FK506 Blocks its Immunosuppressive Activity	113

4.3	Discussion	115
4.3.1	Potential Implications of this Synthetic Route for the Rapid Creation of New CIDs	115
4.4	Experimental Procedures	115
4.4.1	General Method for Cross Metathesis	115
4.4.2	Quantification of the Cross Metathesis Reaction	116
4.4.3	Synthetic Scale-Up of Select Reactions	116
4.4.4	Synthesis of a Bifunctional Protease Inhibitor	117
4.4.5	<i>In vitro</i> Evaluation of Tacrolimavir	117
4.4.6	<i>Ex vivo</i> Evaluation of Tacrolimavir	118
4.5	Appendix of Selected Spectra	118
4.5.1	FK506 Coupled to 3,4-Epoxy-1-butene	118
4.5.2	FK506 Coupled to Acrylic Acid	119
4.5.3	FK506 Coupled to Acrylamide	119
4.5.4	FK506 Coupled to 4-Vinylbenzoic Acid	119
4.5.5	FK506 Coupled to 4-Hexenenitrile	120
4.5.6	FK506 Coupled to N-Boc Allyl Amine	120
4.5.7	FK506 Coupled to an HIV Protease Inhibitor	121
4.6	References	123

## **V. Conclusions & Future Directions**

5.1	Conclusions	127
5.1.1	A Look Back	128
5.2	Future Directions	130

5.2.1	The Promise of FKBP-Binding Antibiotics	130
5.2.2	Diversifying the Chemistry of the Synthetic Linker	134
5.2.3	Dual-Targeting of HIV-1 Infected Lymphocytes	136
5.3	References	138

## List of Figures

<b>1-1</b>	Chemical Inducers of Dimerization	5
<b>1-2</b>	Agonist Independent Recruitment of $\beta$ arrestin2 to GPCRs	8
<b>1-3</b>	MISTs Based on the Vesicular VAMP2 Protein	11
<b>1-4</b>	Conditional Control of Cohesin Gating	13
<b>1-5</b>	Bifunctional Molecules Can Create New, Non-native Protein-Protein Interactions	16
<b>1-6</b>	Engineering Chemical Specificity	18
<b>1-7</b>	Chemical Intervention in a Hypothetical Receptor Signaling Pathway	20
<b>2-1</b>	FKBP Protects FK506 from Binding to CYP3A4	42
<b>2-2</b>	The Chemical Structures of FKBP Ligands	43
<b>2-3</b>	Synthesis of Bifunctional Molecules	45
<b>2-4</b>	Protection of Bifunctional Molecules by FKBP	47
<b>2-5</b>	Bifunctional Molecules Partition into FKBP-Rich Compartments	49
<b>2-6</b>	COS Cells Protect Bifunctional Compound 6 from Metabolism by CYP3A4	50

<b>3-1</b>	Synthesis of a Bifunctional HIV Protease Inhibitor	71
<b>3-2</b>	Functional Analysis of SLFavir	72
<b>3-3</b>	Addition of FKBP does not Block Anti-HIV Protease Activity	74
<b>3-4</b>	SLFavir is Selectively Partitioned into Blood Cells and is a Prodrug <i>ex vivo</i>	75
<b>3-5</b>	Anti-HIV Protease Activity is Maintained in the SLFavir Treated Samples	76
<b>3-6</b>	SLFavir is Sequestered into Blood Cells and has a Dramatically Enhanced Half-Life <i>in vivo</i>	78
<b>3-7</b>	Anti-HIV Protease Activity Persists Longer in the SLFavir-Treated Mice	79
<b>3-8</b>	A Fluorescent SLF Conjugate is Selectively Sequestered in FKBP-Expressing Cells	81
<b>3-9</b>	A Bifunctional Protease Inhibitor has Potent Antiviral Activity in an HIV Infectivity Model	82
<b>3-10</b>	Model for Selective Protection of SLFavir	84
<b>4-1</b>	Cross Metathesis of 3,4-epoxy-1-butene to FK506 Creates A Reactive Derivative	103
<b>4-2</b>	Varying the Reaction Time and Temperature Reveals Optimal Cross Metathesis Conditions	104
<b>4-3</b>	Synthesis of Reactive FK506 Derivatives	108
<b>4-4</b>	Removal of Ruthenium Byproducts by Scavenger Resin	109



<b>4-5</b>	Modular Synthesis of a Modified HIV Protease Inhibitor by Installation of FK506	110
<b>4-6</b>	An FK506-modified Inhibitor Retains Anti-Protease Activity <i>in vitro</i>	111
<b>4-7</b>	An FK506-coupled HIV Protease Inhibitor is Partitioned into Blood Cells	112
<b>4-8</b>	SLFavir is Dose-Dependently Displaced by the Higher Affinity FK506-Modified Compound	113
<b>4-9</b>	Covalently Modifying the C39 Terminal Alkene of FK506 Disrupts Calcineurin Binding	114
<b>5-1</b>	Crystal Structure of Ampicillin Bound to Penicillin Binding Protein	131
<b>5-2</b>	The Synthesis of a Bifunctional Antibiotic	132
<b>5-3</b>	An FKBP-Binding Beta Lactam Retains Picomolar Activity Against <i>S. Aureus</i>	133
<b>5-4</b>	Designing a Library of Amprenavir Conjugates	135

## List of Tables

<b>2-1</b>	Table of CYP3A4 Assay Results	46
<b>4-1</b>	Summary of Cross Metathesis Reactions Between FK506 and 3,4-epoxy-1-butene in Different Solvents (5 min, 150°C)	105
<b>4-2</b>	Summary of Cross Metathesis Reactions Between FK506 and Functionalized Olefins	106

## List of Abbreviations

A $\beta$	$\beta$ -amyloid
ACN	acetonitrile
AcOH	acetic acid
AD	Alzheimer's disease
ADME	absorption, distribution, metabolism, excretion
AIDS	acquired immunodeficiency syndrome
APCI	atmospheric pressure chemical ionization
ATP	adenosine triphosphate
AVP	vasopressin
Boc	<i>tert</i> -butoxycarbonyl
Br <sub>2</sub>	bromine
°C	degrees Celsius
C57BL/6	C57 black 6 mice
Ca	calcium
CEM	a T-lymphocyte cell line
CHAPS	3[3-Cholamidopropyldimethylammonio]-propanesulfonic acid
CIDs	chemical inducers of dimerization
Cl <sub>3</sub> CCN	trichloroacetonitrile
CM	cross metathesis
CO <sub>2</sub>	carbon dioxide

CYP3A4	cytochrome P450 subtype 3A4
1,4-DAB	1,4-diaminobutane
DCB	1,2-dichlorobutane
DCE	1,2-dichloroethane
DCM	dichloromethane
DHFR	dihydrofolate reductase
DIC	N,N'-diisopropylcarbodiimide
DMF	dimethylformamide
DMAP	4-dimethylaminopyridine
DMEM	Dulbecco's modified eagle medium
DMSO	dimethylsulfoxide
DNA	deoxyribonucleic acid
DTT	dithiothreitol
EDTA	ethylenediaminetetraacetic acid
ELISA	enzyme-linked immunosorbent assay
equiv	equivalent
ESI	electrospray ionization
Et <sub>3</sub> N	triethylamine
EtOH	ethanol
FBS	fetal bovine serum
FDA	Food and Drug Administration
FKBP	FK506-binding protein
Fmoc	9-fluorenylmethoxycarbonyl

FRB	FKBP-Rapamycin binding domain
g	gram
GPCR	G protein-coupled receptor
GRK	G protein-coupled receptor kinase
GSK3 $\beta$	glycogen synthase kinase 3 beta
h	hour
H <sub>2</sub> O	water
HAART	highly active antiretroviral therapy
HCl	hydrochloric acid
HIV	human immunodeficiency virus
HOBt	N-hydroxybenzotriazole
HPLC	high pressure liquid chromatography
HTS	high throughput synthesis
IC <sub>50</sub>	concentration producing a half-maximal inhibition
IL-2	interleukin 2
IN	integrase
IP	intraperitoneal
K <sub>d</sub>	dissociation constant at equilibrium
K <sub>i</sub>	inhibition constant
K <sub>2</sub> EDTA	dipotassium ethylenediaminetetraacetic acid
K <sub>2</sub> HPO <sub>4</sub>	dipotassium phosphate
KF	potassium fluoride
LC-MS	liquid chromatography-mass spectrometry

MAOS	microwave-assisted organic synthesis
MAPK	mitogen-activated protein kinase
MB	methylene blue
MeOH	methanol
MEFs	murine embryonic fibroblasts
Mg(ClO <sub>4</sub> ) <sub>2</sub>	magnesium perchlorate
min	minute
MISTs	molecular systems for inactivation of synaptic transmission
μL	microliter
μM	micromolar
mL	milliliter
mmol	millimole
mM	millimolar
MOI	multiplicity of infection
mTOR	mammalian target of rapamycin
MTX	methotrexate
m/z	mass per charge
NaBH <sub>4</sub>	sodium borohydride
NaHCO <sub>3</sub>	sodium bicarbonate
Na <sub>2</sub> SO <sub>4</sub>	sodium sulfate
NFAT	nuclear factor of activated T-cells
NF-κB	nuclear factor kappa of activated B cells
NLS	nuclear localization signal

nM	nanomolar
O/N	overnight
OPTI-MEM	reduced serum media
p24	a component of the HIV virus particle capsid
P450	cytochrome superfamily of enzymes
PBCs	peripheral blood cells
PBS	phosphate buffered saline
PD	Parkinson's disease
PEG	polyethylene glycol
PIs	protease inhibitors
PPAR	peroxisome proliferation-activated receptor
POCl <sub>3</sub>	phosphorus oxychloride
PPIs	protein-protein interactions
PR	protease
rpm	revolutions per minute
RPMI	media for the culture of human leukocytes
RT	room temperature
s	seconds
SAR	structure-activity relationships
SE	succinimidyl ester
SMC	structural maintenance of chromosomes family of proteins
SNAP-25	25 kDa synaptosome-associated protein
SNARE	soluble NSF-attachment protein receptor

$t_{1/2}$	half-life
TFA	trifluoroacetic acid
THF	tetrahydrofuran
VAMP	vesicle-associated membrane protein
WHO	World Health Organization
WT	wild-type
Zn	zinc
$Zn(BH_4)_2$	zinc borohydride
$ZnCl_2$	zinc chloride
$ZnSO_4$	zinc sulfate



## Abstract

### Exploring a “Nature-Inspired” Strategy for Enhancing the Pharmacology of Small Molecules: Towards the Development of Next Generation Anti-Infectives

by

Paul Stephen Marinec

**Chair: Jason E. Gestwicki**

HIV is now a pandemic of staggering proportions. Unfortunately, the current generation of antiretroviral therapeutics is only partially and temporarily effective in suppressing viral replication due to rapid metabolism leading to liver toxicity, resistance, and poor pharmacokinetics. Thus, there is a burgeoning need to develop innovative approaches for prolonging the lifetimes of these drugs.

Here, we propose a novel and potentially general methodology for enhancing the stability of HIV-1 protease inhibitors and other small molecules. This strategy emerged from our interest in understanding the unusual pharmacology behind the natural product FK506, a compound that is an excellent substrate for metabolic P450 enzymes *in vitro*, yet has an unexpectedly long half-life in humans ( $t_{1/2}$  ~40 hours). This apparent contradiction may partially be explained by the observation that FK506 is predominantly sequestered into the cytosol of peripheral blood cells. Both erythrocytes and leukocytes are a rich

source of FKBP, yet little metabolism occurs here as these cells do not express significant levels of P450 enzymes. Therefore, we hypothesized that FKBP-binding compounds, such as FK506, might be protected from exposure to metabolic enzymes by partitioning into this protected cellular niche.

During my thesis research, we tested this model by designing and synthesizing a series of bifunctional, FKBP-binding small molecules and evaluating their pharmacokinetic properties *in vitro* and *in vivo*. These efforts led to the discovery of SLFavir, an FKBP-binding antiviral with nanomolar potency against HIV-1 protease. We determined that SLFavir is sequestered into the cytosol of erythrocytes and that its lifetime in mice is improved by >20-fold. Furthermore, we observed that binding to FKBP partially blocks its interactions with the CYP3A4 P450 isozyme, making it less susceptible to degradation. Finally, to enable modular synthesis of additional bifunctional compounds, we developed a chemical platform using microwave-assisted olefin cross metathesis to rapidly append FK506 to other drugs, including the antibiotics ampicillin and ciprofloxacin. The key discovery made during my thesis research is that covalently tethering FKBP-binding groups to existing drugs dramatically improves their persistence via cellular partitioning. We expect this “nature-inspired” strategy to yield antivirals and other small molecules with exciting new pharmacokinetic profiles.

# Chapter I

## Prologue

### 1.1 Introduction to Protein-Protein Interactions

Contacts between proteins are widespread in biology; recent analyses in yeast have revealed that the network of protein-protein interactions, termed the “interactome”, is more extensive than might have previously been predicted.<sup>1-6</sup> Through these physical connections, proteins provide structural support and pattern the flow of information through the cell. Within this framework one might ask: what would happen if the interactome were rationally manipulated? What if specific interactions were disconnected or if transient contacts were stabilized? What if proteins were brought together that normally do not interact? Chemical probes that control specific protein-protein contacts might open the interactome to exploration.

#### 1.1.1 Inhibitors of Protein-Protein Interactions

The interactome can, in theory, be manipulated in one of two ways: either by inhibiting or promoting protein-protein interactions. Traditionally viewed as exceedingly difficult, recent breakthroughs have provided a template for the development of low molecular weight, “drug-like” inhibitors.<sup>7-12</sup> A key insight was made by the Wells group when they observed that protein-protein interactions often contain “hot spots” on their surfaces.<sup>13-15</sup> These regions contribute a

disproportionate percentage of the binding energy, and thus, can serve as critical focal points for chemical intervention. By leveraging this knowledge and structural information, inhibitors of IL-2,<sup>16, 17</sup> the MDM2-p53 interaction,<sup>18</sup> ubiquitin recognition,<sup>19</sup> HSV DNA polymerase subunit interactions,<sup>20</sup> HIV protease dimerization,<sup>21</sup> and Myc-Max<sup>22</sup> have been uncovered. Together, these successes are challenging the dogma that protein-protein interactions are impervious to inhibition by small molecules.

### **1.1.2 Promoters of Protein-Protein Interactions**

While inhibitors are being identified with increasing regularity, another class of compounds for rationally controlling the interactome has emerged: small molecules that promote binding. Why might it be desirable to promote a protein-protein interaction? The answer lies in identifying whether a specific contact is both necessary and sufficient to drive a biological process. For example, if dimerization of a receptor is required, and moreover, is sufficient for initiating signal transduction, then user-controlled, chemically-induced dimerization should suffice for activation in the absence of other stimuli. In addition to studying native interactions, one can also create new contacts (i.e. those not utilized in nature due to subcellular segregation or lack of shape complementarity). In some cases, chemical recombination of artificial pairs produces novel activities to materialize that are not observed in either target protein. Thus, bifunctional molecules can be used to either enforce known contacts or create new ones. We propose that along with inhibitors, chemical stimulators of protein-protein

contacts should be considered as part of the essential toolbox of reagents for studying protein networks. Together, these compounds might be combined with genomic and proteomic efforts to provide new insight into biological systems.

## **1.2 Chemical Inducers of Dimerization (CIDs)**

### **1.2.1 Inspirations from Nature**

Small molecules that are able to promote protein contacts have precedent in natural systems. For example, the immunosuppressants rapamycin and FK506 and the antibiotic brefeldin are natural products whose mode of action involves simultaneous binding to two protein targets.<sup>23,24</sup> Rapamycin has high affinity ( $K_d \sim 1$  nM) for the cytosolic, 12 kDa FK506-binding protein (FKBP).<sup>25-27</sup> Subsequently, the drug-FKBP complex acquires an affinity for the FK506-rapamycin binding (FRB) domain of the mammalian target of rapamycin (mTOR).<sup>28-29</sup> Similarly, FK506 binds with high affinity to FKBP and this drug-protein complex then binds to and inhibits the protein phosphatase calcineurin. Interestingly, FKBP has little affinity for FRB or calcineurin in the absence of the appropriate small molecule. Thus, rapamycin and related compounds stabilize protein interfaces that normally have weak associations.

Based on observations of FK506 and rapamycin, the Crabtree and Schreiber laboratories developed a “nature inspired” method to selectively regulate protein-protein interactions using synthetic ligands. They termed these reagents Chemical Inducers of Dimerization (CIDs) and the defining feature of

this class of molecules is that they are, like FK506 or rapamycin, bifunctional. Specifically, CIDs are molecules possessing two chemical faces that each exhibit affinity for a protein; the targets can either be the same protein (homodimerizer) or different proteins (heterodimerizer). The hallmark of these compounds is that they control protein-protein interactions in the absence of other influences.<sup>30-31</sup> Thus, the goal of any CID strategy is to gain temporal and spatial control over biological processes. In this way, the CIDs can mirror classical temperature-sensitive alleles, as they permit an investigator-initiated switch between active and inactive states. Temperature sensitivity is a powerful methodology in yeast and other organisms, but its use in higher animals is limited. Like temperature sensitive mutations, CIDs were envisioned to provide similar exogenous control over the function of proteins, specifically those that are normally regulated by protein dimerization. Additionally, these reagents might have the advantage of being used in any organism (e.g. warm- and cold-blooded).

### **1.2.2 A Synthetic Homodimerizer**

In the first example of this approach, the CID was a synthetic, homobifunctional derivative of FK506, termed FK1012 (Figure 1-1). FK1012 binds an FKBP with each end, such that binding brings together two target proteins if the genes are “tagged” with an FKBP domain. This molecule has been used to demonstrate that oligomerization is sufficient for activation of a variety of cellular responses, including T-cell receptor signaling,<sup>32</sup> triggering FGF receptor,<sup>33-35</sup> Fas activation,<sup>36</sup> transcriptional initiation,<sup>37</sup> Akt stimulation,<sup>38</sup> ZAP70 activity,<sup>39</sup> and signaling through Src.<sup>40</sup> In an effort to extend the utility of CIDs,

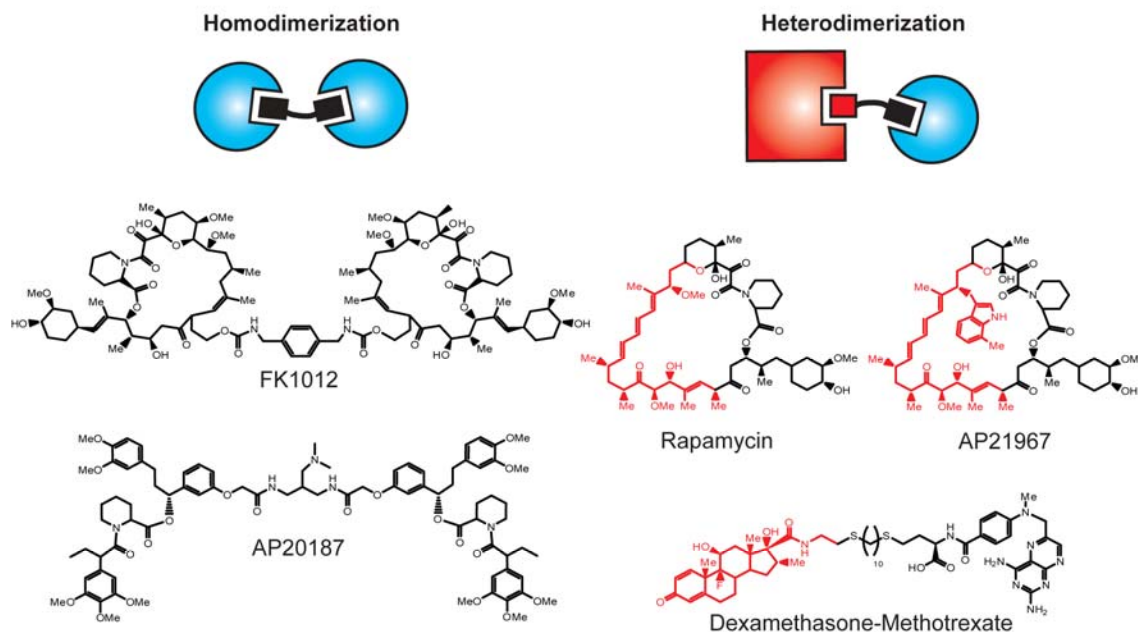


**Figure 1-1. Chemical Inducers of Dimerization (CIDs).** The chemical structures and mechanisms of dimerization for select CIDs are shown.

heterodimerizers were also developed.<sup>41,42</sup> Like rapamycin, these compounds bridge two different proteins. Heterobifunctional CIDs have been used to investigate caspase activation,<sup>43,44</sup> pre-RNA splicing,<sup>45</sup> GTPase function,<sup>46</sup> protein complementation,<sup>47,48</sup> translation initiation,<sup>49</sup> glycosylation,<sup>50,51</sup> induced degradation by the proteasome,<sup>52,53</sup> phosphoinositide signaling,<sup>54,55</sup> secretion,<sup>56,57</sup> and transcriptional activation<sup>29, 58-60</sup> and have found exceptional use in drug discovery applications.<sup>31,58, 61-64</sup> These dimerization systems are all based, in part, on the chemical structure of rapamycin or FK506. In addition, other scaffolds have been explored,<sup>53, 65-70</sup> such as the coumermycin system,<sup>71, 72</sup> alkyltransferase,<sup>73</sup> estradiol-biotin chimeras,<sup>74</sup> acyl homoserine lactone-based methods,<sup>75</sup> and methotrexate-derived dimerizers.<sup>76</sup> Together, CIDs provide a versatile collection of synthetic reagents for controlling protein-protein

interactions.

Most CID systems rely on genetic manipulation of the target proteins to provide selectivity. For example, expressing a protein as a fusion to FKBP places it under control of FK1012, as addition of the divalent compound will drive the dimerization of the FKBP-tagged proteins. This feature provides extraordinary versatility. The same compound can be used to control virtually any target because proteins tend to tolerate the addition of small, appended tags. This strategy has even been combined with “knock-in” technology to generate CID-sensitive proteins in mice.<sup>77, 78</sup> However, genetic intervention is oftentimes undesirable or impractical, such as when drug therapies are being developed. Thus, there is a need for systems in which tagging is not required. In these cases, the desired bifunctional molecule needs to have affinity for the intrinsic protein surfaces instead of a fusion tag. The major challenges to this approach are that each system requires extensive chemical optimization and the resulting CIDs are not generally applicable to other targets. The choice of strategy (genetic fusion vs. intrinsic affinity) is dictated by the question being addressed and the goals of the study. To illustrate these design challenges, we highlight a few recent examples that have provided important insights.

### **1.2.3 Agonist-Independent Internalization of GPCRs**

Heterotrimeric G protein-coupled receptors (GPCRs) are the largest class of cell surface receptors in multicellular organisms and are one of the primary mediators of intracellular communication. Upon agonist activation, GPCRs



undergo homologous desensitization, an essential regulatory mechanism that attenuates the signal in the presence of continued stimulation. Desensitization is carried out by G protein-coupled receptor kinases (GRKs), a family of serine/threonine kinases that phosphorylate activated receptors at specific amino acid residues on their intracellular loops and carboxy-terminal tails.<sup>79</sup> Phosphorylation by GRKs decreases the affinity of the GPCR for its cognate G protein and promotes a high-affinity association with an arrestin adapter protein. Arrestin binding further impedes G protein coupling and initiates internalization of the receptor *via* clathrin-coated pits.<sup>80</sup> The receptors are then either recycled back to the plasma membrane or targeted to endosomes for degradation. Thus, the fate of a GPCR is believed to be influenced by its coupling to arrestin; however, the details of this interaction (e.g. its stability, duration, etc) are not clear.

In an effort to characterize the intrinsic signaling properties of the arrestin family of proteins, Terrillon and coworkers fused a single FKBP tag to the carboxy terminal regions of the G protein-coupled V1a and V2 vasopressin receptors, while concomitantly attaching an FRB domain to the amino terminus of a fluorescently-tagged  $\beta$ arrestin2 (Figure 1-2).<sup>81</sup> Their approach would thus allow for the agonist-independent recruitment of arrestin to the vasopressin receptor upon treatment with a bivalent rapamycin analog. Remarkably, upon exposure to the heterobifunctional rapamycin derivative AP21967 (Figure 1-1), transfected cells exhibited a dose-dependent internalization of the modified receptors

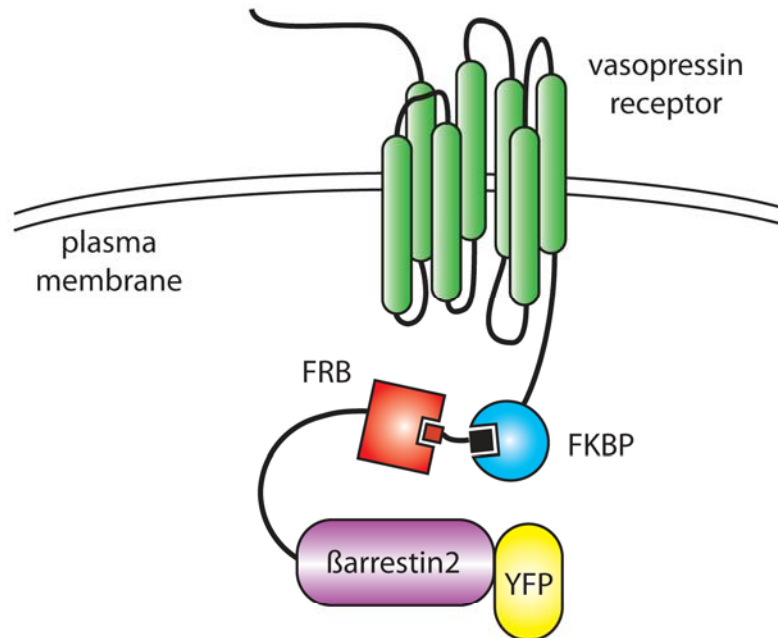


**Figure 1-2. Agonist Independent Recruitment of βarrestin2 to GPCRs.**  
 The carboxy terminal tails of the V1a and V2 vasopressin receptors were fused with FKBP while a single FRB domain was attached to the amino terminus of a fluorescent βarrestin2. Transfected cells treated with the AP21967 heterodimerizer exhibited an agonist-independent internalization of the receptor.

functionally identical to the internalization seen in the agonist-induced state, indicating that βarrestin2 is necessary and sufficient for engaging the cell's endocytotic machinery in the absence of agonist.

However, chemically-induced, agonist-independent activation also significantly alters the trafficking of the GPCRs. Whereas stimulation with the vasopressin-specific agonist AVP promoted internalization followed by efficient receptor recycling back to the plasma membrane, treatment with AP21967 trapped the receptors within endocytic compartments with no observable cell surface recycling. These results suggest that AP21967 drives the formation of

an unusually high-affinity interaction between the chimeric arrestin and vasopressin receptors, synthetically forging a heterodimeric complex that is much more stable than the transient arrestin association exhibited during agonist-mediated desensitization. The stability of this interaction, in turn, dictates the recycling pattern and ultimately, the fate of the receptor.

Additional experiments showed that agonist-independent recruitment of  $\beta$ arrestin2 to the vasopressin receptors was sufficient to activate the MAPK pathway. Taken together, these results provide insights into the properties of the arrestin-GPCR interaction.

#### **1.2.4 Inducible Inactivation of Neurotransmission**

For efficient intracellular signaling to occur in the nervous system, target neurotransmitters must be packaged in transport vesicles before being released from the presynaptic neuron into the synaptic cleft. Calcium-dependent fusion of the vesicle with the plasma membrane is critical to this process, and SNARE (soluble NSF-attachment protein receptor) proteins are key components of the molecular machinery mediating this fusion event. These proteins can be subdivided into the syntaxin, VAMP (vesicle-associated membrane protein, also known as synaptobrevin), and SNAP-25 (25 kDa synaptosome-associated protein) families based on their domain structure and sequence homology. However, all three families share a conserved heptad repeat sequence that forms functionally significant coiled domains. When a single, vesicular coil of VAMP interacts with that of membrane-bound syntaxin and SNAP-25, they

intertwine to create a stable four-stranded coiled-coil complex remarkably resistant to dissociation. This SNARE core complex fuses the vesicular and plasma membranes by bringing them into close proximity with one another, allowing exocytosis to occur (Figure 1-3). Prompted by the lack of non-transcriptional approaches for specifically inactivating synaptic activity, Svoboda and coworkers set out to develop a method for temporally blocking neuronal transmission.<sup>82</sup> In doing so, they created so-called “MISTs” or Molecular systems for inducible and reversible Inactivation of Synaptic Transmission. These molecules rely on the inducible crosslinking of genetically modified VAMP proteins that dimerize in the presence of small molecules, thus preventing their association with the other SNARE partner proteins. Fusing rat VAMP2/synaptobrevin with two domains of FKBP, the authors introduced the construct into cortical neuronal slices using viral vector-mediated gene delivery. Application of the homobifunctional compound AP20187 (Figure 1-1) into transfected neurons resulted in remarkably rapid and robust decreases in the amplitude of both excitatory and inhibitory postsynaptic currents. These effects were completely reversed following a 60 minute wash with medium, demonstrating that MISTs provide conditional control over neuronal synaptic activity that is analogous (or equivalent to) a temperature-sensitive allele.

Further characterization of the MIST system was performed in the context of cerebellum-dependent behavior *in vivo*. Expressing the VAMP2-MIST construct under the control of the Purkinje cell-specific L7 promoter, transgenic

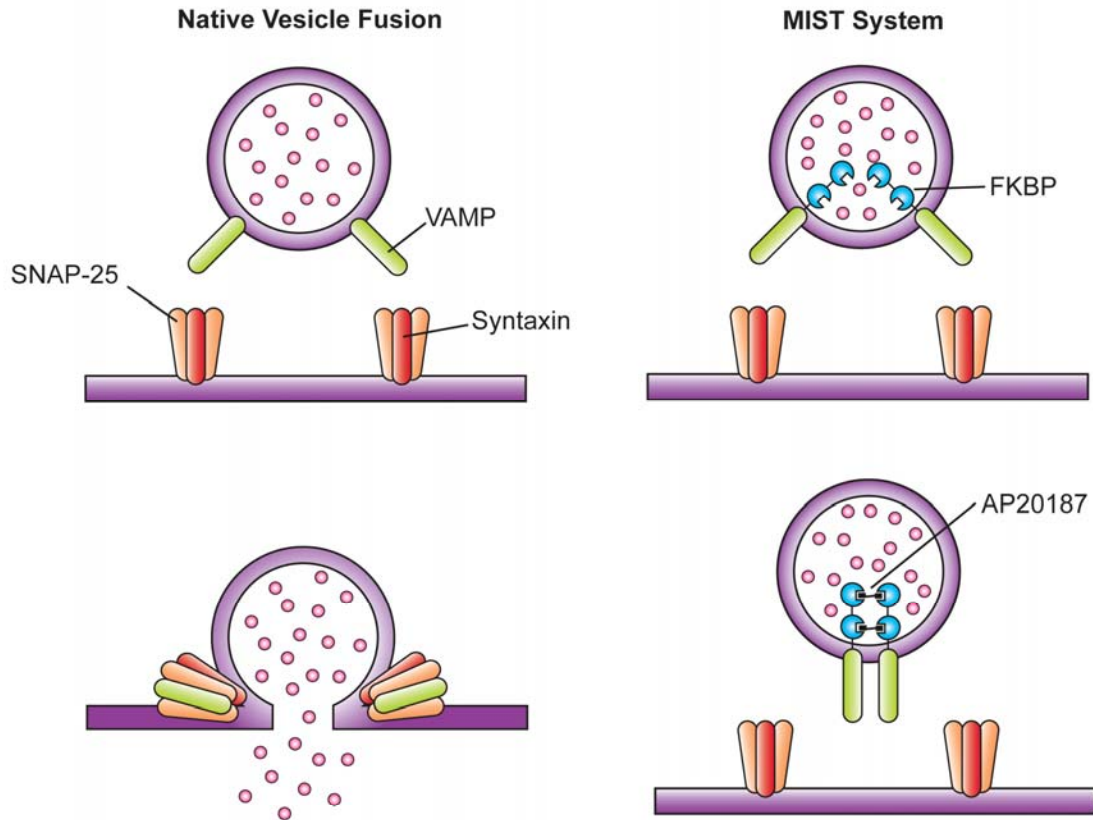


**Figure 1-3. MISTs Based on the Vesicular VAMP2 Protein.** Two FKBP domains were fused to rat VAMP2/Synaptobrevin. Addition of the homodimerizer AP20187 resulted in a rapid and reversible decrease in the amplitude of both excitatory and inhibitory postsynaptic currents.

mice treated with AP20187 exhibited profound impairment in rotarod performance during learning. Furthermore, once learning was saturated in the animals, application of the rapamycin analog transiently decreased task performance. These experiments demonstrate that chemical inducers of dimerization based on the VAMP family of vesicular proteins can rapidly and reversibly block synaptic transmission in genetically targeted cerebellar Purkinje neurons and are powerful tools for probing neural circuits with inducible, temporal control.

### 1.2.5 Conditional Control of Chromosomal Cohesion

During cellular growth and differentiation, sister-chromatids are held together by a large, multi-subunit complex collectively known as cohesin. This complex serves as a molecular harness, establishing the necessary tension to stabilize kinetochore-microtubule attachments and properly align chromosomes on the mitotic spindle.<sup>83</sup> Structurally, cohesin is composed of two members of the Structural Maintenance of Chromosomes (Smc) family of proteins, a kleisin Scc1 subunit, and an accessory Scc3 binding partner. Both Smc subunits are 50 nm-long antiparallel coiled-coils, possessing an ATPase head at one end and a dimerization domain at the other. Interaction of Smc1 with Smc3 creates a heterodimeric hinge bridged by the binding of Scc1 to the two apical ATPase motifs (Figure 1-4). Together, these proteins form a large, three-membered ring that acts as a molecular lasso, trapping mitotic chromosomes within its central core. During anaphase, the enzyme separase cleaves the Scc1 subunit, thereby opening the ring, abolishing sister-chromatid cohesion and restoring chromatid autonomy.

Although several working models have been proposed, many of the details surrounding the entry of chromosomes into the cohesin core are unresolved. To address this cryptic sequence of events, Gruber and coworkers developed a conditional synthetic platform using rapamycin-dependent dimerization with which they could test many of the postulated gating mechanisms.<sup>84</sup> Their approach relied on fusing an FKBP domain to one subunit

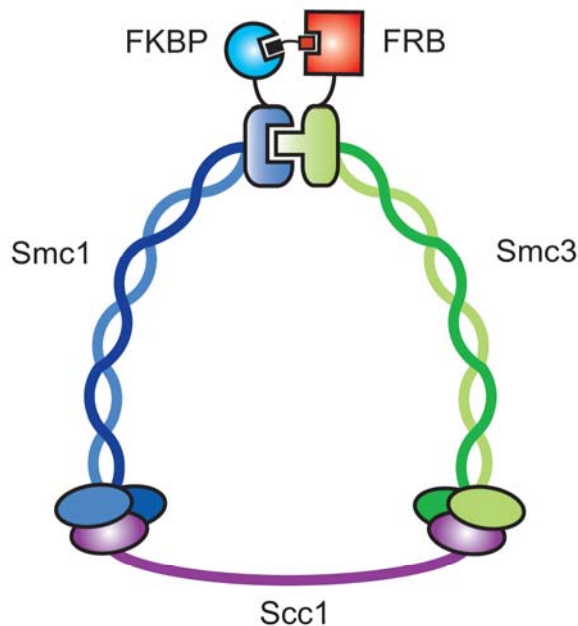


**Figure 1-4. Conditional Control of Cohesin Gating.** FKBP and FRB were fused to the hinge regions of Smc1 and Smc3 respectively. Addition of rapamycin to the modified cohesin complex blocked the transient opening of the hinge region and abolished association with chromosomes.

of the cohesin complex while attaching the FRB domain to another at potential sites of chromosomal entry. The addition of rapamycin would thus block any transient ring opening and abrogate cohesin's association with chromosomes.

After examining a number of possible gating mechanisms in yeast cells, the authors found the hinge region of the cohesin complex to be critically important for DNA entry. Because the hinge domains of cohesin are highly conserved throughout their entire length, it was particularly striking to find that adding an FKBP domain to Smc1's hinge region via a decapeptide linker, and an

analogous fusion of FRB to Smc3, did not compromise the function of either subunit or the cohesin complex. However, addition of rapamycin to the cells essentially blocked cohesin function and severely inhibited its association with chromosomes. These findings suggest that the hinge region of the cohesin complex is not only essential for heterodimerization of the Smc1 and Smc3 subunits, but its transient dissociation is required for chromosomal entry.

### **1.3 Creating New Protein Functions**

Natural bifunctional molecules, such as rapamycin and FK506, bind two distinct proteins *via* non-overlapping chemical domains. While these compounds and their related derivatives are useful tools, application of bifunctional molecule technologies to drug discovery requires one to circumvent the requirement for genetic modification of the target. In these cases, affinity for the native, unmodified target must be synthetically installed in the bifunctional ligand. For example, regions of rapamycin or FK506 could be replaced with domains that have affinity for new targets. Alternatively, entirely new ligands can be created by covalently coupling two small molecules that have known targets.<sup>85</sup> As an extension of this idea, multivalent scaffolds can be used to display multiple copies of a ligand to generate multi-pronged reagents capable of binding dozens of proteins at the same time.<sup>86-88</sup> Although these approaches require more extensive investments in chemical synthesis, the resulting products are powerful, “nature inspired” tools.



### 1.3.1 A Bifunctional Inhibitor of Amyloid Beta Aggregation

By rationally designing these synthetic probes, two proteins that under normal circumstances would never come together can be forced to interact. In this way, unique combinations of protein pairs can be created and novel functions may emerge. To test this hypothesis, we recently developed a bifunctional inhibitor for the self-assembly of amyloid beta (A $\beta$ ) peptides. Oligomers of A $\beta$  are implicated in Alzheimer's disease,<sup>89-91</sup> but traditional small molecule inhibitors of aggregation have been difficult to identify.<sup>92-98</sup> One reason for this failure might be due to the large and complex surface that stabilizes the A $\beta$ -A $\beta$  interaction. We envisioned a synthetic molecule that could block aggregation by recruiting an endogenous cellular protein to the A $\beta$  interface (Figure 1-5). To this end, we altered the selectivity of an FK506 derivative such that it bound FKBP on one end and A $\beta$  on the other. We predicted that this compound would inhibit A $\beta$  self-assembly by recruiting the bulk of FKBP to the surface, thereby enveloping a larger area than would normally be accessible to a small molecule.<sup>99-100</sup> Consistent with this idea, the bifunctional compound was a potent inhibitor *in vitro* (IC<sub>50</sub> ~ 50 nM), but only in the presence of FKBP. Interestingly, the combination of FKBP and the bifunctional molecule also blocked formation of toxic A $\beta$  oligomers, suggesting that this general approach might lead to compounds that can reduce the toxicity of amyloids. These studies, along with others in which FKBP has been chemically co-opted,<sup>101-102</sup> demonstrate how a protein can synthetically acquire new functions. In the discussed example, the new protein-protein interaction between FKBP and A $\beta$

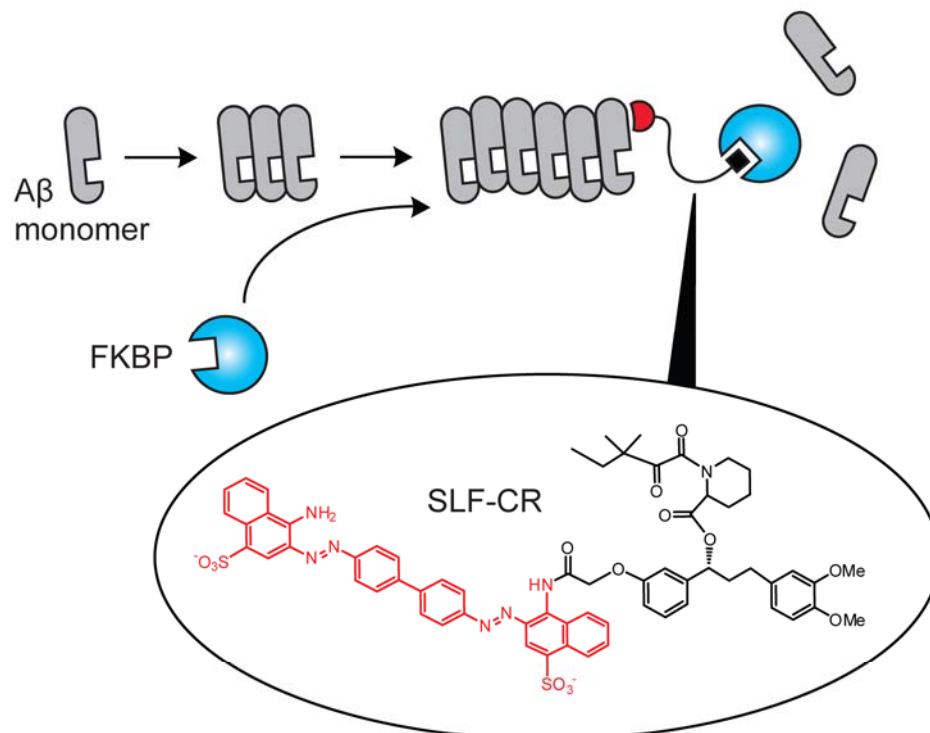


**Figure 1-5. Bifunctional Molecules Can Create New, Non-native Protein-Protein Combinations.** A bifunctional molecule composed of an Aβ ligand (CR) coupled to SLF recruits FKBP to sites of aggregation. The combined mass of the drug and the protein serves as a potent barrier to further self-association.

(enforced by the synthetic compound) endows the FKBP with a new capability: inhibition of amyloid formation. One can imagine the numerous ways in which other endogenous proteins might be coerced into forming unconventional partnerships.

### 1.3.2 Targeting Based on Dual Protein Availability

A primary goal of any drug discovery platform is specificity. The more discriminating a drug is for its intended target, the more likely it is to be therapeutically effective without causing unwanted side effects. In many cases,

contrasting expression profiles confer the specificity. For example, antibacterial drugs with low toxicity typically target prokaryotic proteins that lack good orthologs in the human host. This feature favors binding in the desired pathogen while sparing adjacent cells lacking the protein target.

In a recent effort to improve the molecular specificity of the dihydrofolate reductase inhibitor methotrexate (MTX), Sellmyer and coworkers utilized a previously synthesized bifunctional molecule consisting of MTX at one end and the synthetic ligand for FKBP (SLF) at the other.<sup>101-103</sup> Their strategy, however, differs from the aforementioned bifunctional approaches in that it relies on binding only one protein partner at a time. By installing the shortest possible linker between the two moieties of their bifunctional molecule, they ensured that steric repulsions would impinge on the bivalent binding of proteins. This group had already demonstrated that their bifunctional MTX-SLF molecule exhibited context-dependent cellular activity, whereby it was extremely cytotoxic toward the malaria parasite but relatively harmless toward human cell lines endogenously expressing FKBP.<sup>102</sup> Now, they wanted to further improve the specificity of their bifunctional compound by taking advantage of the differential expression of non-target proteins. Using a mouse embryonic fibroblast (MEF) cell line that expressed similar levels of FKBP to humans, they genetically disrupted the FKBP gene *via* homologous recombination to generate FKBP-null cells. When MTX-SLF was added to wild type MEFs, a mild, dose-dependent cytotoxicity was observed with an IC<sub>50</sub> of 3200 nM. This effect is likely due to binding to FKBP,

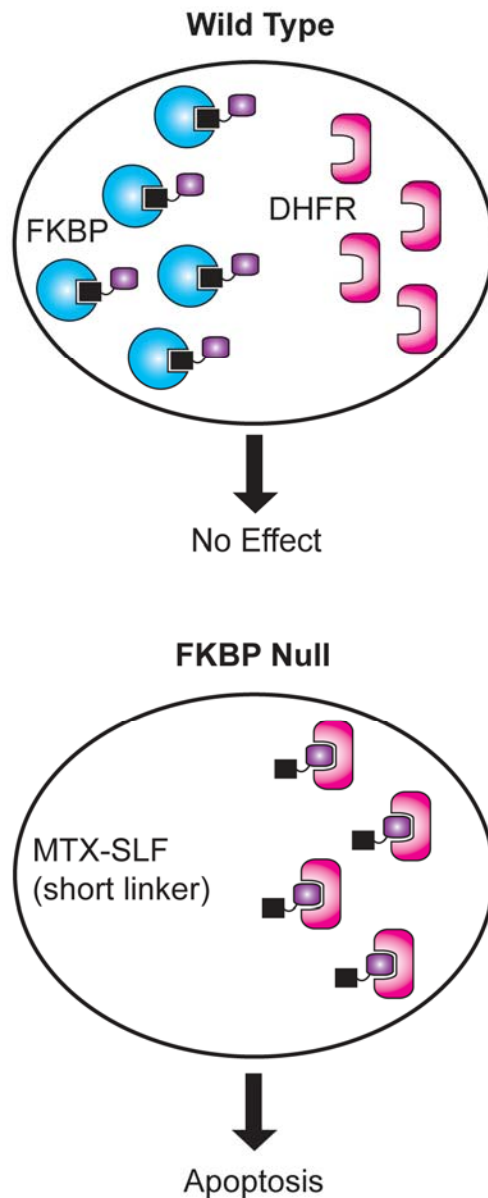


**Figure 1-6. Engineering Chemical Specificity.** A bifunctional molecule was synthesized with MTX on one side and SLF on the other. Control cells exhibited no harmful effects upon addition of compound. However, in an FKBP-null environment, MTX-SLF was exceedingly cytotoxic.

which detoxifies the MTX-SLF by precluding interactions with dihydrofolate reductase (DHFR) (Figure 1-6).

Consistent with this mechanism, when the same bifunctional molecule was added to the FKBP-null MEF cells, there was a 40-fold increase in toxicity with an  $IC_{50}$  of 78 nM. Interestingly, addition of a high-affinity, competitive FKBP ligand to the wild type MEFs abolished most of the protective effect of the FKBP genomic background. These data demonstrate that chemical specificity can be genetically engineered into cells to discriminate between nearly identical cellular environments.

#### **1.4 Outlook for the Future**

Protein-protein interactions are generally under-explored as targets for chemical intervention. Beyond inhibitors, these interfaces may be susceptible to manipulation by compounds that prolong their association and even create new contacts (Figure 1-7). However, in comparison to the base of knowledge guiding discovery of traditional small molecules, the field of bifunctional molecule synthesis remains largely enigmatic. Although we have highlighted a number of exceptional published reports, there are instances in which existing CIDs have failed to operate for known or unknown reasons. Furthermore, while CIDs have been used to address important questions in both mammalian cell lines and rodents, other model systems, such as *Xenopus laevis* and *C. elegans*, remain virtually unexplored.<sup>104</sup> Moreover, because these technologies use small molecules, they are, by definition, reliant on the pharmacological properties of the probes and in some experiments, limited stability might preclude activity. There is clearly a need for continued exploration.

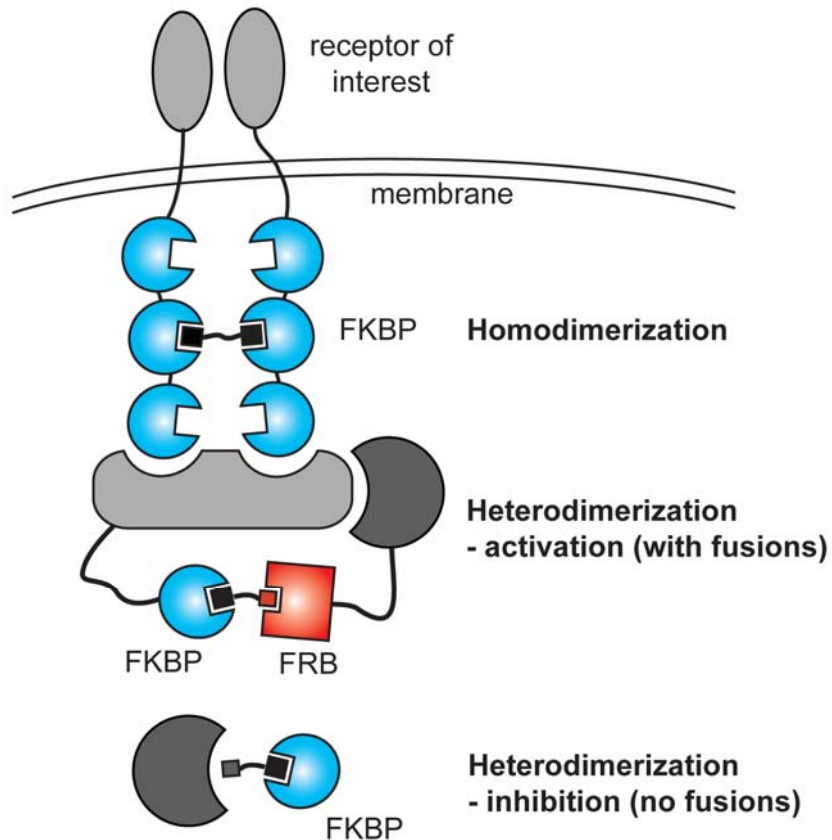


**Figure 1-7. Chemical Intervention in a Hypothetical Receptor Signaling Pathway.**

Depending on the choice of the system, CIDs can be used to manipulate protein-protein interactions in a variety of ways. For example, a homodimerizer could be used to regulate receptor-receptor association. Downstream, the interaction between an associated protein with its partner might be driven by a heterodimerizer. Likewise, a compound with affinity for unmodified targets might be used to block binding by covering a surface with endogenous FKBP.

#### 1.4.1 Creating Orthogonal Binding Pairs to Expand the Toolbox

In the rapamycin-induced heterodimerization system, addition of the small molecule rapidly dimerizes proteins expressed as FKBP- and FRB-fusions. However, if two proteins are each expressed as fusions to FRB, then addition of rapamycin will indiscriminately trigger incorporation of both targets with an FKBP partner. To avoid this problem, new rapamycin analogs with chemical

modifications in the FRB-binding surface have been developed. These synthetic alterations can be combined with engineered mutants to create orthogonal binding pairs.<sup>105-108</sup> This system is a variation on the “bump-hole” technology used to provide orthogonal molecular recognition by creating compensatory modifications in both the small molecule and the protein target. In the rapamycin-FRB system, “bumped” rapamycin analogs only bind to FRB mutants that have a matching “hole” created by replacing bulky amino acids with smaller residues. Thus, in the same cell, two different FRB fusion proteins can be selectively engaged.<sup>105</sup> Conceptually similar modifications were used in earlier investigations to decrease binding of rapamycin to endogenous mTOR, thus avoiding immunosuppression,<sup>109-111</sup> and recent efforts building on this idea have created an expanded series of orthogonal binding pairs.<sup>105</sup> The end result of these efforts is a series of rapamycin-derived compounds that can be added sequentially to a system to enact serial recruitment of tagged protein targets.

#### **1.4.2 Protein Mislocalization**

The subcellular localization of a protein determines the context in which its function will be interpreted, and this position is often dictated by the nature of a short “address” signal found within its primary sequence. For example, a nuclear localization signal (NLS) is typically encoded on the termini of many transcription factors, which retains the protein within the nuclear compartment. This tag is used to mediate the dynamic trafficking of some transcription factors, such as NF- $\kappa$ B and NFAT, between the nucleus and cytoplasm. In these cases, the cellular signals are masked or unmasked in response to external stimuli.

Similarly, proteolytic processing can irreversibly remove these signals to alter protein localization. A chemical method to achieve these same regulatory capacities, without the input from native signaling pathways, would be a powerful tool.

Based on these natural examples, a synthetic simulacrum has been developed whereby a cellular address signal can be added or removed depending on the availability of a bifunctional molecule.<sup>105, 112, 114-117</sup> Using this “conditional chemical splicing” approach, an NLS sequence can be appended to FKBP and the resulting FKBP-NLS fusion is only recruited to the FRB-tagged target protein in the presence of rapamycin. Thus, a multi-domain protein (e.g. a transcription factor and its NLS) is reversibly and noncovalently assembled and disassembled in response to a chemical stimulus. In theory, similar methods could be used to direct protein localization to other compartments. This trafficking might inactivate a protein (e.g. remove a transcription factor from the nucleus with an export signal) or promote a favorable distribution (e.g. recruit a required signaling kinase to the plasma membrane).

### **1.4.3 Inducible Stabilization**

Another variation of the theme comes from the observation that during the course of engineering FRB mutants that bind specific rapamycin analogs, certain mutations produce thermodynamically unstable products.<sup>77, 107</sup> Interestingly, tagging a number of different targets with this FRB mutant generates unstable chimeric proteins where the instability of the tag is manifest in the fusion.



Importantly, addition of the appropriate rapamycin analog restores the folding stability of the FRB domain and the protein. This system is analogous to temperature-sensitive alleles in which the protein product is only stable at the permissive temperature. By supplying rapamycin or its analogs, temporal windows of function can be created. This approach was recently used to explore the requirements for GSK3 $\beta$  function during mouse embryonic development.<sup>78</sup> Importantly, stabilization of the FRB mutant requires recruitment of the FKBP partner.<sup>107</sup> Thus, it is the formation of the protein-protein complex that is necessary. Related systems have also explored the use of small molecules to regulate protein stability, typically *via* association with the proteasome and its components.<sup>52, 53, 113, 118-120</sup>

#### **1.4.4 Integration of Bifunctional Molecules with –Omics**

Recent large-scale proteomic analyses have revealed a widespread network of interconnected protein-protein interactions termed the interactome. Because of the unique features of bifunctional molecules, it is likely that these reagents will become increasingly important for studying the interactome. In particular, these tools might be leveraged to identify key contacts and understand the dynamics of these connections. In this way, a putative protein-protein contact that was identified by proteomic analyses (e.g. by large-scale yeast two hybrid) might be verified and studied using small molecule probes. However, fulfilling this promise will require extensive advances in the synthesis of large-scale libraries of bifunctional molecules and/or the genomic integration of FKBP and FRB tags. A few examples of chemical library synthesis have been

reported,<sup>64</sup> but additional insights may be gained by application of more diverse collections. One of the challenges in the integration of proteomics/interactomics with chemical genomics is the establishment of a broad base of chemical transformations to address the sophisticated questions emerging in these fields.

## **1.5 Prospectus**

The overarching goal of this thesis work, described in the following chapters, is to explore a novel application of these CID systems. Although there are many interesting examples of bifunctional molecules being used to control protein localization, stability and function, as described above, we envisioned a conceptually different way of using CIDs and protein-protein interactions to control the pharmacokinetic properties of drugs. Specifically, our central hypothesis is that FKBP-binding compounds, such as FK506, avoid hepatic extraction and are shielded from contact with key metabolic enzymes through high-affinity interactions with the FKBP protein. Moreover, synthetically tethering FKBP-binding groups onto other compounds may endow the new chimeric molecules with similar metabolically-evasive properties, thus enhancing their pharmacological profiles. In Chapter 2, we begin investigating the limits of this model by supplementing FK506 with recombinant FKBP12 in the context of a P450 assay. Chapter 3 focuses on the synthesis and comprehensive pharmacokinetic evaluation of a bifunctional molecule, the FKBP-binding HIV-1 protease inhibitor SLFavir. In Chapter 4, we design a rapid and modular chemical platform for the facile synthesis of new bifunctional molecules using

microwave-assisted olefin cross metathesis. The last chapter outlines several of our most compelling ideas for future work and describes potential applications of this approach towards antibiotics and other drug classes. The ultimate goal of this thesis work is to deliberately and systematically modulate the pharmacokinetics of target molecules by covalent conjugation to select FKBP-binding groups.

## Notes

A portion of this work has been published as “Chemical Control Over Protein-Protein Interactions: Beyond Inhibitors,” Gestwicki, J.E., and Marinec, P.S., *Combinatorial Chemistry & High Throughput Screening*, 2007, 10: 667-675.

## 1.6 References

1. Parrish, J.R.; Gulyas, K.D.; Finley, R.L., Jr. Yeast two-hybrid contributions to interactome mapping. *Curr. Opin. Biotechnol.*, **2006**, *17*, 387.
2. Valente, A.X.; Cusick, M.E. Yeast Protein Interactome topology provides framework for coordinated-functionality. *Nucleic Acids Res.*, **2006**, *34*, 2812.
3. Warner, G.J.; Adeleye, Y.A.; Ideker, T. Interactome networks: the state of the science. *Genome Biol.*, **2006**, *7*, 301.
4. Vidal, M. Interactome modeling. *FEBS Lett.*, **2005**, *579*, 1834.
5. Li, S.; Armstrong, C.M.; Bertin, N.; Ge, H.; Milstein, S.; Boxem, M.; Vidalain, P.O.; Han, J.D.; Chesneau, A.; Hao, T.; Goldberg, D.S.; Li, N.; Martinez, M.; Rual, J.F.; Lamesch, P.; Xu, L.; Tewari, M.; Wong, S.L.; Zhang, L.V.; Berriz, G.F.; Jacotot, L.; Vaglio, P.; Reboul, J.; Hirozane-Kishikawa, T.; Li, Q.; Gabel, H.W.; Elewa, A.; Baumgartner, B.; Rose, D.J.; Yu, H.; Bosak, S.; Sequerra, R.; Fraser, A.; Mango, S.E.; Saxton, W.M.; Strome, S.; Van Den Heuvel, S.; Piano, F.; Vandenhaute, J.; Sardet, C.; Gerstein, M.; Doucette-Stamm, L.; Gunsalus, K.C.; Harper, J.W.; Cusick, M.E.; Roth, F.P.; Hill, D.E.; Vidal, M. A map of the interactome network of the metazoan *C. elegans*. *Science*, **2004**, *303*, 540.
6. Ge, H.; Liu, Z.; Church, G.M.; Vidal, M. Correlation between transcriptome and interactome mapping data from *Saccharomyces cerevisiae*. *Nat. Genet.*, **2001**, *29*, 482.
7. Berg, T. Modulation of protein-protein interactions with small organic molecules. *Angew. Chem. Int. Ed. Engl.*, **2003**, *42*, 2462.
8. Arkin, M. Protein-protein interactions and cancer: small molecules going in for the kill. *Curr. Opin. Chem. Biol.*, **2005**, *9*, 317.
9. Reayi, A.; Arya, P. Natural product-like chemical space: search for chemical dissectors of macromolecular interactions. *Curr. Opin. Chem. Biol.*, **2005**, *9*, 240.
10. Veselovsky, A.V.; Ivanov, Y.D.; Ivanov, A.S.; Archakov, A.I.; Lewi, P.; Janssen, P. Protein-protein interactions: mechanisms and modification by drugs. *J. Mol. Recognit.*, **2002**, *15*, 405.
11. Toogood, P.L. Inhibition of protein-protein association by small molecules: approaches and progress. *J. Med. Chem.*, **2002**, *45*, 1543.

12. Fletcher, S.; Hamilton, A.D. Protein surface recognition and proteomimetics: mimics of protein surface structure and function. *Curr. Opin. Chem. Biol.*, **2005**, *9*, 632.
13. Wells, J.A. Systematic mutational analyses of protein-protein interfaces. *Methods Enzymol.*, **1991**, *202*, 390.
14. DeLano, W.L.; Ultsch, M.H.; de Vos, A.M.; Wells, J.A. Convergent solutions to binding at a protein-protein interface. *Science*, **2000**, *287*, 1279.
15. Clackson, T.; Wells, J.A. A hot spot of binding energy in a hormone-receptor interface. *Science*, **1995**, *267*, 383.
16. Thanos, C.D.; Randal, M.; Wells, J.A. Potent small-molecule binding to a dynamic hot spot on IL-2. *J. Am. Chem. Soc.*, **2003**, *125*, 15280.
17. Arkin, M.R.; Randal, M.; DeLano, W.L.; Hyde, J.; Luong, T.N.; Oslob, J.D.; Raphael, D.R.; Taylor, L.; Wang, J.; McDowell, R.S.; Wells, J.A.; Braisted, A.C. Binding of small molecules to an adaptive protein-protein interface. *Proc. Natl. Acad. Sci. USA*, **2003**, *100*, 1603.
18. Ding, K.; Lu, Y.; Nikolovska-Coleska, Z.; Wang, G.; Qiu, S.; Shangary, S.; Gao, W.; Qin, D.; Stuckey, J.; Krajewski, K.; Roller, P.P.; Wang, S. Structure-based design of spiro-oxindoles as potent, specific small-molecule inhibitors of the MDM2-p53 interaction. *J. Med. Chem.*, **2006**, *49*, 3432.
19. Verma, R.; Peters, N.R.; D'Onofrio, M.; Tochtrop, G.P.; Sakamoto, K.M.; Varadan, R.; Zhang, M.; Coffino, P.; Fushman, D.; Deshaies, R.J.; King, R.W. Ubistatins inhibit proteasome-dependent degradation by binding the ubiquitin chain. *Science*, **2004**, *306*, 117.
20. Pilger, B.D.; Cui, C.; Coen, D.M. Identification of a small molecule that inhibits herpes simplex virus DNA Polymerase subunit interactions and viral replication. *Chem. Biol.*, **2004**, *11*, 647.
21. Shultz, M. D.; Ham, Y.W.; Lee, S.G.; Davis, A.; Brown, C.; Chmielewski, J. Small-molecule dimerization inhibitors of wild-type and mutant HIV protease: a focused library approach. *J. Am. Chem. Soc.*, **2004**, *126*, 9886.
22. Xu, Y.; Shi, J.; Yamamoto, N.; Moss, J.A.; Vogt, P.K.; Janda, K.D. A credit-card library approach for disrupting protein-protein interactions. *Bioorg. Med. Chem.*, **2006**, *14*, 2660.

23. Sehgal, S.N. Rapamune (RAPA, rapamycin, sirolimus): mechanism of action immunosuppressive effect results from blockade of signal transduction and inhibition of cell cycle progression. *Clin. Biochem.*, **1998**, *31*, 335.
24. Mossessova, E.; Corpina, R.A.; Goldberg, J. Crystal structure of ARF1\*Sec7 complexed with Brefeldin A and its implications for the guanine nucleotide exchange mechanism. *Mol. Cell*, **2003**, *12*, 1403.
25. Harding, M.W.; Galat, A.; Uehling, D.E.; Schreiber, S.L. A receptor for the immunosuppressant FK506 is a cis-trans peptidyl-prolyl isomerase. *Nature*, **1989**, *341*, 758.
26. Siekierka, J.J.; Hung, S.H.; Poe, M.; Lin, C.S.; Sigal, N.H. A cytosolic binding protein for the immunosuppressant FK506 has peptidyl-prolyl isomerase activity but is distinct from cyclophilin. *Nature*, **1989**, *341*, 755.
27. Banaszynski, L.A.; Liu, C.W.; Wandless, T.J. Characterization of the FKBP.rapamycin.FRB ternary complex. *J. Am. Chem. Soc.*, **2005**, *127*, 4715.
28. Chen, J.; Zheng, X.F.; Brown, E.J.; Schreiber, S.L. Identification of an 11-kDa FKBP12-rapamycin-binding domain within the 289-kDa FKBP12-rapamycin-associated protein and characterization of a critical serine residue. *Proc. Natl. Acad. Sci. USA*, **1995**, *92*, 4947.
29. Liberles, S.D.; Diver, S.T.; Austin, D.J.; Schreiber, S.L. Inducible gene expression and protein translocation using nontoxic ligands identified by a mammalian three-hybrid screen. *Proc. Natl. Acad. Sci. USA*, **1997**, *94*, 7825.
30. Crabtree, G.R.; Schreiber, S.L. Three-part inventions: intracellular signaling and induced proximity. *Trends Biochem. Sci.*, **1996**, *21*, 418.
31. Clackson, T. Dissecting the functions of proteins and pathways using chemically induced dimerization. *Chem. Biol. Drug Des.*, **2006**, *67*, 440.
32. Spencer, D.M.; Wandless, T.J.; Schreiber, S.L.; Crabtree, G.R. Controlling signal transduction with synthetic ligands. *Science*, **1993**, *262*, 1019.
33. Pownall, M.E.; Welm, B.E.; Freeman, K.W.; Spencer, D.M.; Rosen, J.M.; Isaacs, H.V. An inducible system for the study of FGF signaling in early amphibian development. *Dev. Biol.*, **2003**, *256*, 89.

34. Welm, B.E.; Freeman, K.W.; Chen, M.; Contreras, A.; Spencer, D.M.; Rosen, J.M. Inducible dimerization of FGFR1: development of a mouse model to analyze progressive transformation of the mammary gland. *J. Cell Biol.*, **2002**, *157*, 703.
35. Freeman, K.W.; Gangula, R.D.; Welm, B.E.; Ozen, M.; Foster, B.A.; Rosen, J.M.; Ittmann, M.; Greenberg, N.M.; Spencer, D.M. Inducible prostate intraepithelial neoplasia with reversible hyperplasia in conditional FGFR1-expressing mice. *Cancer Res.*, **2003**, *63*, 6237.
36. Spencer, D.M.; Belshaw, P.J.; Chen, L.; Ho, S.N.; Randazzo, F.; Crabtree, G.R.; Schreiber, S.L. Functional analysis of Fas signaling in vivo using synthetic inducers of dimerization. *Curr. Biol.*, **1996**, *6*, 839.
37. Freiberg, R.A.; Ho, S.N.; Khavari, P.A. Transcriptional control in keratinocytes and fibroblasts using synthetic ligands. *J. Clin. Invest.*, **1997**, *99*, 2610.
38. Li, B.; Sun, A.; Youn, H.; Hong, Y.; Terranova, P.F.; Thrasher, J.B.; Xu, P.; Spencer, D. Conditional Akt activation promotes androgen-independent progression of prostate cancer. *Carcinogenesis*, **2007**, *28*, 572.
39. Graef, I.A.; Holsinger, L.J.; Diver, S.; Schreiber, S.L.; Crabtree, G.R. Proximity and orientation underlie signaling by the non-receptor tyrosine kinase ZAP70. *Embo J.*, **1997**, *16*, 5618.
40. Spencer, D.M.; Graef, I.; Austin, D.J.; Schreiber, S.L.; Crabtree, G.R. A general strategy for producing conditional alleles of Src-like tyrosine kinases. *Proc. Natl. Acad. Sci. USA*, **1995**, *92*, 9805.
41. Belshaw, P.J.; Ho, S.N.; Crabtree, G. R.; Schreiber, S.L. Controlling protein association and subcellular localization with a synthetic ligand that induces heterodimerization of proteins. *Proc. Natl. Acad. Sci. USA*, **1996**, *93*, 4604.
42. Althoff, E.A.; Cornish, V.W. A bacterial small-molecule three-hybrid system. *Angew. Chem. Int. Ed. Engl.*, **2002**, *41*, 2327.
43. Belshaw, P.J.; Spencer, D.M.; Crabtree, G.R.; Schreiber, S.L. Controlling programmed cell death with a cyclophilin-cyclosporin-based chemical inducer of dimerization. *Chem. Biol.*, **1996**, *3*, 731.
44. Mallet, V.O.; Mitchell, C.; Guidotti, J.E.; Jaffray, P.; Fabre, M.; Spencer, D.; Arnoult, D.; Kahn, A.; Gilgenkrantz, H. Conditional cell ablation by tight control of caspase-3 dimerization in transgenic mice. *Nat. Biotechnol.*, **2002**, *20*, 1234.

45. Graveley, B.R. Small molecule control of pre-mRNA splicing. *RNA*, **2005**, *11*, 355.
46. Inoue, T.; Heo, W.D.; Grimley, J.S.; Wandless, T.J.; Meyer, T. An inducible translocation strategy to rapidly activate and inhibit small GTPase signaling pathways. *Nat. Methods*, **2005**, *2*, 415.
47. Mootz, H.D.; Muir, T.W. Protein splicing triggered by a small molecule. *J. Am. Chem. Soc.*, **2002**, *124*, 9044.
48. Wehrman, T.; Kleaveland, B.; Her, J.H.; Balint, R.F.; Blau, H.M. Protein-protein interactions monitored in mammalian cells via complementation of beta -lactamase enzyme fragments. *Proc. Natl. Acad. Sci. USA*, **2002**, *99*, 3469.
49. Schlatter, S.; Senn, C.; Fussenegger, M. Modulation of translation-initiation in CHO-K1 cells by rapamycin-induced heterodimerization of engineered eIF4G fusion proteins. *Biotechnol. Bioeng.*, **2003**, *83*, 210.
50. Kohler, J.J.; Bertozzi, C.R. Regulating cell surface glycosylation by small molecule control of enzyme localization. *Chem. Biol.*, **2003**, *10*, 1303.
51. Lin, H.; Tao, H.; Cornish, V.W. Directed evolution of a glycosynthase via chemical complementation. *J. Am. Chem. Soc.*, **2004**, *126*, 15051.
52. Janse, D. M., Crosas, B., Finley, D. and Church, G. M. Localization to the proteasome is sufficient for degradation. *J Biol Chem*, **2004**, *279*, 21415.
53. Schneekloth, J.S. Jr.; Crews, C.M. Chemical approaches to controlling intracellular protein degradation. *ChemBiochem.*, **2005**, *6*, 40.
54. Heo, W.D.; Inoue, T.; Park, W.S.; Kim, M.L.; Park, B.O.; Wandless, T.J.; Meyer, T. PI(3,4,5)P3 and PI(4,5)P2 lipids target proteins with polybasic clusters to the plasma membrane. *Science*, **2006**, *314*, 1458.
55. Suh, B.C.; Inoue, T.; Meyer, T.; Hille, B. Rapid chemically induced changes of PtdIns(4,5)P2 gate KCNQ ion channels. *Science*, **2006**, *314*, 1454.
56. Rivera, V.M.; Wang, X.; Wardwell, S.; Courage, N.L.; Volchuk, A.; Keenan, T.; Holt, D.A.; Gilman, M.; Orci, L.; Cerasoli, F. Jr.; Rothman, J.E.; Clackson, T. Regulation of protein secretion through controlled aggregation in the endoplasmic reticulum. *Science*, **2000**, *287*, 826.



57. Johnston, J.; Tazelaar, J.; Rivera, V.M.; Clackson, T.; Gao, G.P.; Wilson, J.M. Regulated expression of erythropoietin from an AAV vector safely improves the anemia of beta-thalassemia in a mouse model. *Mol. Ther.*, **2003**, *7*, 493.
58. Pollock, R.; Issner, R.; Zoller, K.; Natesan, S.; Rivera, V.M.; Clackson, T. Delivery of a stringent dimerizer-regulated gene expression system in a single retroviral vector. *Proc. Natl. Acad. Sci. USA*, **2000**, *97*, 13221.
59. Pollock, R.; Rivera, V.M. Regulation of gene expression with synthetic dimerizers. *Methods Enzymol.*, **1999**, *306*, 263.
60. Rivera, V.M. Controlling gene expression using synthetic ligands. *Methods*, **1998**, *14*, 421.
61. Becker, F.; Murthi, K.; Smith, C.; Come, J.; Costa-Roldan, N.; Kaufmann, C.; Hanke, U.; Degenhart, C.; Baumann, S.; Wallner, W.; Huber, A.; Dedier, S.; Dill, S.; Kinsman, D.; Hediger, M.; Bockovich, N.; Meier-Ewert, S.; Kluge, A.F.; Kley, N. A three-hybrid approach to scanning the proteome for targets of small molecule kinase inhibitors. *Chem. Biol.*, **2004**, *11*, 211.
62. Firestine, S.M.; Salinas, F.; Nixon, A.E.; Baker, S.J.; Benkovic, S.J. Using an AraC-based three-hybrid system to detect biocatalysts in vivo. *Nat. Biotechnol.*, **2000**, *18*, 544.
63. Henthorn, D.C.; Jaxa-Chamiec, A.A.; Meldrum, E. A GAL4-based yeast three-hybrid system for the identification of small molecule-target protein interactions. *Biochem. Pharmacol.*, **2002**, *63*, 1619.
64. Koide, K.; Finkelstein, J.M.; Ball, Z.; Verdine, G.L. A synthetic library of cell-permeable molecules. *J. Am. Chem. Soc.*, **2001**, *123*, 398.
65. Banaszynski, L.A.; Wandless, T.J. Conditional control of protein function. *Chem. Biol.*, **2006**, *13*, 11.
66. Clackson, T. Controlling mammalian gene expression with small molecules. *Curr. Opin. Chem. Biol.*, **1997**, *1*, 210.
67. Rossi, F.M.; Blau, H.M. Recent advances in inducible gene expression systems. *Curr. Opin. Biotechnol.*, **1998**, *9*, 451.
68. Lin, H.; Cornish, V.W. Screening and selection methods for large-scale analysis of protein function. *Angew. Chem. Int. Ed. Engl.*, **2002**, *41*, 4402.

69. Kley, N. Chemical dimerizers and three-hybrid systems: scanning the proteome for targets of organic small molecules. *Chem. Biol.*, **2004**, *11*, 599.
70. Buskirk, A.R.; Liu, D.R. Creating small-molecule-dependent switches to modulate biological functions. *Chem. Biol.*, **2005**, *12*, 151.
71. Farrar, M.A.; Alberol, I.; Perlmutter, R.M. Activation of the Raf-1 kinase cascade by coumermycin-induced dimerization. *Nature*, **1996**, *383*, 178.
72. Mizuguchi, R.; Hatakeyama, M. Conditional activation of Janus kinase (JAK) confers factor independence upon interleukin-3-dependent cells. Essential role of Ras in JAK-triggered mitogenesis. *J. Biol. Chem.*, **1998**, *273*, 32297.
73. Gendreizig, S.; Kindermann, M.; Johnsson, K. Induced protein dimerization in vivo through covalent labeling. *J. Am. Chem. Soc.*, **2003**, *125*, 14970.
74. Hussey, S.L.; Muddana, S.S.; Peterson, B.R. Synthesis of a beta-estradiol-biotin chimera that potently heterodimerizes estrogen receptor and streptavidin proteins in a yeast three-hybrid system. *J. Am. Chem. Soc.*, **2003**, *125*, 3692.
75. Neddermann, P.; Gargioli, C.; Muraglia, E.; Sambucini, S.; Bonelli, F.; De Francesco, R.; Cortese, R. A novel, inducible, eukaryotic gene expression system based on the quorum-sensing transcription factor TraR. *EMBO Rep.*, **2003**, *4*, 159.
76. Abida, W.M.; Carter, B.T.; Althoff, E.A.; Lin, H.; Cornish, V.W. Receptor-dependence of the transcription read-out in a small-molecule three-hybrid system. *Chembiochem.*, **2002**, *3*, 887.
77. Stankunas, K.; Bayle, J.H.; Gestwicki, J.E.; Lin, Y.M.; Wandless, T.J.; Crabtree, G.R. Conditional protein alleles using knockin mice and a chemical inducer of dimerization. *Mol. Cell*, **2003**, *12*, 1615.
78. Liu, K.J.; Arron, J.R.; Stankunas, K.; Crabtree, G.R.; Longaker, M.T. Chemical rescue of cleft palate and midline defects in conditional GSK-3beta mice. *Nature*, **2007**, *446*, 79.
79. Rankin, M.L.; Marinec, P.S.; Cabrera, D.M.; Wang, Z.; Jose, P.A.; Sibley, D.R. The D1 dopamine receptor is constitutively phosphorylated by G protein-coupled receptor kinase 4. *Mol. Pharmacol.*, **2006**, *69*, 759.

80. Premont, R.T.; Gainetdinov, R.R. Physiological roles of G protein-coupled receptor kinases and arrestins. *Annu. Rev. Physiol.*, **2007**, *69*, 511.
81. Terrillon, S.; Bouvier, M. Receptor activity-independent recruitment of beta arrestin2 reveals specific signalling modes. *Embo J.*, **2004**, *23*, 3950.
82. Karpova, A.Y.; Tervo, D.G.; Gray, N.W.; Svoboda, K. Rapid and reversible chemical inactivation of synaptic transmission in genetically targeted neurons. *Neuron*, **2005**, *48*, 727.
83. Nasmyth, K.; Haering, C.H. The structure and function of SMC and kleisin complexes. *Annu. Rev. Biochem.*, **2005**, *74*, 595.
84. Gruber, S.; Arumugam, P.; Katou, Y.; Kuglitsch, D.; Helmhart, W.; Shirahige, K.; Nasmyth, K. Evidence that loading of cohesin onto chromosomes involves opening of its SMC hinge. *Cell*, **2006**, *127*, 523.
85. Portoghese, P.S. From models to molecules: opioid receptor dimers, bivalent ligands, and selective opioid receptor probes. *J. Med. Chem.*, **2001**, *44*, 2259.
86. Kiessling, L.L.; Gestwicki, J.E.; Strong, L.E. Synthetic multivalent ligands as probes of signal transduction. *Angew. Chem. Int. Ed. Engl.*, **2006**, *45*, 2348.
87. Lowe, J.N.; Fulton, D.A.; Chiu, S.H.; Elizarov, A.M.; Cantrill, S.J.; Rowan, S.J.; Stoddart, J.F. Polyvalent interactions in unnatural recognition processes. *J. Org. Chem.*, **2004**, *69*, 4390.
88. Fan, E.; Merritt, E.A. Combating infectious diseases through multivalent design. *Curr Drug Targets Infect. Disord.*, **2002**, *2*, 161.
89. Selkoe, D.J. Alzheimer disease: mechanistic understanding predicts novel therapies. *Ann. Intern. Med.*, **2004**, *140*, 627.
90. Gong, Y.; Chang, L.; Viola, K.L.; Lacor, P.N.; Lambert, M.P.; Finch, C.E.; Krafft, G.A.; Klein, W.L. Alzheimer's disease-affected brain: presence of oligomeric A beta ligands (ADDLs) suggests a molecular basis for reversible memory loss. *Proc. Natl. Acad. Sci. USA*, **2003**, *100*, 10417.
91. Walsh, D.M.; Klyubin, I.; Fadeeva, J.V.; Cullen, W.K.; Anwyl, R.; Wolfe, M.S.; Rowan, M.J.; Selkoe, D.J. Naturally secreted oligomers of amyloid beta protein potently inhibit hippocampal long-term potentiation in vivo. *Nature*, **2002**, *416*, 535.

92. Aisen, P.S. The development of anti-amyloid therapy for Alzheimer's disease: from secretase modulators to polymerisation inhibitors. *CNS Drugs*, **2005**, *19*, 989.
93. LeVine, H. 3rd. Challenges of targeting A beta fibrillogenesis and other protein folding disorders. *Amyloid*, **2003**, *10*, 133.
94. Findeis, M.A. Peptide inhibitors of beta amyloid aggregation. *Curr. Top. Med. Chem.*, **2002**, *2*, 417.
95. Lansbury, P.T. Jr. Inhibition of amyloid formation: a strategy to delay the onset of Alzheimer's disease. *Curr. Opin. Chem. Biol.*, **1997**, *1*, 260.
96. Ghanta, J.; Shen, C.L.; Kiessling, L.L.; Murphy, R.M. A strategy for designing inhibitors of beta-amyloid toxicity. *J. Biol. Chem.*, **1996**, *271*, 29525.
97. Cairo, C.W.; Strzelec, A.; Murphy, R.M.; Kiessling, L.L. Affinity-based inhibition of beta-amyloid toxicity. *Biochemistry*, **2002**, *41*, 8620.
98. Sacchettini, J.C.; Kelly, J.W. Therapeutic strategies for human amyloid diseases. *Nat. Rev. Drug Discov.*, **2002**, *1*, 267.
99. Gestwicki, J.E.; Crabtree, G.R.; Graef, I.A. Harnessing chaperones to generate small-molecule inhibitors of amyloid beta aggregation. *Science*, **2004**, *306*, 865.
100. Bose, M.; Gestwicki, J.E.; Devasthali, V.; Crabtree, G.R.; Graef, I.A. 'Nature-inspired' drug-protein complexes as inhibitors of Abeta aggregation. *Biochem. Soc. Trans.*, **2005**, *33*, 543.
101. Briesewitz, R.; Ray, G.T.; Wandless, T.J.; Crabtree, G.R. Affinity modulation of small-molecule ligands by borrowing endogenous protein surfaces. *Proc. Natl. Acad. Sci. USA*, **1999**, *96*, 1953.
102. Braun, P.D.; Barglow, K.T.; Lin, Y.M.; Akompong, T.; Briesewitz, R.; Ray, G.T.; Haldar, K.; Wandless, T.J. A bifunctional molecule that displays context-dependent cellular activity. *J. Am. Chem. Soc.*, **2003**, *125*, 7575.
103. Sellmyer, M.A.; Stankunas, K.; Briesewitz, R.; Crabtree, G.R.; Wandless, T.J. Engineering small molecule specificity in nearly identical cellular environments. *Bioorg. Med. Chem. Lett.*, **2007**, *17*, 2703.

104. Liu, K.J.; Gestwicki, J.E.; Crabtree, G.R. Bringing Small Molecule Regulation of Protein Activity to Developmental Systems. Taylor & Francis, **2007**.
105. Bayle, J.H.; Grimley, J.S.; Stankunas, K.; Gestwicki, J. E.; Wandless, T.J.; Crabtree, G.R. Rapamycin analogs with differential binding specificity permit orthogonal control of protein activity. *Chem. Biol.*, **2006**, 13, 99.
106. Rollins, C.T.; Rivera, V.M.; Woolfson, D.N.; Keenan, T.; Hatada, M.; Adams, S.E.; Andrade, L.J.; Yaeger, D.; van Schravendijk, M.R.; Holt, D.A.; Gilman, M.; Clackson, T. A ligand-reversible dimerization system for controlling protein-protein interactions. *Proc. Natl. Acad. Sci. USA*, **2000**, 97, 7096.
107. Stankunas, K.; Bayle, J.H.; Havranek, J.J.; Wandless, T.J.; Baker, D.; Crabtree, G.R.; Gestwicki, J.E. Rescue of degradation-prone mutants of the FK506-rapamycin binding (FRB) protein with chemical ligands. *Chembiochem.*, **2007**, 8, 1162.
108. Yang, W.; Rozamus, L.W.; Narula, S.; Rollins, C.T.; Yuan, R.; Andrade, L.J.; Ram, M.K.; Phillips, T.B.; van Schravendijk, M.R.; Dalgarno, D.; Clackson, T.; Holt, D.A. Investigating protein-ligand interactions with a mutant FKBP possessing a designed specificity pocket. *J. Med. Chem.*, **2000**, 43, 1135.
109. Clackson, T.; Yang, W.; Rozamus, L.W.; Hatada, M.; Amara, J.F.; Rollins, C.T.; Stevenson, L.F.; Magari, S.R.; Wood, S.A.; Courage, N.L.; Lu, X.; Cerasoli, F. Jr.; Gilman, M.; Holt, D.A. Redesigning an FKBP-ligand interface to generate chemical dimerizers with novel specificity. *Proc. Natl. Acad. Sci. USA*, **1998**, 95, 10437.
110. Clackson, T. Redesigning small molecule-protein interfaces. *Curr. Opin. Struct. Biol.*, **1998**, 8, 451.
111. Amara, J.F.; Clackson, T.; Rivera, V.M.; Guo, T.; Keenan, T.; Natesan, S.; Pollock, R.; Yang, W.; Courage, N.L.; Holt, D.A.; Gilman, M. A versatile synthetic dimerizer for the regulation of protein-protein interactions. *Proc. Natl. Acad. Sci. USA*, **1997**, 94, 10618.
112. Klemm, J.D.; Beals, C.R.; Crabtree, G.R. Rapid targeting of nuclear proteins to the cytoplasm. *Curr. Biol.*, **1997**, 7, 638.
113. Pratt, M.R.; Schwartz, E.C.; Muir, T.W. Small-molecule-mediated rescue of protein function by an inducible proteolytic shunt. *Proc. Natl. Acad. Sci. USA*, **2007**, 104, 11209.

114. Patury, S.; Geda, P.; Dobry, C.J.; Kumar, A.; Gestwicki, J.E. Conditional nuclear import and export of yeast proteins using a chemical inducer of dimerization. *Cell Biochem. Biophys.*, **2009**, 53, 127.
115. Geda, P.; Patury, S.; Ma, J.; Bharucha, N.; Dobry, C.J.; Lawson, S.K.; Gestwicki, J.E.; Kumar, A. A small molecule-directed approach to control protein localization and function. *Yeast*, **2008**, 25, 577.
116. Haruki, H.; Nishikawa, J.; Laemmli, U.K. The anchor-away technique: rapid, conditional establishment of yeast mutant phenotypes. *Mol. Cell.*, **2008**, 31, 925.
117. Xu, T.; Johnson, C.A.; Gestwicki, J.E.; Kumar, A. Conditionally controlling nuclear trafficking in yeast by chemical-induced protein dimerization. *Nat. Protoc.*, **2010**, 10, 1831.
118. Iwamoto, M.; Bjorklund, T.; Lundberg, C.; Kirik, D.; Wandless, T.J. A general chemical method to regulate protein stability in the mammalian central nervous system. *Chem. Biol.*, **2010**, 17, 981.
119. Banaszynski, L.A.; Sellmyer, M.A.; Contag, C.H.; Wandless, T.J.; Thorne, S.H. Chemical control of protein stability and function in living mice. *Nat. Med.*, **2008**, 18, 5941.
120. Lau, H.D.; Yaegashi, J.; Zaro, B.W.; Pratt, M.R. Precise control of protein concentration in living cells. *Angew. Chem. Int. Ed. Engl.*, **2010**, 49, 8458.

## Chapter II

### **Bifunctional Molecules Evade Cytochrome P450 Metabolism by Forming Protective Complexes with FK506-Binding Protein**

#### **2.1 Abstract**

Despite their large size and complexity, the bifunctional, macrolide natural products rapamycin and FK506 have excellent pharmacological characteristics. We hypothesize that these unexpected properties may arise from protective, high-affinity interactions with the cellular FK506-binding protein, FKBP. In this model, the drug–FKBP complex might sequester the small molecule and limit its degradation by restricting access to metabolic enzymes. In support of this idea, we found that adding FKBP blocks binding of FK506 to the common cytochrome P450 enzyme CYP3A4 *in vitro*. To further test this idea, we have systematically modified a small collection of otherwise unrelated compounds, such that they acquire affinity for FKBP. Strikingly, we found that many of these synthetic derivatives, but not the unmodified parent compounds, are also protected from CYP3A4-mediated metabolism. Depending on the properties of the linker, the bifunctional molecules exhibited up to a 3.5-fold weaker binding to CYP3A4, and this protective effect was observed in the presence of either purified FKBP or FKBP-expressing cells. Together, these results suggest that the surprising pharmacology of rapamycin and FK506 might arise, in part, from binding to their

abundant intracellular target, FKBP. Furthermore, these findings provide a framework by which other small molecules might be systematically modified to impart this protective effect.

### **2.1.1 The Interesting Pharmacology Behind Rapamycin and FK506**

The macrolide natural products rapamycin and FK506 are potent immunosuppressive drugs that are used clinically to prevent transplant rejection. Based solely on the common “rule of five”,<sup>1</sup> these compounds would be expected to possess poor pharmacological characteristics; however, in practice, they have exceedingly long half-lives. For example, despite its high molecular weight (914 Da) and large number of functional groups (~13 hydrogen bond donors and acceptors), rapamycin has a terminal half-life ( $t_{1/2}$ ) of greater than 5 hours in rats and approximately 60 hours in humans.<sup>2-4</sup> Thus, rapamycin and FK506 avoid rapid metabolism, despite their chemical and structural complexity. Moreover, they are orally bioavailable and rapidly absorbed, with rapamycin reaching its peak concentration less than 1 hour after administration.<sup>2,5</sup> These compounds do not conform to the normal patterns of drug design, and therefore, provide an interesting model from which to understand how large molecules might be used as drugs.

### **2.1.2 Protein Binding as a Protective Mechanism**

The mechanism responsible for the better-than-predicted pharmacology of rapamycin and FK506 may involve the protein binding abilities of these drugs.<sup>6</sup>



Interestingly, both drugs are naturally bifunctional; they first bind to the cytoplasmic FK506-binding protein (FKBP), and then the FKBP-bound complex gains affinity for another target. For example, rapamycin takes part in a ternary interaction with FKBP and the mammalian target of rapamycin (mTOR).<sup>7-9</sup> Similarly, FK506 first binds FKBP, and then the FKBP-FK506 complex inhibits the phosphatase calcineurin.<sup>10-12</sup> The shared target of both drugs, FKBP, is an abundant *cis-trans* prolyl isomerase, which is highly expressed in the cytosol of muscle cells, neurons, red blood cells and leukocytes, among other tissues.<sup>12</sup> Interestingly, orally-administered rapamycin is preferentially localized in the cellular component of whole blood ( blood : plasma distribution ratio of 4.5 : 1 ).<sup>2,3</sup> Based on these observations, Levin *et al.* speculated that certain large natural products, such as rapamycin and paclitaxel, might accumulate in protected cellular environments through high-affinity interactions with their targets.<sup>6</sup> However, the specific contribution of FKBP to the metabolism, half-life, and biodistribution of rapamycin and FK506 has not been systematically explored.

### **2.1.3 Synthetic Chemical Inducers of Dimerization**

Inspired by FK506, synthetic molecules were developed by Crabtree *et al.* in the early 1990s.<sup>14, 15</sup> Since they were first described, these chemical inducers of dimerization (CIDs) have been used widely to study the effects of protein juxtaposition in a wide variety of organisms and biological systems.<sup>16-18</sup> As discussed in Chapter 1, synthetic CIDs are composed of two non-overlapping chemical domains that each provide affinity for a specific protein target. Similar

to the natural products, at least one of the domains often retains a high affinity for FKBP. The linker that bridges the two domains is also one of their important features, and extensive studies have documented the effects of this group on potency.<sup>19-21</sup> In one example, Briesewitz *et al.* found that very short linkers gave rise to compounds that could not bind both targets simultaneously.<sup>22</sup> In these short linker systems, a steric clash between the FKBP surface and the adjoining protein is believed to disallow formation of the ternary complex. This property was exploited to create compounds that display context-specific activity; their function could be tuned by the differential expression of FKBP in various cell types.<sup>23, 24</sup>

Because many synthetic CIDs bind FKBP, we envisioned that these molecules could be good models for exploring the role of this interaction in controlling the persistence of FK506 and rapamycin. To test this idea, we generated a series of CIDs that are all coupled to FK506-like groups and explored the binding of these compounds to the P450 isozyme, CYP3A4. Interestingly, we found that, like the natural products, some of the bifunctional derivatives were protected by FKBP. These findings support a model in which FKBP sequesters small molecules and limits their access to metabolic enzymes. We speculate that this property contributes to the surprisingly long half-lives of rapamycin and FK506.

## 2.2 Results

### 2.2.1 FK506 is Protected from CYP3A4 Metabolism by FKBP *in vitro*

We hypothesized that rapamycin and FK506 might possess long half-lives, in part, because of their affinity for FKBP. More specifically, formation of the drug–protein complex might directly shield the compounds from interactions with metabolic P450 enzymes (Figure 2-1A). In this model, the drug no longer reaches the active site because of steric clashes between the FKBP surface and the P450 enzyme. To test this idea, we first explored whether FKBP could protect FK506 from CYP3A4, which is the cytochrome P450 that is principally responsible for degradation of FK506 *in vivo*.<sup>31</sup> Towards this goal, we employed a well-known assay in which metabolism is indirectly measured by the ability of the query compound to compete with the conversion of a fluorescent model substrate. Using this approach, we first added FK506 to microsome-bound CYP3A4 and confirmed that it was a good substrate (Figure 2-1B). Next, we added a mixture of FK506 and recombinant FKBP (1  $\mu$ M). Strikingly, we found that FKBP significantly protected the drug. As expected, the protective effects were lost when the drug concentration (e.g. 20  $\mu$ M) greatly exceeded the levels of FKBP. In addition, we found that FKBP had no effect on the turnover of the fluorescent substrate in the absence of FK506 (Figure 2-1C), which suggests that the protective effects were mediated by direct interactions between FK506 and FKBP. By plotting the results across a range of concentrations, we found that the apparent  $K_i$  of FK506 for CYP3A4 was improved nearly 3-fold by FKBP

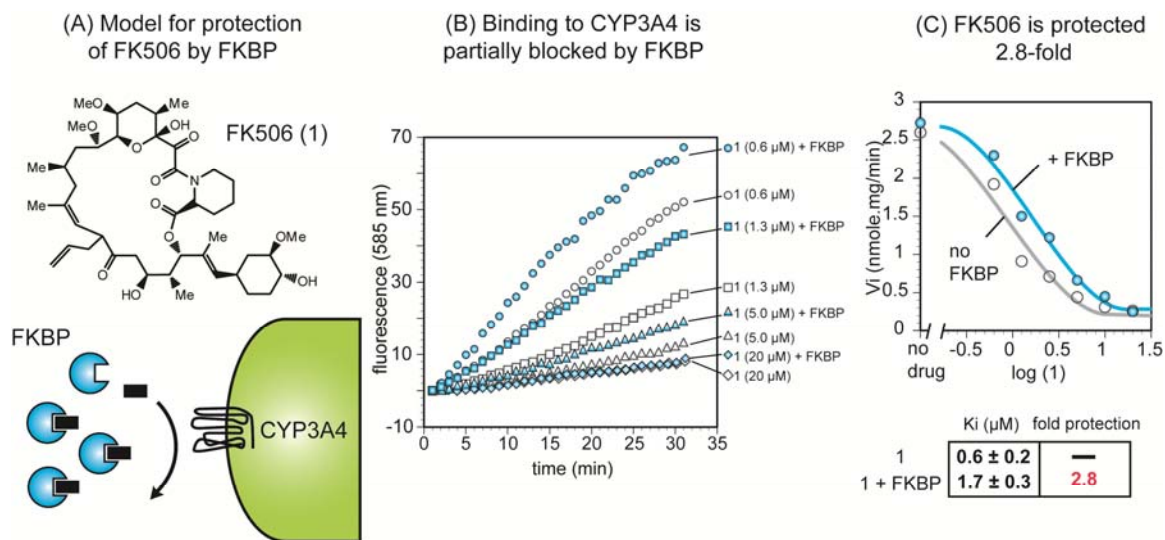


**Figure 2-1. FKBP Protects FK506 from Binding to CYP3A4.** (A) The chemical structure of FK506 and a model for FKBP-mediated protection is shown. The arrow represents binding to the enzyme and subsequent metabolism. (B) Cytochrome P450 assay using a green fluorescent probe and the recombinant CYP3A4 enzyme incorporated into liposomes. Addition of FKBP makes FK506 less susceptible to enzyme binding, and therefore favors faster turnover of the model fluorescent substrate (fluorescence emission 585 nm). FKBP was added at a final concentration of 1 μM. Results are representative of three independent experiments, and only 4 of the 7 total drug concentrations are shown for clarity. (C) K<sub>i</sub> for FK506 in the presence and the absence of FKBP (1 μM) is shown.

(Figure 2-1C). These results suggest that FK506 is partially protected from binding to CYP3A4 *in vitro* by the formation of a complex with FKBP.

## 2.2.2 Synthesis of FKBP-binding Bifunctional Molecules

We envisioned that if binding to FKBP provides protection, then systematically installing FKBP-binding groups into a series of otherwise unrelated compounds should enhance their stability. To complete the synthesis of the desired compounds, we required FKBP-binding groups with a functionality suitable in coupling reactions. Towards this goal, we generated **2** and **4**, which each have a single activated carboxylate (Figure 2-2). The succinimidyl ester, **2**, was derived from FK506 (**1**) through an established route.<sup>14</sup> Likewise, compound **4**

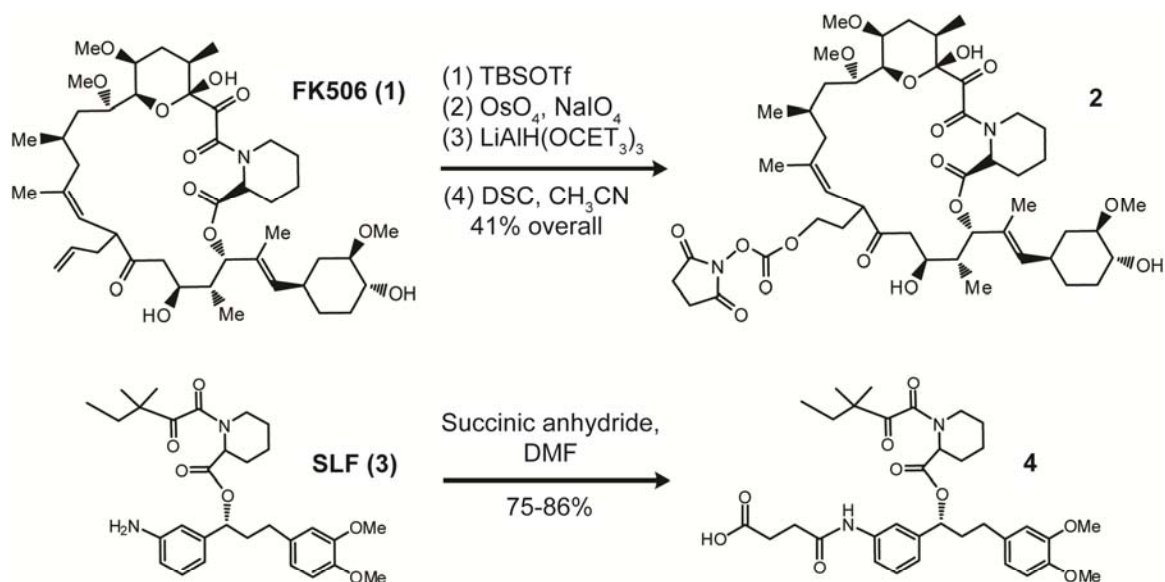


**Figure 2-2. The Chemical Structures of FKBP Ligands.** Commercially available **1** and **3** were converted to intermediates **2** and **4** using established routes. The intermediates contain a single reactive carboxylate group that is suitable for installation into amine-bearing parent ligands.

was available through the straightforward reaction of succinic anhydride with commercially available Synthetic Ligand for FKBP (SLF). **1** and **3** bind FKBP with good affinity, approximately 1.0 and 10 nM, respectively, and the sites that we modified are known to be dispensable for binding.<sup>32</sup> Thus, compounds **2** and **4** are suitable as reactive intermediates for installing FKBP-binding groups into compounds that normally do not have this potential.

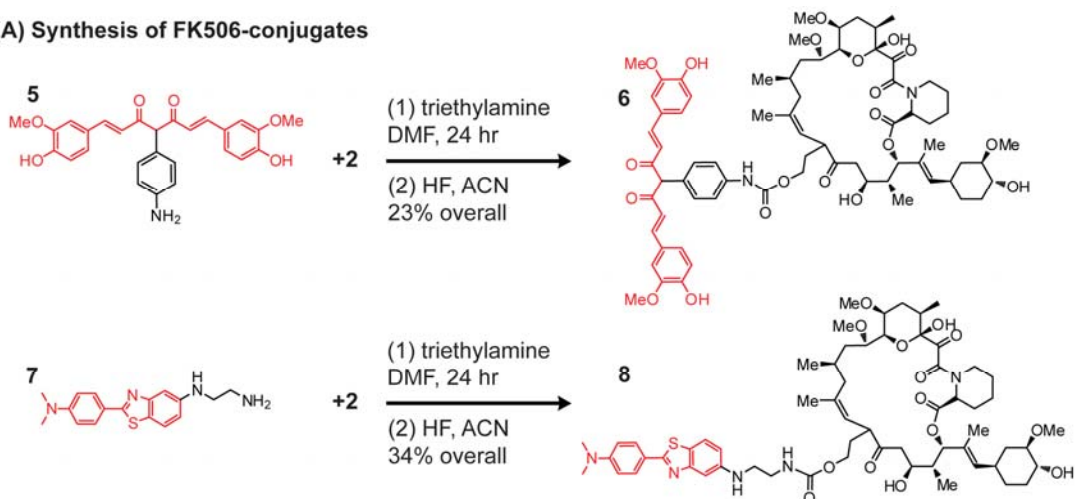
Next, we selected four compounds as parent ligands. Congo red, curcumin and thioflavin T (ThT) are known ligands for amyloid beta.<sup>33-36</sup> Because our previous work has focused on generating new inhibitors of amyloid formation,<sup>19, 37, 38</sup> we included these targets in the pilot study. Congo red (**10**)

was used without further purification, while the amine-containing curcumin analog **5** and ThT-like benzothiazole **7** were readily available using minor adaptations of published routes. Lastly, we chose a derivative, **12**, of the known HIV protease inhibitor Amprenavir.<sup>39</sup> Peptide-based HIV protease inhibitors, including Amprenavir, have a challenging pharmacology that complicates their dosing schedules and reduces patient compliance.<sup>40</sup> Thus, we included this example to explore whether FKBP-binding might improve the lifetime of drugs in this class. The intermediate, **12**, was available by a well-known route.<sup>29</sup> Importantly, the sites of coupling to the amyloid and HIV protease ligands were chosen such that installation of FKBP-binding groups would have minimal impact on their interaction with their normal binding partner.<sup>19, 27, 38, 39</sup> The resulting bifunctional compounds (**6**, **8**, **9**, **11** and **13**; Figure 2-3) were purified by chromatography and their identities confirmed by mass spectrometry. The compounds were synthesized in average-to-poor overall yields, but because only milligram amounts were needed for the pilot studies *in vitro*, we proceeded without optimization.

### **2.2.3 Bifunctional Molecules are Protected from Binding to CYP3A4 *in vitro***

Using the cytochrome P450 assay outlined above, we studied the ability of FKBP to protect compounds **5–13**. The apparent  $K_i$  for each compound was used to estimate its suitability as a substrate for CYP3A4, and the relative binding in the presence and absence of 1.0  $\mu\text{M}$  FKBP was compared. Using this approach, we first measured the binding of the unmodified, parent compounds **5**,

**(A) Synthesis of FK506-conjugates**



**(B) Synthesis of SLF-conjugates**

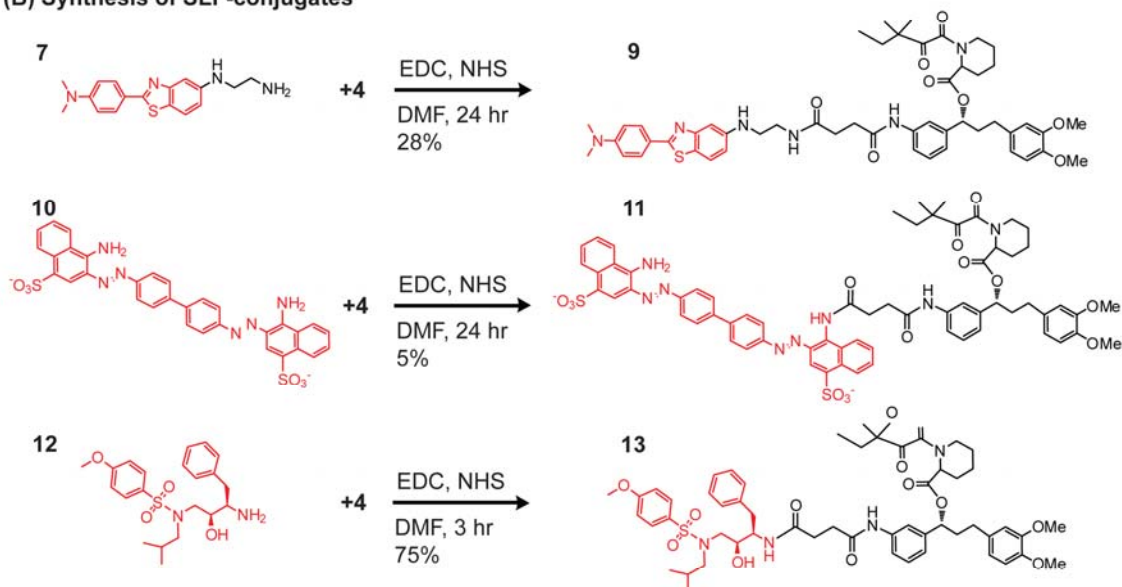


**Figure 2-3. Synthesis of Bifunctional Molecules.** (A) Reactive intermediate **2** was used to install FK506 into compounds **5** and **7** to generate the bifunctional derivatives **6** and **8**. (B) Modified SLF **4** was appended to the parent compounds **7**, **10**, and **12** to yield the bifunctional compounds **9**, **11**, and **13**.

**7**, **10** and **12**. Consistent with their varied chemical structures, the parent ligands had different intrinsic affinities for CYP3A4; for example, compounds **5** and **12** were good substrates, with  $K_i$  values less than 3  $\mu\text{M}$  (Table 2-1). As expected, none of the parent compounds were influenced by the addition of FKBP (Figure 2-4). Next, we explored the activity of the bifunctional derivatives. In the

**Table 2-1** Table of CYP3A4 Assay Results

Compound	$K_i/\mu\text{M}$		Fold protection vs. no FKBP <sup>a</sup>	Fold protection vs. parent <sup>b</sup>
	No FKBP	+FKBP		
<b>5</b>	0.7 ± 0.1	0.7 ± 0.3	1.0	
<b>6</b>	0.4 ± 0.2	1.4 ± 0.5	<b>3.5</b>	<b>2.0</b>
<b>7</b>	5.8 ± 1.2	5.1 ± 1.3	0.9	
<b>8</b>	5.0 ± 1.2	5.3 ± 0.8	1.1	1.0
<b>9</b>	0.9 ± 0.3	3.1 ± 0.6	<b>3.4</b>	<b>0.6</b>
<b>10</b>	4.3 ± 0.7	4.4 ± 0.7	1.0	
<b>11</b>	4.2 ± 1.0	6.2 ± 1.3	<b>1.5</b>	<b>1.4</b>
<b>12</b>	2.8 ± 0.4	2.8 ± 0.2	1.0	
<b>13</b>	2.3 ± 0.5	4.8 ± 0.9	<b>2.1</b>	<b>1.7</b>

<sup>a</sup>  $K_i$  (bifunctional + FKBP) /  $K_i$  (bifunctional, no FKBP).    <sup>b</sup>  $K_i$  (parent + FKBP) /  $K_i$  (bifunctional + FKBP).

absence of FKBP, we noticed that, compared to their parents, the bifunctional molecules were uniformly more susceptible to CYP3A4. For example, the  $K_i$  of bifunctional compound **6** was 0.4  $\mu\text{M}$ , compared to 0.7  $\mu\text{M}$  for its parent ligand, **5**. This result suggests that, not surprisingly, the larger, more complex bifunctional molecule provides additional opportunities for metabolism. However, the addition of FKBP provided resistance to a number of the bifunctional compounds. For example, FKBP improved the  $K_i$  of **6** to 1.4  $\mu\text{M}$ , which is 2-fold better than parent compound **5**, and 3.5-fold better than **6** in the absence of the binding protein. Similarly, compounds **11** and **13** were protected 1.4- and 1.7-fold over their parent ligands, respectively (Table 2-1). These results suggest that the installation of FKBP-binding groups can, in some cases, provide partial relief from binding to CYP3A4.



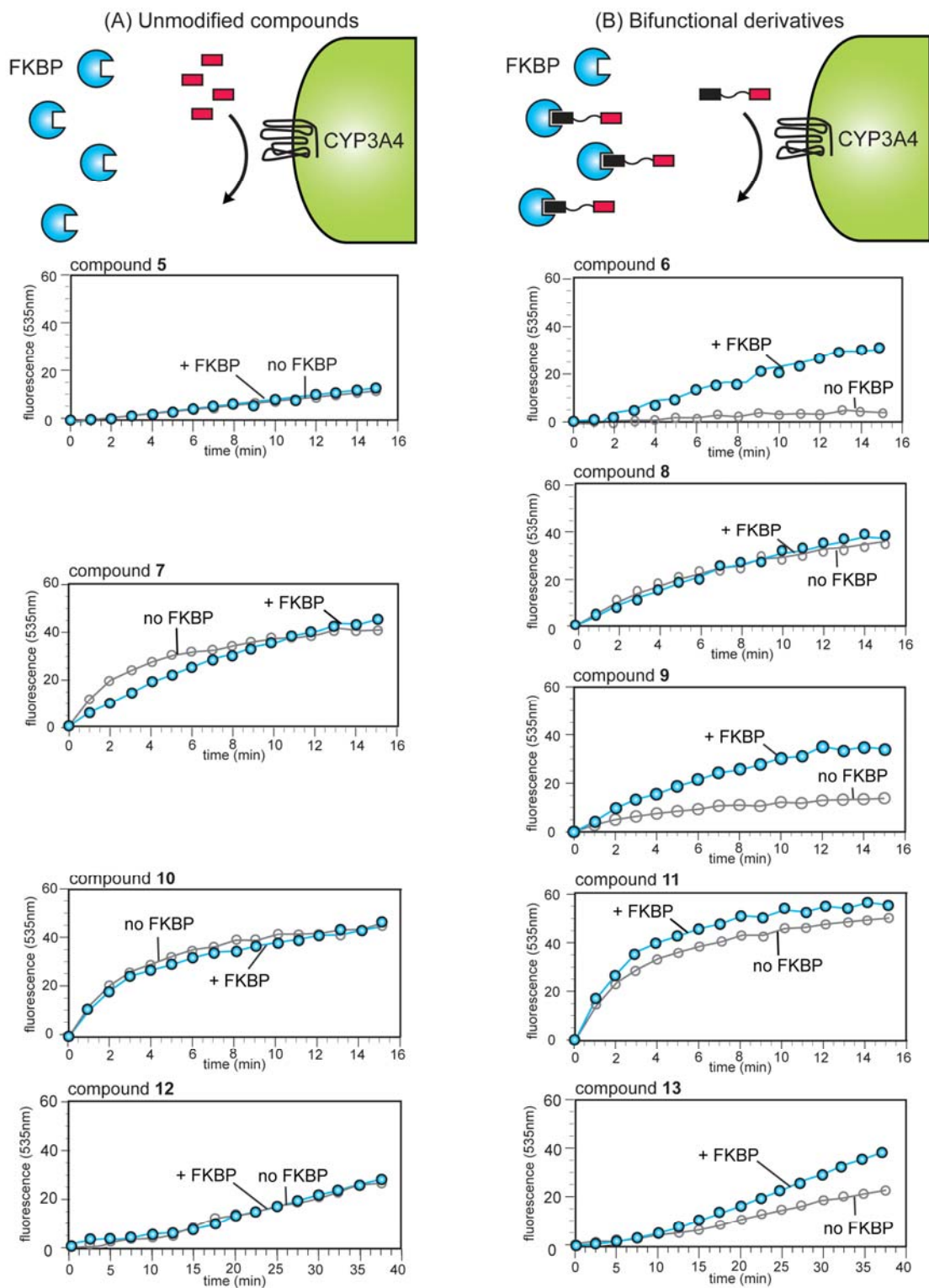


**Figure 2-4. Protection of Bifunctional Molecules by FKBP.** (A) CYP3A4 assay results for the unmodified parent compounds. FKBP was added to a final concentration of 1  $\mu$ M. Only single concentrations are shown as representative of the full 7-point concentration range. (B) CYP3A4 assay results for the bifunctional derivatives (see Table 2-1).

#### **2.2.4 Some Bifunctional Molecules are Membrane Permeable**

Many cells express high levels of FKBP, and in some systems it represents up to 1% of the total protein.<sup>13</sup> Thus, we considered the possibility that tight binding to this protein might lead bifunctional molecules to accumulate inside FKBP-rich cells. This binding might further shield the compounds from interactions with P450 enzymes, which are principally oriented to act upon extracellular targets. To test this idea, we first examined the membrane permeability of the compounds. In these experiments, the intrinsic fluorescence of the ligands was used to measure the uptake into COS cells, and as expected we found that highly charged molecules **10** and **11** were not permeable (Figure 2-5A). In contrast, incubating COS cells for 30 min with curcumin analogs **5** and **6** resulted in extensive intracellular fluorescence following washing. Interestingly, the benzothiazole, **7**, was not permeable, but appending SLF (compound **9**) permitted uptake, perhaps through improved hydrophobicity (cLogP increased from ~4 to 9).

#### **2.2.5 FKBP Alters the Partitioning of a Bifunctional Compound**

After establishing the permeability of compounds **5** and **6**, we wanted to explore whether these ligands might be preferentially localized into FKBP-rich compartments by their high-affinity interactions with this protein. To directly test this hypothesis, we filled one chamber of an equilibrium dialysis cassette with FKBP. A low mass filter (10,000 Da) was used to restrict the protein to a single compartment, and either **5** or **6** were added to the other side. After 24 hours, the

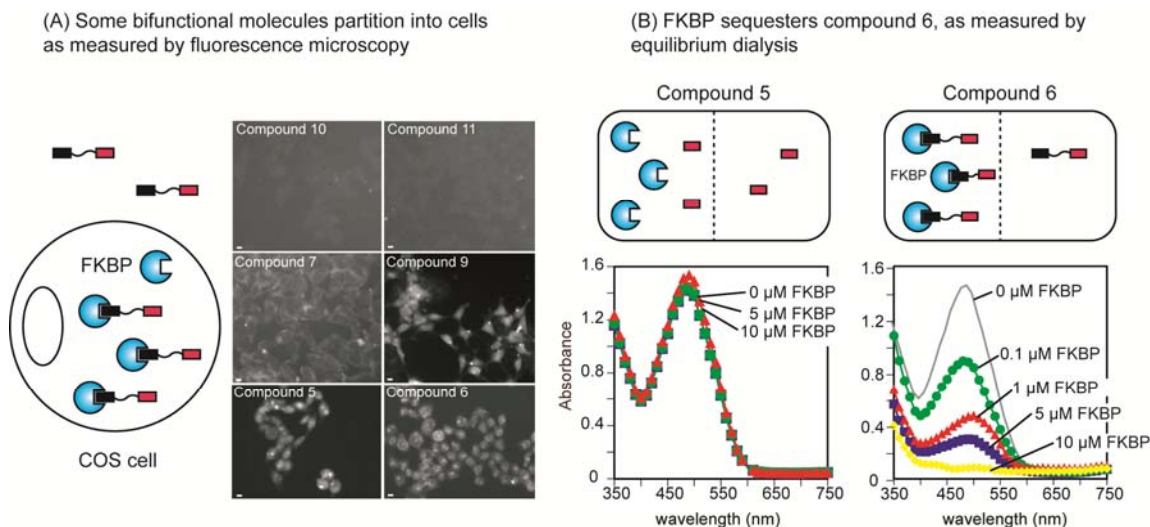


**Figure 2-5. Bifunctional Molecules Partition into FKBP-rich Compartments.** (A) Intrinsic fluorescence was used to monitor the uptake of bifunctional compounds and their parent ligands in COS cells. Cells were treated for 30 minutes with the compound, washed, and fixed with paraformaldehyde. The cellular load of compound was revealed by microscopy. Note that all compounds were visible at excitation 485 nm / emission of 535 nm. The scale bar is 2.5 micron. (B) Equilibrium dialysis was performed using 10 kDa pore size, such that compounds could freely distribute but FKBP was retained in one compartment. Results are representative of three independent experiments.

compound remaining in the protein-free compartment was quantified using a characteristic absorbance signature at ~500 nm. Using this approach, we found that FKBP significantly influenced the distribution of the bifunctional compound **6**, but not parent compound **5** (Figure 2-5B). These results demonstrate that FKBP can alter the partitioning of molecules across diffusion layers.

## 2.2.6 Cells Protect a Bifunctional Molecule

Because many cells are rich in FKBP, we hypothesized that they might also sequester bifunctional ligands (Figure 2-6B). Moreover, this interaction might provide resistance to metabolism, because the intracellular environment is largely inaccessible to P450 enzymes. To test this idea *in vitro*, we repeated the CYP3A4 assays using COS cells as a replacement for recombinant FKBP.

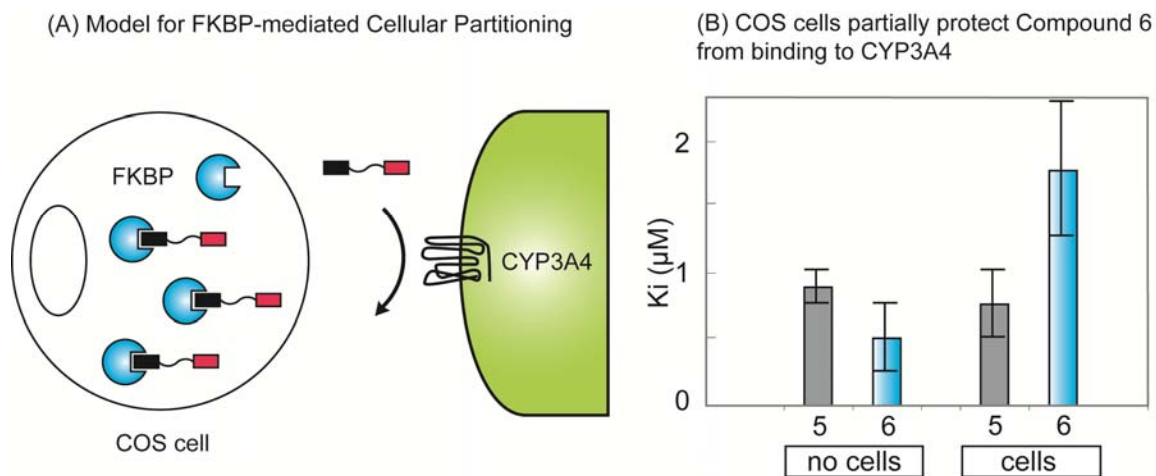


**Figure 2-6. COS Cells Protect Bifunctional Compound 6 from Metabolism by CYP3A4.** (A) Schematic depiction of the model, in which cellular FKBP retains the bifunctional molecule. (B) Addition of COS cells provides some relief from CYP3A4 metabolism. Results are the average of 3 experiments and error is the standard deviation.

Consistent with our model, compound **6** was partially protected in this system. The effect was modest ( $K_i$  improved approximately 2-fold) (Figure 2-6B), and we hypothesize that increasing the number of cells might improve protection; unfortunately, more cells seemed to disrupt liposome integrity (data not shown). Despite this technical limitation, these results provide preliminary evidence that the partitioning of bifunctional molecules into cells removes them from the pool that is accessible for modification.

## 2.3 Discussion

### 2.3.1 Binding to FKBP Augments the Pharmacology of FK506

Considering their size and complexity, rapamycin and FK506 have surprisingly long half-lives.<sup>2, 3, 5, 41</sup> To directly test whether this property might arise from their affinity for FKBP, we employed methods common in the

synthesis of CIDs to generate compounds that share this binding profile. Using *in vitro* CYP3A4 assays, we found that some of the bifunctional ligands are indeed less prone to metabolism when complexed with FKBP. Thus, these findings illustrate one possible mechanism, by which some large natural products might acquire better-than-expected pharmacological properties.<sup>42</sup> In bacteria, considerable energy is committed to the biosynthesis of secondary metabolites, and it is interesting to speculate that the size and complexity of certain macrolides may, counterintuitively, be a result of evolutionary pressure for improved stability. The inhibition of FKBP is not thought to contribute directly to the immunosuppressive activity of either rapamycin or FK506; rather, the other binding partner (mTOR or calcineurin) is the pharmacologically important target. Thus, the reason that these compounds bind FKBP hasn't been made entirely clear. We propose that the FKBP-binding half of the molecule might primarily contribute to favorable pharmacology. Therefore, counter to the common guidelines that dominate drug design, the desired selectivity and potency might have been produced by making the compound larger and more complex. Finally, we speculated that other natural products might access similarly interesting mechanisms, and that a deeper understanding of these pathways could aid efforts to synthesize drugs that truly mimic natural scaffolds.<sup>43</sup>

### **2.3.2 Synthetic Considerations for Bifunctional Molecules**

In this study, we found that certain FKBP-binding CIDs are protected from CYP3A4 *in vitro*. Although the exact molecular mechanism is not entirely clear,

one hypothesis is that repulsive interactions between the FKBP surface and the membrane-embedded P450 preclude entry to the active site. This theory resembles one previously reported as underlying the interesting binding properties of other CIDs.<sup>22</sup> Additionally, it is well known that binding to serum proteins, such as albumin, can greatly prolong drug lifetimes by reducing contact with metabolic enzymes.<sup>44</sup> For bifunctional molecules, the length of the linker is expected to be an especially important feature, because long, flexible linkers would place one end of the compound too far from the surface of FKBP to be shielded from P450. For example, compounds **8** and **9** are similar, except that the distance between the ThT-like group and the FKBP binding functionality is approximately 3.4 angstroms longer in **8**. Despite their similarities, compound **9** was protected 3.4-fold by FKBP, while the  $K_i$  of **8** was largely independent of FKBP (5.0 vs. 5.3  $\mu\text{M}$ ). This effect is probably not due to a difference between the affinities of SLF and FK506 for FKBP, because compound **6**, **11**, and **13** behave similarly, despite the identities of their FKBP-binding groups. Rather, we conclude that shorter linkers tend to limit enzyme accessibility, and thus these types of connections might be preferred in attempts to yield compounds with reduced binding to metabolic proteins. Of course, binding to the other target (e.g. amyloid and HIV protease, in the present case) must also be considered. Thus, there is likely to be a complex relationship between competing surface topologies that dominate the productive formation of ternary complexes.

### **2.3.3 Dual Mechanisms for Metabolic Protection**

Based on our preliminary findings, it seems possible that binding to FKBP may provide two levels of protection from metabolism: one being the involvement of direct shielding via steric exclusion and the other being partitioning away from extracellular pools of P450 enzymes. In this Chapter, we present evidence in support of a steric exclusion mechanism. In support of the second mechanism, we found that binding to FKBP sequesters compounds into FKBP-rich environments, and that FKBP-expressing cells can partly shield a CID from CYP3A4. This particular mechanism is studied in greater detail in Chapter 3.

### **2.3.4 Looking Forward**

Previous methods for generating drugs with enhanced pharmacological profiles include constructing prodrugs, installing polyethylene glycol chains, and formulating liposomes. The model we propose for rapamycin and FK506 is distinct from these strategies. Specifically, we propose that intracellular localization alters the environment of the compound and contributes to its stability. The generality of this mechanism and its applicability to other drug classes remain to be explored.

One class of compounds that may be particularly amenable to this strategy are HIV-1 antivirals. The majority of these inhibitors possess low metabolic stability due to their extensive metabolism by CYP3A4, the most prevalent form of the cytochrome P450 enzymes. Protease inhibitors in

particular exhibit poor pharmacokinetics as demonstrated by their short half-lives ranging from 1-6 hours. These apparent shortcomings in the current generation of antiretroviral therapeutics, however, open the door for cutting edge chemical intervention.

## 2.4 Experimental Procedures

### 2.4.1 Synthesis of Bifunctional Molecules

**(1*E*,6*E*)-4-(4-Aminophenyl)-1,7-bis(4-hydroxy-3-methoxyphenyl)hepta-1,6-diene-3,5-dione (5).** Compound **5** was generated by an adaptation of a published route.<sup>26</sup> Briefly, curcumin (Sigma; 150 mg; 0.407 mmol) and NaOH (Sigma; 112 mg; 0.6512 mmol) were added to 4-bromoaniline in ~5 mL of ethanol/NaOEt. After 1 hour at room temperature, the product was poured over crushed ice and extracted with EtOAc (3 X 20 mL). The organic phase was concentrated in vacuo and purified by flash chromatography (DCM : MeOH) to yield a bright yellow solid product (22% yield).  $m/z = 460.5$  [M + H] (calc. 460.49).

**N<sup>1</sup>-(2-(4-(Dimethylamino) phenyl) benzothiazol-5-yl) butane-1,4-diamine (7).** Compound **7** was generated from 2-chlorobenzothiazole (100 mg)<sup>27</sup> using Buchwald's catalyst (1%) and mono-N-Boc-protected ethylenediamine (Sigma; 1.2 equiv.), similar to previous reports.<sup>28</sup> The product was extracted from the aqueous layer, deprotected in 50% TFA : DCM, and the pale yellow solid purified on silica gel (1 : 1 hexanes : ethyl acetate; 62% yield,



3 steps).  $m/z = 341.5$  [M + H] (calc. 341.49).

**N-((2S,3R)-3-Amino-2-hydroxy-4-phenylbutyl)-N-isobutyl-4-nitrobenzene-sulfonamide (12).** Compound **12** was generated by an established route. <sup>29</sup>  $m/z = 422.6$  [M + H] (calc. 422.51).

Coupling the FKBP-binding group, **3** or **4**, to the appropriate amine-bearing parent ligand generated the bifunctional derivatives **5**, **7**, **10** or **12**. These reactions were carried out on a small scale (20–50 mg) in dry DMF at room temperature (see Figure 2-3). For the reactions involving intermediate **3**, triethylamine (Sigma) was added at ~1%. For the amide couplings with intermediate **4**, 1-ethyl-3-(3-dimethylaminopropyl) carbodiimide hydrochloride (EDC; 5 equiv.) and N-hydroxysuccinimide (NHS; 5 equiv.) were used. In some reactions, 4-dimethylaminopyridine (DMAP; 0.1 equiv.) was also added. The products were separated by silica gel chromatography (2 : 1 ethyl acetate : MeOH for **6** and **11**; ethyl acetate for **8**, **9** and **13**). Each was isolated as a single, UV-active spot by TLC, except for compound **11**, which was only ~75% pure (the major contaminant was unreacted starting material **10**). The remainder of the products were >90% pure, as crudely estimated by HPLC. The products were primarily characterized by ESI mass spectrometry because of their low overall yields and complex <sup>1</sup>H NMR spectra: compound (**6**)  $m/z = 1316.5$  [M + Na] (calc. 1316.49); compound (**8**)  $m/z = 1174.2$  [M + H] (calc. 1174.19); compound (**9**)  $m/z = 906.2$  [M + H] (calc. 906.11); compound (**11**)  $m/z = 1301.0$  [M + 2Na]

(calc. 1300.44); compound (**13**)  $m/z = 1052.2$  [M + Na] (calc. 1052.22). The products were stored as solids and dissolved in DMSO (to 100 mM) prior to use in biological assays. Compounds **5**, **6** and **11** were unstable after prolonged (>12 months) storage in DMSO at -80°C.

#### **2.4.2 CYP3A4 Metabolism Assays**

The CYP3A4 VIVID assay was purchased from Invitrogen and used according to the manufacturer's specifications. A fluorescent standard was used to convert the fluorescence signal to the initial velocity ( $V_i$ ), and the inhibitory constant ( $K_i$ ) was generated using published equations.<sup>30</sup> FKBP (from a 25 mM stock in 10 mM Tris-HCl, 100 mM NaCl, pH 7.0) was pre-mixed with the query compound, such that the final concentration was 1  $\mu$ M. This concentration is likely to be similar to (or less than) the physiological concentration in the cytosol.<sup>13</sup> COS cells were maintained in RPMI without phenol red at 37°C and 5% CO<sub>2</sub>, counted using a hemocytometer and washed 3 times with cold PBS prior to being added to the assay. FKBP at up to 10  $\mu$ M had no effect on the conversion of the substrate in the absence of competitors (not shown). In contrast, COS cells slowed the kinetics of the reaction and, at higher concentrations, disrupted the signal. In control experiments, we found that 1,500 cells provided optimal protection with minimal disruption.

#### **2.4.3 Fluorescence Assay for Cellular Uptake**

COS cells were grown in tissue culture-treated 12-well plates containing a

single poly-L-lysine-coated cover slip. At ~70% confluency, the cells were washed 3 times with PBS to remove the RPMI media, and then treated with 10  $\mu$ M of compound in PBS for 30 min in the dark. The compound-treated media was removed, and the cells were washed once with fresh PBS, before being fixed with 4% paraformaldehyde for 30 min at 4°C. After two additional PBS washing steps, the cover slips were mounted on slides treated with Vectashield. Ten random fields were collected on a Zeiss fluorescence microscope using the GFP filter ( $E_{\text{excitation}} = 485$  /  $E_{\text{emission}} = 535$  nm). Compounds **7**, **8**, **9**, **10** and **11** exhibited fluorescence (with identical patterns and variable intensities) in multiple filter sets, precluding the use of DAPI stain.

#### **2.4.4 Equilibrium Dialysis**

Harvard Apparatus DispoEquilibrium dialyzers (10 kDa MWCO; 50 mL volume) were used according to manufacturer's specifications. The absorbance of compounds **5** and **6** (10  $\mu$ M) were measured from the protein-free chamber after 24 h of equilibration at 4°C with gentle agitation. All experiments were performed in 50 mM Tris, 100 mM NaCl, pH 7.0, less than 1% final DMSO concentration.

## Notes

Portions of this work have been published as “Bifunctional Molecules Evade Cytochrome P450 Metabolism by Forming Protective Complexes with FK506-Binding Protein,” Marinec, P. S., Lancia, J. K., and Gestwicki, J. E., *Molecular Biosystems*, 2008, 4: 571-578.

P. S. Marinec and J. E. Gestwicki designed the experiments and prepared the manuscript. P. S. Marinec and J. E. Gestwicki performed the synthetic work, equilibrium dialysis and CYP3A4 assays. P. S. Marinec performed the computational simulations. J. K. Lancia performed the experiments with cells.

## 2.5 References

1. Lipinski, C.A.; Lombardo, F.; Dominy, B.W.; Feeney, P.J. Experimental and computational approaches to estimate solubility and permeability in drug discovery and development settings. *Adv. Drug Delivery Rev.*, **2001**, 46, 3.
2. Trepanier, D.J.; Gallant, H.; Legatt, D.F.; Yatscoff, R.W. Rapamycin: distribution, pharmacokinetics and therapeutic range investigations: an update. *Clin. Biochem.*, **1998**, 31, 345.
3. Zimmerman, J.J.; Kahan, B.D. Pharmacokinetics of sirolimus in stable renal transplant patients after multiple oral dose administration. *J. Clin. Pharmacol.*, **1997**, 37, 405.
4. Yatscoff, R.W. Pharmacokinetics of rapamycin. *Transplant Proc.*, **1996**, 28, 970.
5. Takahara, S. Efficacy of FK506 in renal transplantation. *Ann. N. Y. Acad. Sci.*, **1993**, 696, 235.
6. Levin, A.D.; Vukmirovic, N.; Hwang, C.W.; Edelman, E.R. Specific binding to intracellular proteins determines arterial transport properties for rapamycin and paclitaxel. *Proc. Natl. Acad. Sci. U.S.A.*, **2004**, 101, 9463.
7. Chen, J.; Zheng, X.F.; Brown, E.J.; Schreiber, S.L. Identification of an 11-kDa FKBP12-rapamycin-binding domain within the 289-kDa FKBP12-rapamycin-associated protein and characterization of a critical serine residue. *Proc. Natl. Acad. Sci. USA*, **1995**, 92, 4947.
8. Harding, M.W.; Galat, A.; Uehling, D.E.; Schreiber, S.L. A receptor for the immunosuppressant FK506 is a cis-trans peptidyl-prolyl isomerase. *Nature*, **1989**, 341, 758.
9. Siekierka, J.J.; Hung, S.H.; Poe, M.; Lin, C.S.; Sigal, N.H. A cytosolic binding protein for the immunosuppressant FK506 has peptidyl-prolyl isomerase activity but is distinct from cyclophilin. *Nature*, **1989**, 341, 755.
10. Ho, S.; Clipstone, N.; Timmermann, L.; Northrop, J.; Graef, I.; Fiorentino, D.; Nourse, J.; and Crabtree, G.R. The mechanism of action of cyclosporin A and FK506. *Clin. Immun. Immunopathol.*, **1996**, 80, S40.
11. Liu, J.; Albers, M.W.; Wandless, T.J.; Luan, S.; Alberg, D.G.; Belshaw, P.J.; Cohen, P.; MacKintosh, C.; Klee, C.B.; and Schreiber, S.L. Inhibition of T cell signaling by immunophilin-ligand complexes correlates with loss of calcineurin phosphatase activity. *Biochemistry*, **1992**, 31, 3896.

12. Griffith, J.P.; Kim, J.L.; Kim, E.E.; Sintchak, M.D.; Thomson, J.A.; Fitzgibbon, M.J.; Fleming, M.A.; Caron, P.R.; Hsiao, K.; Navia, M.A. X-ray structure of calcineurin inhibited by the immunophilin-immunosuppressant FKBP12-FK506 complex. *Cell*, **1995**, 82, 507.
13. Galat, A. Peptidylprolyl cis/trans isomerases (immunophilins): biological diversity--targets--functions. *Curr. Top. Med. Chem.*, **2003**, 3, 1315.
14. Spencer, D.M.; Wandless, T.J.; Schreiber, S.L.; Crabtree, G.R. Controlling signal transduction with synthetic ligands. *Science*, **1993**, 262, 1019.
15. Crabtree, G.R.; Schreiber, S.L. Three-part inventions: intracellular signaling and induced proximity. *Trends Biochem. Sci.*, **1996**, 21, 418.
16. Banaszynski, L.A.; Wandless, T.J. Conditional control of protein function. *Chem. Biol.*, **2006**, 13, 11.
17. Gestwicki, J.E.; Marinec, P.S. Chemical control over protein-protein interactions: beyond inhibitors. *Comb. Chem. High Throughput Screening*, **2007**, 10, 667.
18. Clackson, T. Controlling Protein-Protein Interactions Using Chemical Inducers and Disrupters of Dimerization, in *Chemical Biology: From Small Molecules to Systems Biology and Drug Design*, ed. S. L. Schreiber, T. M. Kapoor and G. Weiss, Wiley-VCH Verlag GmbH & Co., Weinheim, **2007**, 3, 227.
19. Gestwicki, J.E.; Crabtree, G.R.; Graef, I.A. Harnessing chaperones to generate small-molecule inhibitors of amyloid beta aggregation. *Science*, **2004**, 306, 865.
20. Amara, J.F.; Clackson, T.; Rivera, V.M.; Guo, T.; Keenan, T.; Natesan, S.; Pollock, R.; Yang, W.; Courage, N.L.; Holt, D.A.; Gilman, M. A versatile synthetic dimerizer for the regulation of protein-protein interactions. *Proc. Natl. Acad. Sci. USA*, **1997**, 94, 10618.
21. Abida, W.M.; Carter, B.T.; Althoff, E.A.; Lin, H.; Cornish, V.W. Receptor-dependence of the transcription read-out in a small-molecule three-hybrid system. *Chembiochem.*, **2002**, 3, 887.
22. Briesewitz, R.; Ray, G.T.; Wandless, T.J.; Crabtree, G.R. Affinity modulation of small-molecule ligands by borrowing endogenous protein surfaces. *Proc. Natl. Acad. Sci. USA*, **1999**, 96, 1953.

23. Braun, P.D.; Barglow, K.T.; Lin, Y.M.; Akompong, T.; Briesewitz, R.; Ray, G.T., Haldar, K.; Wandless, T.J. A bifunctional molecule that displays context-dependent cellular activity. *J. Am. Chem. Soc.*, **2003**, 125, 7575
24. Sellmyer, M.A.; Stankunas, K.; Briesewitz, R.; Crabtree G.R.; Wandless, T. J. Engineering small molecule specificity in nearly identical cellular environments. *Bioorg. Med. Chem. Lett.*, **2007**, 17, 2703.
25. Stankunas, K.; Bayle, J.H.; Havranek, J.J.; Wandless, T.J.; Baker, D.; Crabtree, G.R.; Gestwicki, J.E. Rescue of degradation-prone mutants of the FK506-rapamycin binding (FRB) protein with chemical ligands. *Chembiochem.*, **2007**, 8, 1162.
26. Kumar, S.; Narain, U.; Tripathi, S.; Misra, K. Syntheses of Curcumin Bioconjugates and Study of Their Antibacterial Activities against beta-Lactamase-Producing Microorganisms. *Bioconjugate Chem.*, **2001**, 12, 464.
27. Mathis, C.A.; Bacskai, B.J.; Kajdasz, S.T.; McLellan, M.E.; Frosch, M.P.; Hyman, B.T.; Holt, D.P.; Wang, Y.; Huang, G.F.; Debnath M.L.; Klunk, W.E. A lipophilic thioflavin-T derivative for positron emission tomography (PET) imaging of amyloid in brain. *Bioorg. Med. Chem. Lett.*, **2002**, 12, 295.
28. Hoffman-La Roche, AG; Flohr, A.; Jakob-Roetne, R.; Norcross, R.D.; Riemer, C. 2-Imidazo-Benzothiazoles as Adenosine Receptor Ligands. *World Pat.*, **2004**, WO/2004/101558, 2004.
29. Yeung, C. M.; Klein, L.L.; Flentge, C.A.; Randolph, J.T.; Zhao, C.; Sun, M.; Dekhtyar, T.; Stoll, V.S.; Kempf, D.J. Oximinoarylsulfonamides as potent HIV protease inhibitors. *Bioorg. Med. Chem. Lett.*, **2005**, 15, 2275.
30. Kuzmic, P.; Sideris, S.; Cregar, L.M.; Elrod, K.C.; Rice, K.D.; Janc, J.W. High-throughput screening of enzyme inhibitors: automatic determination of tight-binding inhibition constants. *Anal. Biochem.*, **2000**, 281, 62.
31. Sattler, M.; Guengerich, F.P.; Yun, C.H.; Christians, U.; Sewing, K.F. Cytochrome P-450 3A enzymes are responsible for biotransformation of FK506 and rapamycin in man and rat. *Drug Metab. Dispos.*, **1992**, 20, 753.
32. Clackson, T.; Yang, W.; Rozamus, L.W.; Hatada, M.; Amara, J.F.; Rollins, C.T.; Stevenson, L.F.; Magari, S.R.; Wood, S.A.; Courage, N.L.; Lu, X.; Cerasoli, F. Jr.; Gilman, M.; Holt, D.A. Redesigning an FKBP-ligand interface to generate chemical dimerizers with novel specificity. *Proc. Natl. Acad. Sci. USA*, **1998**, 95, 10437.

33. Lee, V.M. Amyloid binding ligands as Alzheimer's disease therapies. *Neurobiol. Aging*, **2002**, 23, 1039.
34. Ye, L.; Morgenstern, J.L.; Gee, A.D.; Hong, G.; Brown, J.; Lockhart, A. Delineation of positron emission tomography imaging agent binding sites on beta-amyloid peptide fibrils. *J. Biol. Chem.*, **2005**, 280, 23599.
35. Bacskai, B.J.; Klunk, W.E.; Mathis, C.A.; Hyman, B.T. Imaging amyloid-beta deposits in vivo. *J. Cereb. Blood Flow Metab.*, **2002**, 22, 1035.
36. Klunk, W.E.; Debnath, M.L.; Pettegrew, J.W. Development of small molecule probes for the beta-amyloid protein of Alzheimer's disease. *Neurobiol. Aging*, **1994**, 15, 691.
37. Bose, M.; Gestwicki, J.E.; Devasthali, V.; Crabtree, G.R.; Graef, I.A. 'Nature-inspired' drug-protein complexes as inhibitors of A $\beta$  aggregation. *Biochem. Soc. Trans.*, **2005**, 33, 543.
38. Reinke, A.A.; Gestwicki, J.E. Structure-activity relationships of amyloid beta-aggregation inhibitors based on curcumin: influence of linker length and flexibility. *Chem. Biol. Drug Des.*, **2007**, 70, 206.
39. Kim, E.E.; Baker, C.T.; Dwyer, M.D.; Murcko, M.A.; Rao, B.G.; Tung, R.D.; Navia, M.A. Crystal structure of HIV-1 protease in complex with VX-478, a potent and orally bioavailable inhibitor of the enzyme. *J. Am. Chem. Soc.*, **1995**, 117, 1181.
40. Turner, S.R. HIV Protease Inhibitors – The Next Generation. *Curr. Med. Chem.: Anti Infect. Agents*, **2002**, 1, 141.
41. Yatscoff, R.W.; Wang, P.; Chan, K.; Hicks, D.; Zimmerman, J. Rapamycin: distribution, pharmacokinetics, and therapeutic range investigations. *Ther. Drug Monit.*, **1995**, 17, 666.
42. Butler, M.S. Natural products to drugs: natural product derived compounds in clinical trials. *Nat. Prod. Rep.*, **2005**, 22, 162.
43. Schreiber, S.L. Target-oriented and diversity-oriented organic synthesis in drug discovery. *Science*, **2000**, 287, 1964.
44. Thibaudeau, K.; Leger, R.; Huang, X.; Robitaille, M.; Quraishi, O.; Soucy, C.; Bousquet-Gagnon, N.; van Wyk, P.; Paradis, V.; Castaigne, J.P.; Bridon, D. Synthesis and evaluation of insulin-human serum albumin conjugates. *Bioconjugate Chem.*, **2005**, 16, 1000.



45. Kazmierski, W.M.; Bevans, P.; Furfine, E.; Spaltenstein, A.; Yang, H. Novel prodrug approach to amprenavir-based HIV-1 protease inhibitors via O-->N acyloxy migration of P1 moiety. *Bioorg. Med. Chem. Lett.*, **2003**, 13, 2523.
46. Desormeaux A.; Bergeron, M.G. Lymphoid tissue targeting of anti-HIV drugs using liposomes. *Methods Enzymol.*, **2005**, 391, 330.
47. Molineux, G. Pegylation: engineering improved biopharmaceuticals for oncology. *Pharmacotherapy*, **2003**, 23, 3S.
48. Greenwald, R.B.; Choe, Y.H.; McGuire, J.; Conover, C.D.; Effective drug delivery by PEGylated drug conjugates. *Adv. Drug Delivery Rev.*, **2003**, 55, 217.

## Chapter III

### **FKBP Partitions a Modified HIV Protease Inhibitor into Blood Cells and Prolongs its Lifetime *in vivo***

#### **3.1 Abstract**

HIV protease inhibitors are a key component of antiretroviral therapy, but their susceptibility to cytochrome P450 metabolism reduces their systemic availability and necessitates repetitive dosing. Importantly, failure to maintain adequate inhibitor levels is believed to provide an opportunity for resistance to emerge; thus, new strategies to prolong the lifetimes of these drugs are needed. Towards this goal, numerous prodrug approaches have been developed, but these methods all involve creating inactive precursors that require enzymatic processing. Using an alternative strategy inspired by the natural product FK506, we synthetically modified an HIV protease inhibitor such that it acquires high affinity for the abundant, cytoplasmic chaperone FKBP. This bifunctional protease inhibitor maintains nanomolar activity against HIV-1 protease ( $IC_{50} = 19$  nM), and additionally, is partitioned into the cellular component of whole blood via binding to FKBP. Interestingly, redistribution into this protected niche reduces metabolism and improves its half-life in mice by >20-fold compared to the unmodified parent compound. Based on these findings, we propose that addition of FKBP-binding groups might partially overcome the poor pharmacokinetic

properties of existing HIV protease inhibitors and, potentially, other drug classes.

### **3.1.1 The Human Immunodeficiency Virus**

The human immunodeficiency virus (HIV) is a lentivirus of the *Retroviridae* family, and is the etiological agent in developing the acquired immunodeficiency syndrome (AIDS).<sup>1</sup> The virus is roughly spherical, with an average diameter of approximately 145 nm.<sup>2</sup> The outer surface of HIV is composed of a phospholipid bilayer derived from the membrane of an infected host cell and is studded along its surface with gp120 and gp41, envelope glycoproteins mediating viral entry into target cells.<sup>3</sup> A matrix, constructed of the viral p17 protein, lines the inner surface of the HIV membrane and surrounds a cone-shaped core that encapsulates duplicate copies of positive single-stranded viral RNA as well as several virally encoded enzymes essential for replication and subsequent infection.<sup>4</sup>

### **3.1.2. The Protein-Protein Interactions Mediating HIV Infection**

HIV-1 infection is characterized by the progressive depletion of CD4+ T cells with a parallel decrease in cytokine signaling.<sup>5</sup> These combined losses lead to the opportunistic infections and cancers associated with AIDS-immunocompromised individuals. A series of protein-protein interactions are critical to successful HIV propagation, and therefore, provide multiple opportunities for therapeutic intervention.

The initial step in the HIV infectious process begins with binding of the viral gp120 envelope protein to CD4 receptors on the host cell surface. This event triggers a conformational change in the trimeric gp120, stabilizing an architecture that facilitates interaction with the cellular CCR5 or CXCR4 chemokine coreceptors.<sup>6</sup> Binding of these coreceptors induces further conformational changes in the viral spike, uncovering the gp41 glycoprotein buried deep within the envelope and positioning it in close proximity to the cell membrane. While the CD4 and chemokine coreceptors act as molecular anchors, the fusogenic gp41 is inserted into the host creating a gp41 six-helix bundle between the viral and cellular membranes.<sup>7,8</sup> The formation of this molecular channel is essential for fusion and allows for the unobstructed injection of the viral capsid core into the target cell.

Following fusion with the host cell membrane, the viral capsid is uncoated and reverse transcriptase (RT) converts the single-stranded viral RNA into a double-stranded DNA copy of the HIV genome. This, together with matrix, integrase, Vpr and other host proteins, forms the viral preintegration complex that is subsequently transported inside of the nucleus.<sup>9</sup> Here, the viral DNA is integrated into the host chromosome via the catalytic activity of the viral integrase (IN) enzyme.<sup>10</sup> After integration, the host cell initiates transcription of the proviral DNA leading to the synthesis of multiply-spliced mRNA transcripts encoding the Tat, Rev, and Nef regulatory proteins as well as full-length viral RNA.<sup>11</sup> Translation of the unspliced RNA produces the Gag and Gag-Pol polyproteins

and the Env glycoprotein precursor, gp160.<sup>12</sup> These proteins, together with duplicate copies of viral RNA, are then transported to the plasma membrane where the immature virus particles are released from the cell by budding.<sup>13</sup> Cleavage of the Gag and Gag-Pol polyproteins by HIV protease (PR) during viral release generates mature virions capable of infection.

### **3.1.3 Current State of HIV-1 Therapeutics**

Since its introduction over a decade ago, highly aggressive antiretroviral therapy (HAART) has proven to be effective at reducing viral loads and decreasing the morbidity and mortality associated with HIV-1 infection. However, despite the clinical improvements seen with this combination therapy, a residual level of viral replication continues in patients infected with HIV. Factors contributing to this persistence may include the existence of protected cellular reservoirs of the virus, adverse drug-drug interactions, poor adherence to antiviral regimens, and importantly, the rapid emergence of multidrug resistance.<sup>14-16</sup> To combat this propensity for HIV to select resistant variants, maintaining inhibitor concentrations above critical thresholds is vitally important. However, the physiochemical properties of current antiretrovirals make this a challenging task. For example, all ten of the FDA-approved inhibitors of HIV-1 protease are good substrates for cytochrome P450 enzymes, especially CYP3A4, and undergo extensive first-pass hepatic metabolism leading to their rapid clearance.<sup>17</sup> These properties necessitate the co-administration of P450 inhibitors, such as Ritonavir; however, this treatment often exacerbates side

effects and leads to liver toxicity.<sup>18</sup> Thus, there is a burgeoning need for new methods to improve the pharmacology of antiviral therapies.

#### **3.1.4 Prodrug Approaches to Antivirals**

A number of prodrug strategies have been evaluated in an attempt to improve existing HIV protease inhibitors.<sup>19</sup> For example, several groups have conjugated these molecules to amino acids and other nutrients to permit carrier-mediated absorption.<sup>20-22</sup> Others have altered their distribution and persistence via covalent attachment of lipophilic groups,<sup>23</sup> phosphates,<sup>24</sup> polyethylene glycol,<sup>25</sup> or other modifications.<sup>26</sup> In general, these strategies are intended to augment transepithelial delivery into systemic circulation and reduce binding to metabolic enzymes, with the hopes of improving the antiviral's absorption, distribution, metabolism, and excretion (ADME) profile. In all cases, the modified drugs require enzymatic processing to release the active compound because the protected, prodrug form has minimal activity.

#### **3.1.5 Our “Nature-Inspired” Strategy**

As introduced in Chapter 1 and discussed in Chapter 2, our group has been exploring a conceptually different approach to enhancing drug lifetimes that is inspired by the natural product FK506. This compound is a potent immunosuppressive that forms a high-affinity complex with FK506-binding protein (FKBP).<sup>27</sup> Once bound to FKBP, FK506 engages in a ternary interaction with calcineurin through a non-overlapping chemical domain.<sup>28-30</sup> Thus, FK506 is

a bifunctional molecule; it simultaneously binds two distinct proteins. In order to engage in both these interactions, the chemical structure of FK506 is quite large (molecular weight = 804) and rich in functional groups (>10 H-bond donors/acceptors). This complexity would be expected to adversely affect its pharmacological properties and, indeed, FK506 is an excellent substrate for CYP3A4 *in vitro*.<sup>31, 32</sup> Despite these apparently suboptimal features, FK506 is used clinically and it has a surprisingly long half-life (~40 hours). Because of the unexpected persistence of FK506, we became interested in understanding the mechanism by which it avoids metabolism. One potential insight comes from the observation that administration of FK506 results in specific accumulation within the cellular component of whole blood, which is a rich source of FKBP-expressing cells.<sup>33-35</sup> In particular, leukocytes and erythrocytes express high levels of FKBP<sup>35</sup> and low levels of CYP3A4.<sup>36</sup> Therefore, we hypothesized that accumulation of FK506 within these cells might limit exposure to key metabolic enzymes. As illustrated in Chapter 2, we discovered that tethering FKBP-binding groups to otherwise unrelated small molecules reduces their affinity for microsome-immobilized CYP3A4 by up to 3.5-fold when co-administered with purified FKBP or FKBP-expressing cells *in vitro*.<sup>37</sup>

Encouraged by these *in vitro* findings, we wanted to explore whether the *in vivo* lifetime of an HIV protease inhibitor could be modified by installation of an FKBP-binding group. In this model, appending the FKBP-binding portion of FK506 to a known HIV protease inhibitor might be expected to impart some of

the favorable cellular partitioning and longer lifetimes of the natural product. To test this concept, we synthesized a bifunctional derivative of the FDA-approved protease inhibitor Amprenavir. Strikingly, we found that this compound is selectively partitioned into FKBP-expressing blood cells which prolonged its lifetime by >20-fold *in vivo*. Moreover, in a cell-based HIV infectivity model, the antiviral activity of the SLF-modified protease inhibitor was improved >80-fold. Because of the modular synthesis employed, we anticipate that this nature-inspired, prodrug approach might have broad application.

## 3.2 Results

### 3.2.1 Design and Synthesis of a Bifunctional Protease Inhibitor, SLFavir

As discussed above and in Chapter 2, we hypothesized that binding to FKBP might alter the distribution and persistence of existing HIV protease inhibitors. To test this idea, we targeted a derivative of Amprenavir (**4**; 4-methoxy Amprenavir)<sup>38, 39</sup> for modification. Previous structure-activity relationships have demonstrated that chemical diversity may be introduced on the pseudo-amine terminus of Amprenavir without any adverse effects on antiviral activity.<sup>39</sup> Therefore, we reasoned that this core might be coupled to an FKBP ligand at this site without impairing its anti-HIV protease function. To generate these compounds, we followed a precedented route<sup>39</sup> from the known chiral alcohol, **1**, to the key intermediate **3** (Figure 3-1). From this shared core, we either completed the 4-methoxy Amprenavir scaffold, **4**, by installation of hydroxytetrahydrofuran or reacted the amine with succinic anhydride to provide



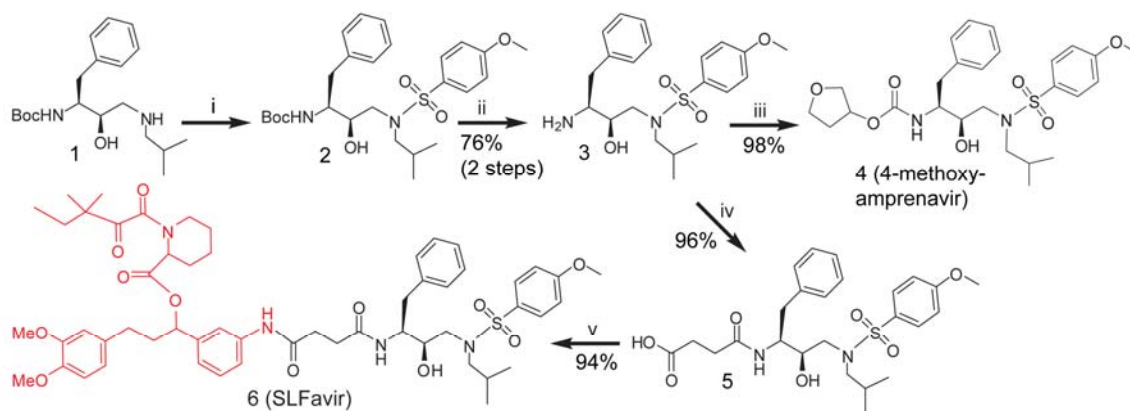


**Figure 3-1. Synthesis of a Bifunctional HIV Protease Inhibitor.** The synthesis of the control inhibitor, 4-methoxy amprenavir, and the bifunctional derivative, SLFavir, are shown. The SLF portion is shown in red. Reagents and conditions: (i) 4-methoxybenzenesulfonyl chloride,  $\text{Et}_3\text{N}$ , DCM (ii) 1:1 TFA:DCM (iii) 2,5-dioxopyrrolidin-1-yl tetrahydrofuran-3-yl carbonate,  $\text{Et}_3\text{N}$ , DCM (iv) succinic anhydride, DCM (v) SLF, DIC, DMAP, DMF.

intermediate **5**. Carbodiimide-mediated coupling of **5** with an FKBP-binding group yielded the bifunctional compound **6**. In this reaction, we took advantage of a well-known, synthetic ligand for FKBP (SLF) that has high affinity for FKBP ( $K_d \sim 10 \text{ nM}$ )<sup>40</sup> but does not interface with calcineurin; thus, installing this group provides tight binding to FKBP without concurrent anti-calcineurin activity.<sup>41-43</sup> We refer to the bifunctional inhibitor as SLFavir because it incorporates chemical domains from both SLF and Amprenavir. These transformations proceeded in good yields and, following HPLC, both the parent compound and SLFavir were obtained in excellent purity (>90%).

### 3.2.2 SLFavir Retains Anti-HIV-1 Protease Activity *in vitro*

To evaluate the potency of compounds **4-6**, we utilized a FRET-based assay in which inhibition of HIV-1 protease is quantified by the ability of a

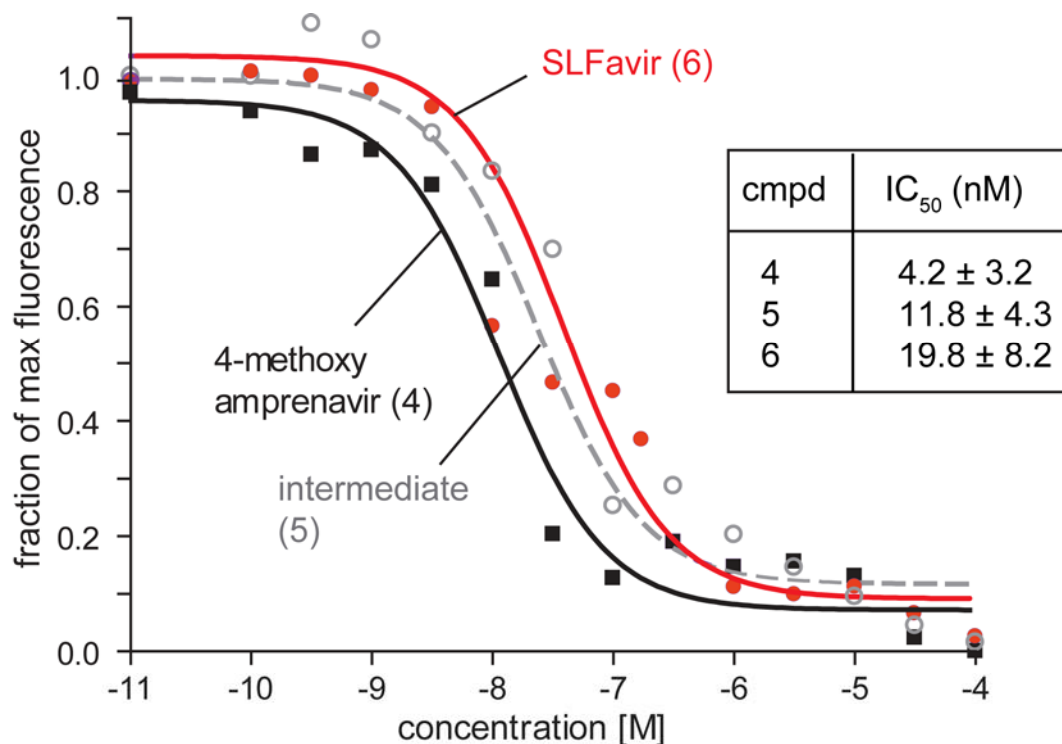


**Figure 3-2. Functional Analysis of SLFavir.** Results of a FRET-based HIV protease assay and the IC<sub>50</sub> values are shown. Compounds 4, 5 and 6 had measurable anti-HIV protease activity. Results are representative of experiments performed in triplicate and the error is standard deviation.

candidate molecule to block cleavage of a quenched fluorescent substrate. Using this approach, we found that the unmodified parent compound, **4**, had an IC<sub>50</sub> of 4.2 nM (Figure 3-2), which agrees with the range of reported values for structurally similar inhibitors.<sup>39, 44</sup> Chemically coupling the SLF moiety resulted in a nominal decrease in potency, with the IC<sub>50</sub> value of SLFavir remaining in the nanomolar range (19.8 nM).

To explore the origins of this modestly diminished activity, we examined the precursor, **5**. This molecule lacks the tetrahydrofuran and, consistent with a role

for this group, compound **5** also had a slightly decreased potency ( $IC_{50} = 11.8$  nM). These results parallel known structure-activity relationships<sup>39</sup> and suggest that replacing the tetrahydrofuran with a short, flexible methylene linker attached to SLF does not drastically alter potency.

### **3.2.3 Binding of SLFavir to Purified FKBP does not Block its Anti-Protease Activity *in vitro***

After confirming that SLFavir maintains anti-protease activity, we wanted to investigate whether binding to FKBP would impact this activity *in vitro*. In some systems, SLF conjugates have been found to bind both protein partners without a loss in affinity for either target,<sup>45</sup> while in other examples, ternary binding is hindered by FKBP.<sup>46</sup> These differences likely arise from variation in the spatial constraints imposed by different protein surfaces and the relative depth of the binding pockets. To empirically test this parameter for SLFavir, we premixed **6** (30 nM) with purified FKBP12 (1  $\mu$ M). Under these conditions, FKBP did not block anti-HIV protease activity (Figure 3-3). This is a key finding as it suggests that SLFavir can bind to FKBP without interrupting its association with the protease.

### **3.2.4 SLFavir is Preferentially Localized within the Cellular Component of Whole Blood *ex vivo***

Because FKBP is abundantly expressed in the cytosol of erythrocytes and leukocytes,<sup>35</sup> we hypothesized that an FKBP-binding group might retain the bifunctional molecule within these cells. To test this idea, we treated mouse

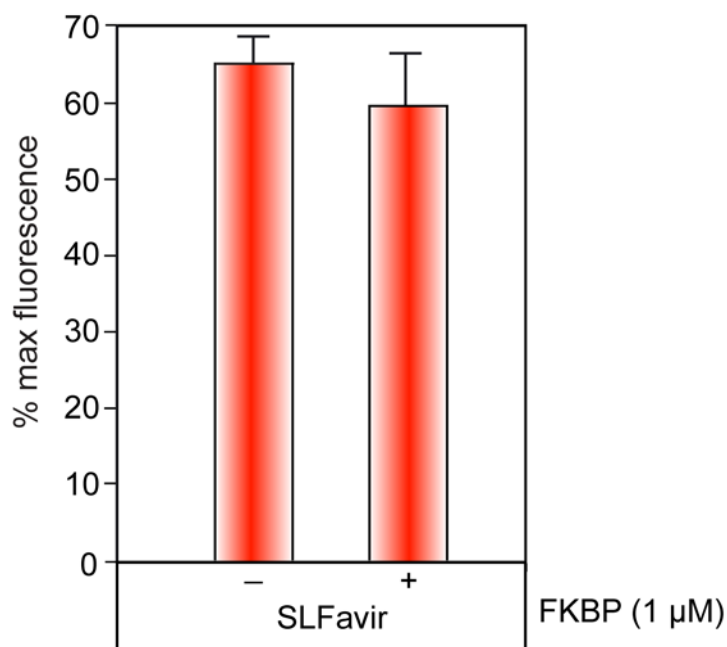


**Figure 3-3. Addition of FKBP does not Block Anti-HIV Protease Activity.** Addition of recombinant, human FKBP did not reduce the anti-protease activity of SLFavir, which suggests that binding to the protease is not disrupted by installation of SLF or the recruitment of FKBP.

whole blood with **4** or SLFavir and analyzed the partitioning of the molecules between the plasma and hematocrit after a 60-minute incubation at 37 °C. We found that compound **4** was distributed equally between the plasma and cells (Figure 3-4A). On the other hand, SLFavir exhibited a striking 8-fold preference for the cellular compartment, suggesting that similar to FK506,<sup>33</sup> binding to FKBP alters partitioning.

### 3.2.5 SLFavir is a Prodrug that Prolongs Anti-Protease Activity *ex vivo*

To evaluate the functional consequences of this cellular distribution on the metabolism of the bifunctional product, we analyzed the levels of the inhibitors

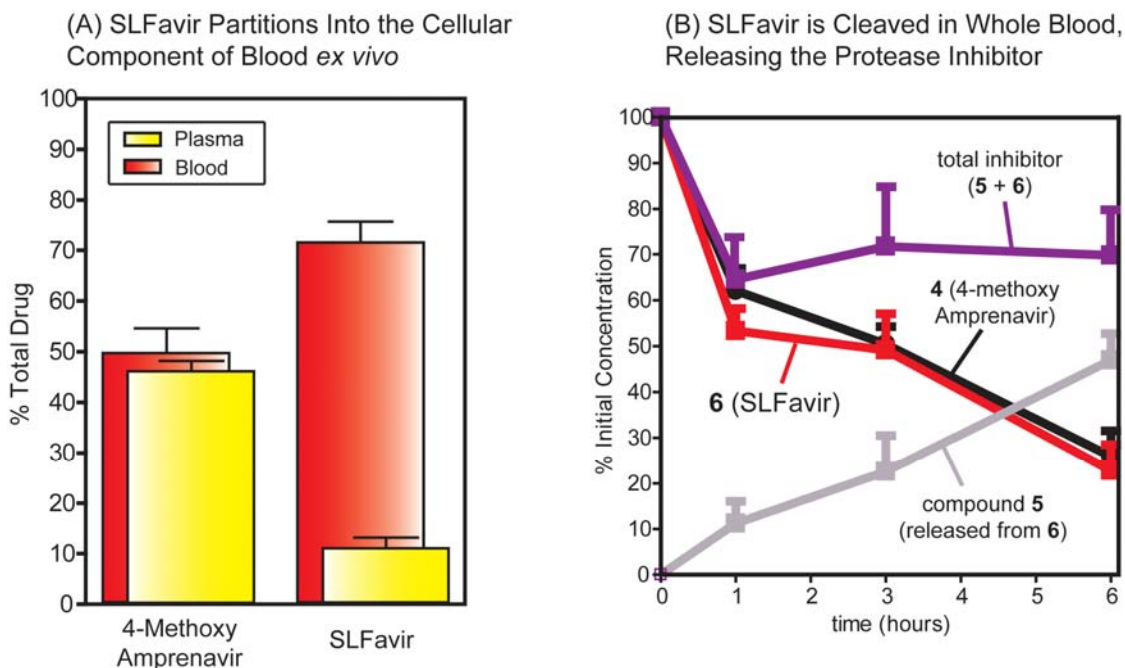


**Figure 3-4. SLFavir is Selectively Partitioned into Blood Cells and is a Prodrug *ex vivo*.** (A) Whole blood treated with compound 4 or 6 was separated into plasma and blood cell fractions and compound levels were assayed by LC-MS. The results are the average of at least three experiments and the error is standard deviation. (B) Both SLFavir and compound 4 are metabolized in whole blood at 37°C, but the total amount of active product remains constant in the SLFavir treated samples because of the release of the active derivative, 5.

over a period of six hours *ex vivo* (Figure 3-4B). At 37 °C, 4 was slowly degraded and only ~25% of the initial concentration remained after six hours. Interestingly, SLFavir had similar kinetics, but the LC-MS spectra revealed that the major cleavage product [ $m/z = 507$ ] was 5, the oxobutanoic acid precursor of the bifunctional compound. As described in Figure 3-2, this intermediate retains nanomolar activity against HIV-1 protease and it might be considered the released product of the prodrug. By adding the observed concentrations of 5 and 6, we calculated that the total amount of viable inhibitor remained elevated (within 70% of the initial value) throughout the experiment. To confirm the anti-protease activity of these samples, we subjected the extracted material to the

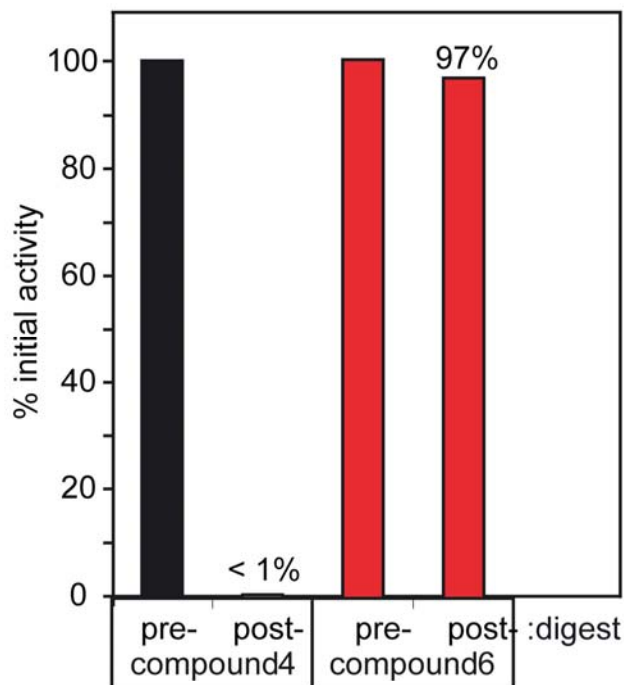


**Figure 3-5. Anti-HIV Protease Activity is Maintained in the SLFavir Treated Samples.** Whole blood samples after 6 h of incubation at 37°C were extracted, dried, and resuspended in DMSO for use in HIV protease assays. The activity of 4 was reduced ~100-fold by incubation in whole blood whereas the activity of the bifunctional drug 6 was largely unchanged.

HIV-1 protease FRET assay. These experiments confirmed that the SLFavir-treated sample retained nearly 100% of its inhibitory activity after 6 hours, while the activity of samples treated with compound 4 was reduced by ~100-fold (Figure 3-5). Together, these results suggest that SLFavir is a prodrug and that it contributes to anti-protease activity longer than the parent compound.

### 3.2.6 SLFavir is Sequestered into Blood Cells *in vivo*

Encouraged by the *ex vivo* results, our next goal was to investigate the

lifetime of the bifunctional molecule in a rodent model. In order to deliver molar equivalents, we used a 2.0 mM dosing solution and administered 10  $\mu\text{L/g}$  intraperitoneally to adult male C57BL/6 mice, equaling 0.4  $\mu\text{mol}$  per gram or approximately 10 mg/kg. One hour after administration, we confirmed that the compounds were accessible to the circulation by extracting with organic solvent and monitoring the parent ion by LC-MS. Analogous to the experiments performed on the *ex vivo* samples, we first examined the partitioning of the compounds between the plasma and cellular components of whole blood. One hour after *i.p.* administration, we found that **4** was distributed equally between the two portions (Figure 3-6A). Consistent with our previous findings, SLFavir had a ~6-fold preference for the cellular fraction; thus, binding to FKBP also alters the distribution of the bifunctional molecule *in vivo*.

### **3.2.7 SLFavir Exhibits a Dramatically Enhanced Lifetime *in vivo***

To evaluate the functional consequences of this enhanced cellular partitioning, we analyzed plasma levels of the inhibitors over a period of 12 hours after *i.p.* injection. After 180 minutes, the plasma levels of the unmodified parent compound, **4**, were undetectable and this compound exhibited a half-life of approximately 30 minutes (Figure 3-6B). This value is consistent with studies of other protease inhibitors in rodents.<sup>34</sup> In contrast, SLFavir had a half-life of >10 hours and persisted in the plasma at levels greater than 1  $\mu\text{M}$  for 12 hours. These results show that the bifunctional molecule exhibits a significantly longer lifetime than the unmodified parent.

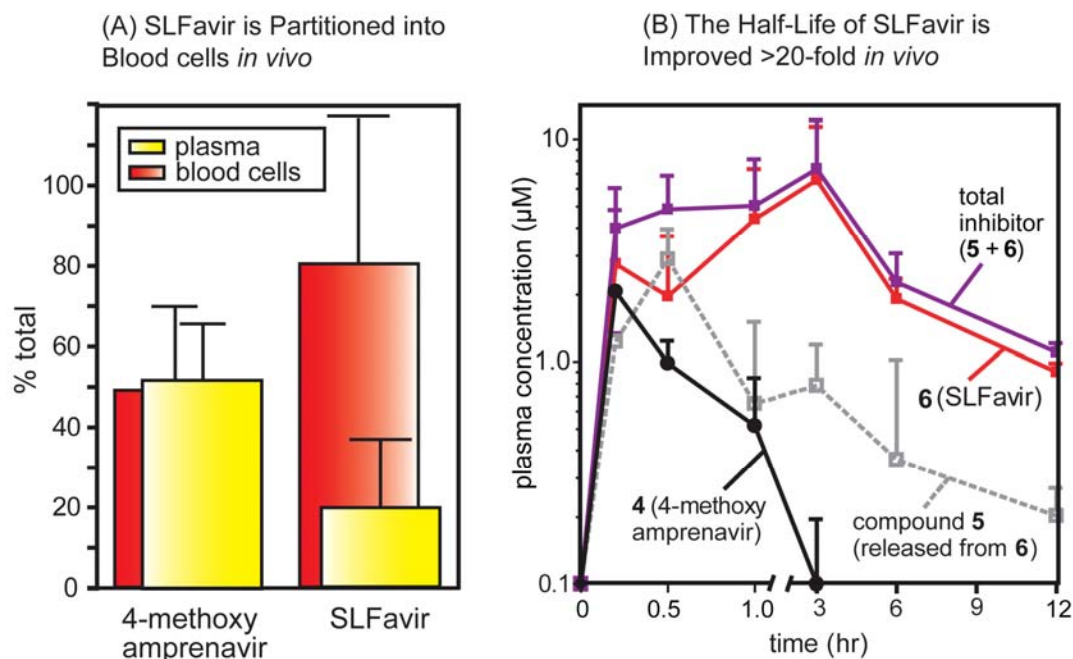


**Figure 3-6. SLFavir is Sequestered into Blood Cells and has a Dramatically Enhanced Half-Life *in vivo*.** (A) After 60 min, whole blood was isolated from treated mice, separated into components and analyzed for drug content by LC-MS. Results are the average of at least three animals. (B) At time 0, adult male mice were injected i.p. with either compound 4 or 6. Whole blood was removed at the indicated times and the plasma drug levels determined. Total inhibitor level was calculated as the concentration of 5 + 6. All results are the average of at least three independent experiments and the error is standard deviation.

### 3.2.8 Anti-HIV Protease Activity is Stably Maintained in SLFavir-Treated Mice

Importantly, SLFavir had an  $IC_{50}$  of ~20 nM *in vitro* (see Figure 3-2), which is 50 times lower than the observed plasma concentration. These results suggest that anti-HIV protease activity might also be maintained in these mice. To directly test this possibility, we subjected the plasma extracts to the HIV-1 protease assay. Using this method, we found that the activity of **4** was quickly lost (Figure 3-7), consistent with its rapid degradation in the rodent. On the other hand, the inhibitory activity of SLFavir remained relatively intact, retaining a high level of potency after 3 hours. Consistent with our previous results, we found



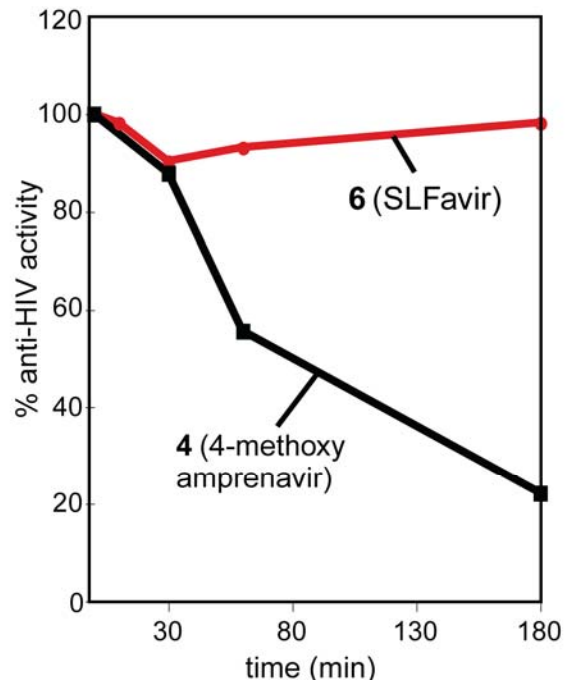


**Figure 3-7. Anti-HIV Protease Activity Persists Longer in the SLFavir-Treated Mice.** Plasma samples were dried and resuspended in DMSO for analysis in the HIV protease assay. Results are shown relative to a control (100% = 10 $\mu$ M drug extracted immediately from whole blood).

that compound **5** was released from the prodrug, which likely contributes to this improved persistence (see Figure 3-6B). Together, these results suggest that the addition of an FKBP-binding group can significantly prolong the duration of anti-protease activity in mice.

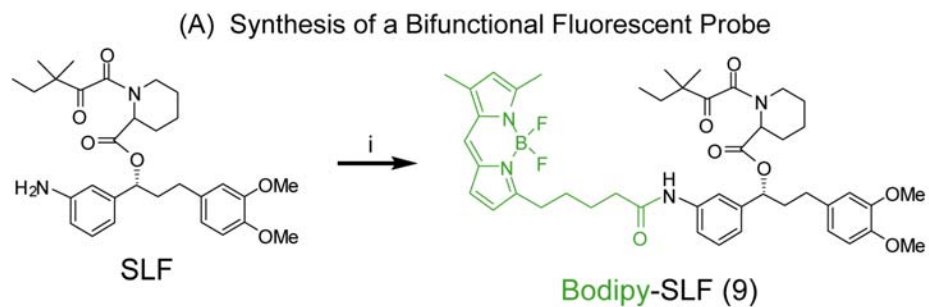
### 3.2.9 Partitioning of a Fluorescent Bifunctional Molecule is Reliant on the Availability of FKBP

Although our strategy is designed to use FKBP-binding to alter partitioning, we wanted to further explore this requirement. Towards this goal, we

synthesized a fluorescent probe (Bodipy-SLF; Figure 3-8A) that enables visualization of binding to this protein. Using confocal fluorescence microscopy, we found that mouse embryonic fibroblasts (MEFs) treated with the mock-conjugated control probe exhibited a diffuse, non-specific membrane staining (Figure 3-8B). Conversely, treatment of wild type MEFs with the bifunctional probe resulted in prominent cytoplasmic fluorescence with no nuclear colocalization, consistent with the fact that FKBP is a cytosolic protein. To confirm an interaction with FKBP, we treated MEFs from a mutant line that fails to express FKBP12 (*fkbp*<sup>NLS/NLS</sup>)<sup>48</sup> and found that neither the control nor the Bodipy-SLF probe were retained. Next, we saturated the ligand-binding sites in wild type MEFs by pre-treating with FK506 (100  $\mu$ M). When these cells were subsequently treated with the fluorescent probe, specific labeling was blocked. Together, these results and previous work<sup>37</sup> suggest that FKBP is responsible for sequestering SLF-bearing, bifunctional molecules.

### **3.2.10 A Bifunctional Protease Inhibitor has Superior Anti-HIV Activity in a Cultured Cell Model**

For this SLF-coupling strategy to produce a clinically viable antiviral, the modified compounds must retain activity against live virus. *In vitro*, addition of recombinant FKBP did not significantly influence anti-protease activity (see Figure 3-3), but this finding does not preclude the possibility that binding to FKBP might positively or negatively influence activity in cells through controlling the subcellular distribution of the modified inhibitor. To directly test this idea, we studied the infectivity of the T-cell tropic HIV-1LAI strain in a CEM cell model



(B) Sequestration of Bifunctional Molecules is FKBP Dependent

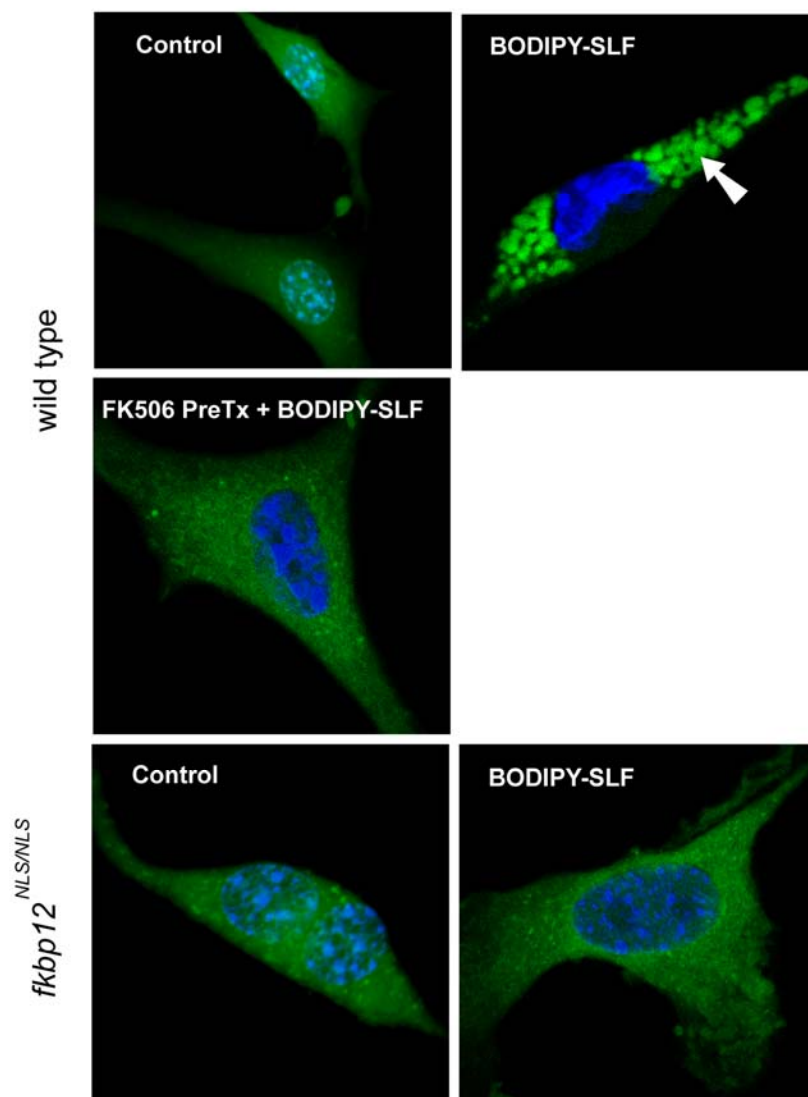


**Figure 3-8. A Fluorescent SLF Conjugate is Selectively Sequestered in FKBP-Expressing Cells.** Wild-type or mutant MEFs (*fkbp12*<sup>NLS/NLS</sup>) were treated with the probe or a Bodipy control (100 $\mu$ M). Only the wild-type MEFs had specific cytoplasmic staining. Nuclei are stained with Hoescht.

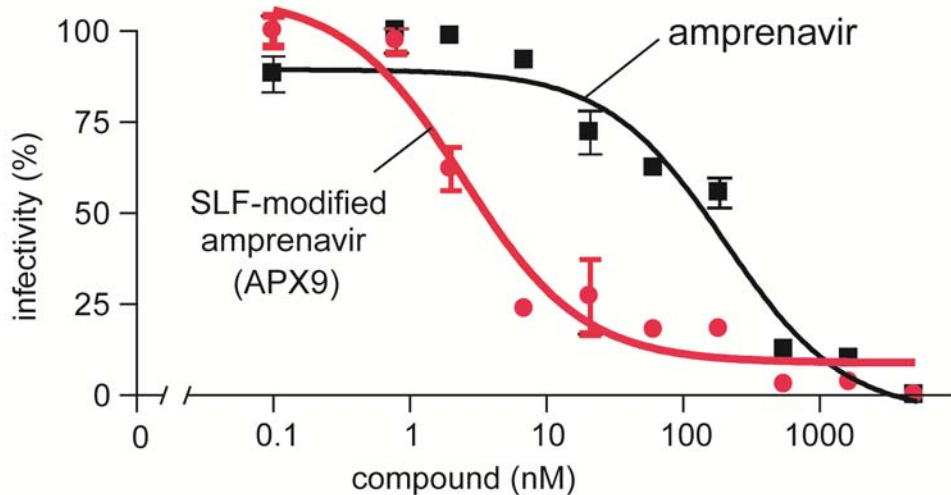


**Figure 3-9. A Bifunctional Protease Inhibitor has Potent Antiviral Activity in an HIV Infectivity Model.** CEM lymphocytes were infected with T-cell tropic HIV-1LA1. The infected cells were treated with either Amprenavir or a SLF-modified protease inhibitor (APX23451). Results are the average of triplicates and error bars are SE.

using a close chemical derivative of SLFavir, APX9. Under these conditions, unmodified Amprenavir inhibited HIV maturation with an  $IC_{50}$  of  $202 \pm 136$  nM, while the bifunctional derivative had an  $IC_{50}$  of  $2.5 \pm 3.2$  nM (Figure 3-9); thus, the SLF-modified compound was approximately 80-fold more potent. These results show that the SLF-modified inhibitor retains antiviral activity.

### 3.3 Discussion

#### 3.3.1 Substantial Room for Improvement in Current Antiviral Treatment Paradigms

A fundamental requirement in any drug treatment protocol is that levels of active compound remain above therapeutically effective concentrations. This feature is especially critical for HIV-1 therapy, as constant antiviral pressure is

required to prevent replication and suppress the emergence of multi-drug resistant strains. While current HAART regimens have been largely successful, significant problems persist. One of the major issues is that current protease inhibitors have limited lifetimes due to rapid metabolism by cytochrome P450 enzymes. In turn, suboptimal pharmacokinetics leads to high pill burdens, liver toxicity and poor patient compliance, especially in developing countries. Thus, there is a continued need for the development of improved therapeutics.

### **3.3.2 A Dramatic Shift in Pharmacology**

As illustrated in Chapter 2, we observed that FKBP significantly protected FK506, and bifunctional derivatives thereof, from interacting with CYP3A4 *in vitro*.<sup>37</sup> Thus, we hypothesized that binding to this protein may improve the pharmacology of HIV protease inhibitors *in vivo*. More specifically, we postulated that tethering FK506-like groups might redistribute the chimeric compounds into a protected biological niche, shielding them from metabolic enzymes, and potentially extending their lifetimes (Figure 3-10). To explicitly test this idea, we generated a bifunctional version of Amprenavir and evaluated its pharmacokinetics both *ex vivo* and *in vivo*. *Ex vivo*, we found that SLFavir is converted to an active metabolite and that the overall anti-HIV protease activity in blood remains high (see Figure 3-2). It is worth noting that, unlike other prodrug methods, both the pre-cleaved and cleaved products are nanomolar inhibitors. The ability of whole blood to cleave the amide of SLFavir is currently not well understood but we are continuing to explore ways of controlling release kinetics.

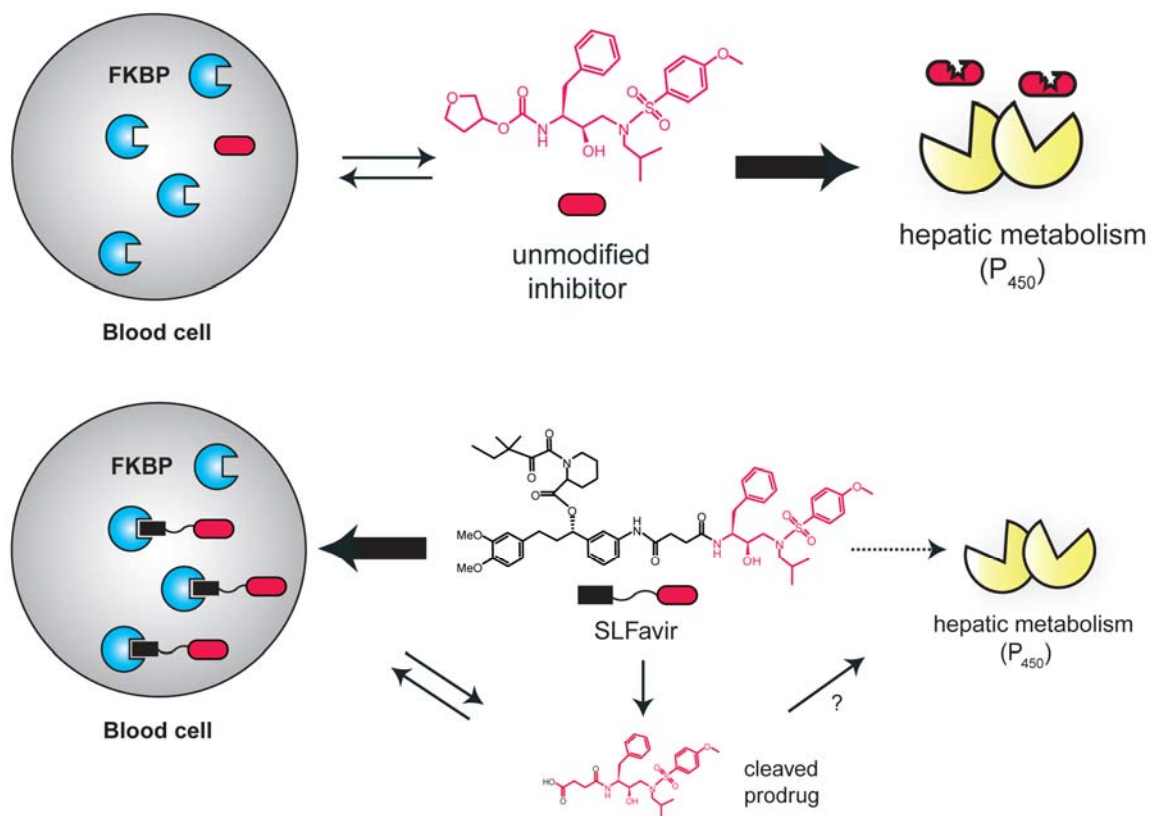


Figure 3-10. Model for Selective Protection of SLFavir.

In infectivity studies with live HIV-1 LA1 strain virions, the activity of the SLF-modified Amprenavir was enhanced >80-fold relative to the unmodified compound ( $IC_{50} \sim 2.5$  nM). This improvement might possibly arise from FKBP-dependent concentration of the SLF-modified material in the cytoplasm or from increased persistence in the culture conditions. *In vivo*, we found that SLFavir has a half-life of more than 10 hours in mice and its anti-protease activity persists unabated for >3 hours (see Figure 3-7). These parameters are approximately 20-fold better than the unmodified Amprenavir and extrapolating these results to human patients would result in a half-life of more than 50 hours (based on a 5.5-fold difference in glomerular filtration rates between humans and rodents). By

comparison, the principal FDA-approved protease inhibitor prodrug used in antiviral cocktails, Fosamprenavir, has a half-life of 7 to 8 hours. Although this is a highly speculative analysis, such a difference would be predicted to have significant benefits in reducing pill burden, minimizing treatment costs, normalizing plasma drug levels, and possibly limiting side effects by lowering the requirement for co-administration of P450 inhibitors.

### **3.3.3. Why is FK506 Bifunctional?**

FK506 inhibits the activity of the phosphatase, calcineurin. More specifically, this compound binds FKBP and then this drug-protein conjugate interacts with the regulatory, calcineurin B subunit. However, a much simpler, synthetic inhibitor that binds directly to the active site of calcineurin A is also active and immunosuppressive. If that is the case, then why does FK506 have such an indirect and relatively complicated mechanism? Why does the producing organism spend extra ATP to synthesize the FKBP-binding portion of FK506, when it could, theoretically, make a much smaller compound that binds in the active site of calcineurin A? What is the evolutionary driving force retaining the biosynthetic machinery to build the large FK506 molecule? We think that the findings in Chapter 2 and 3 might shed light on these evolutionary questions. Specifically, we propose that the FKBP-binding portion of FK506 and rapamycin are evolutionarily conserved because of the favorable pharmacokinetics that it provides. In this model, binding to FKBP is not the target, *per se*, of these compounds. Rather, they simply “utilize” FKBP to achieve useful doses and

avoid metabolism. It is very interesting to note that many other natural products break the modern “Rules” of drug discovery; they have high molecular weight and relatively complex structures. Yet, many natural products are phenomenal drugs with long lifetimes, low toxicity, and good oral bioavailability. We postulate that, perhaps, other natural products also have embedded chemical features that allow them to evade metabolism. However, these mechanisms remain completely unknown. Detailed studies into this possibility might allow drug discovery research groups to describe exactly what makes natural products special and, potentially, to install these special features into other drugs.

### **3.3.4 Outlook for the Future**

While the present study focuses on proof-of-principle validation of a new mechanism, we propose that installation of FKBP-binding groups might constitute a novel strategy to improve therapeutic efficacy in AIDS patients. However, application of this strategy in the clinic will require extensive studies of oral bioavailability and a greater understanding of the design principles that control the distribution and lifetime of such bifunctional therapeutics. Nevertheless, the present study demonstrates that this nature-inspired method combines elements of a cleavable prodrug approach, as well as tissue-targeting, with a slow-release, *in situ* delivery scheme using FKBP as a natural reservoir.

Finally, because our synthetic strategy is modular, other drug classes might also be amenable to this approach. Towards this goal, we developed an



efficient, high-throughput chemical methodology for installing FKBP-binding groups onto a wide range of compounds with differing functionalities discussed in Chapter 4. Together, these studies provide a new way of exploiting naturally bifunctional compounds and CIDs to specifically alter drug pharmacology.

### 3.4 Experimental Procedures

#### 3.4.1 Synthesis of a Bifunctional Protease Inhibitor

***N-((2R,3S)-3-amino-2-hydroxy-4-phenylbutyl)-N-isobutyl-4-methoxybenzenesulfonamide (3)***. (2S, 3S)-1,2-Epoxy-3-(Boc-amino)-4-phenylbutane (Sigma, 50 mg, 0.1898 mmol) and isobutylamine (Sigma; 38.4  $\mu$ L, 0.3797 mmol, 2 equivalents) were stirred in 2.0 mL of methanol overnight at room temperature. The reaction was then concentrated *in vacuo* and brought up in 3.0 mL of dry dichloromethane (DCM). Et<sub>3</sub>N (29.7  $\mu$ L, 0.2128 mmol, 1.1 equivalents) was added dropwise, followed by reaction with 4-methoxybenzenesulfonyl chloride (43.9 mg, 0.2128 mmol, 1.1 equivalents) and the mixture was stirred overnight at room temperature to generate compound **2**. This crude compound was carried forward by addition of 3.0 mL of trifluoroacetic acid and stirring for another 3 hours. The mixture was then brought up in 8.0 mL of DCM and the organic phase was washed once with 50 mL of H<sub>2</sub>O, once with 50 mL of saturated NaHCO<sub>3</sub>, once with 50 mL of H<sub>2</sub>O, once with brine and dried over Na<sub>2</sub>SO<sub>4</sub>. The crude product was filtered and evaporated to dryness. After drying, **3** (58.6 mg, 0.1441 mmol, 76%; 3 steps) was obtained as a white solid. *m/z* 407.05 [M + H, calculated 406.54].

**Tetrahydrofuran-3-yl (2S,3R)-3-hydroxy-4-(N-isobutyl-4-methoxyphenylsulfonamido)-1-phenylbutan-2-ylcarbamate (4; 4-methoxy Amprenavir).** 2,5-dioxopyrrolidin-1-yl tetrahydrofuran-3-yl carbonate (22.5 mg, 0.0984 mmol, 2 equivalents) and EtN<sub>3</sub> (27.4 μL, 0.1968 mmol, 4 equivalents) were added to a stirred solution of **3** (20.0 mg, 0.0492 mmol) in 2.0 mL DCM and allowed to proceed 3 hours at room temperature. The reaction was brought up in 6.0 mL of DCM, washed 3 times with 5% NaHCO<sub>3</sub>, once with brine, and dried over Na<sub>2</sub>SO<sub>4</sub>. The crude product was then filtered and evaporated to dryness. After drying, **4** (25.1 mg, 0.0482 mmol, 98%) was obtained as an oily residue. *m/z* 521.20 [M + H, calculated 520.64].

**4-((2S,3R)-3-hydroxy-4-(N-isobutyl-4-methoxyphenylsulfonamido)-1-phenylbutan-2-ylamino)-4-oxobutanoic acid (5).** Succinic anhydride (49.9 mg, 0.4986 mmol, 5 equivalents) was added to **3** (40.6 mg, 0.0998 mmol) in 3.0 mL DCM and allowed to stir at room temperature. After 2 hours, the reaction was placed in ice bath to precipitate unreacted succinic anhydride, followed by vacuum filtration. The organic layer washed three times with 5% citric acid, once with brine, and dried over Na<sub>2</sub>SO<sub>4</sub>. The crude product was then filtered and evaporated to dryness. After drying, **5** (48.6 mg, 0.0961 mmol, 96%) was obtained as a residue. *m/z* 507.10 [M + H, calculated 506.61].

**(R)-((R)-3-(3,4-dimethoxyphenyl)-1-(3-(4-((2S,3R)-3-hydroxy-4-(N-isobutyl-4-nitrophenylsulfonamido)-1-phenylbutan-2-ylamino)-4-**

**oxobutanamido) phenyl)propyl) 1-(3,3-dimethyl-2-oxopentanoyl)piperidine-2-carboxylate (6; SLFavir).** Diisopropylcarbodiimide (115  $\mu\text{L}$ , 0.7324 mmol, 10 equivalents) was added to **5** (38.2 mg, 0.0732 mmol) in 3.0 mL dimethylformamide (DMF), and stirred for 20 minutes at room temperature. SLF (38.4 mg, 0.0732 mmol, 1.0 equivalent) was then added with dimethylaminopyridine (9.0 mg, 0.0732 mmol, 1.0 equivalent) and the reaction was stirred overnight at room temperature. The reaction mixture was then brought up in 8.0 mL of DCM, washed 3 times with  $\text{H}_2\text{O}$ , once with brine, dried over  $\text{Na}_2\text{SO}_4$ , and evaporated under reduced pressure. The product was further purified by preparative chromatography on a Waters Spherisorb S10 ODS2 column (10 x 250 mm) to yield **6** (48.1 mg, 0.04384 mmol, 64%) as a pale yellow solid.  $m/z$  1028.50 [M + H, calculated 1028.22].

**Fluorescent Probe (Bodipy-SLF).** SLF (1.50 mg, 0.00286 mmol) was dissolved in 2.0 mL DMF and then added to Bodipy FL C<sub>5</sub> SE (Molecular Probes; 1.31 mg, 0.00314 mmol, 1.1 equivalents) with stirring.  $\text{EtN}_3$  (10.0  $\mu\text{L}$ , 0.07175 mmol, 25 equivalents) was then added dropwise and the reaction was allowed to proceed at room temperature for 12 hours. The reaction was quenched by adding Tris-Amine Polystyrene HL Resin (Biotage; 1.0 mg, 1.0 equivalents) and stirring for 60 minutes, followed by vacuum filtration. The filtrate was brought up in 8.0 mL of DCM, washed 3 times with  $\text{H}_2\text{O}$ , once with brine, and dried over  $\text{Na}_2\text{SO}_4$ . The crude product was then evaporated under reduced pressure to yield Bodipy-SLF as a purple solid.

### 3.4.2 HIV Protease Inhibition Assay

To determine the inhibitory potency of PIs, I used a commercially available, FRET-based assay (Bachem, Torrance, CA). Briefly, 5.0  $\mu\text{L}$  of a 120 nM HIV-1 protease solution in Buffer P (20% glycerol, 0.1% CHAPS, 20mM  $\text{K}_2\text{HPO}_4$ , 1.0 mM EDTA, 1.0 mM DTT at pH 5.5) was preincubated with 2.0  $\mu\text{L}$  of inhibitor and 1.0  $\mu\text{L}$  of a 2% PEG-400 solution for 60 minutes at 37°C. 12.0  $\mu\text{L}$  of HIV-1 protease substrate 1 (Arg-Glu(EDANS)-Ser-Gln-Asn-Tyr-Pro-Ile-Val-Gln-Lys(dabcyl)-Arg; Molecular Probes, Eugene OR) diluted in Buffer P was then added to the wells to a final concentration of 30 nM. The change in fluorescence was monitored at 490 nm on a SpectraMax M5 plate reader (Molecular Devices, Mountain View, CA) for 60 minutes at 37°C.

### 3.4.3 Animal Care

The studies reported here adhere to the Stanford University principles of animal care. Mice were housed in groups of four to six at 22°C to 24°C in a 12 hour light/dark cycle and fed chow diet and water *ad libitum*. Male C57BL/6 mice weighing between 16 to 20 g were used for all experiments.

### 3.4.4 *Ex vivo* Pharmacokinetic Studies in Whole Blood

Stock solutions of **4** and **6** in dimethylsulfoxide (10 mM) were diluted into freshly collected mouse blood at a final concentration of 100  $\mu\text{M}$ . The samples were then incubated at 37°C for 0, 1, 3, and 6 hours with shaking and processed as described below.

### **3.4.5 *In vivo* Pharmacokinetic Studies in Mice**

4-Methoxy Amprenavir and SLFavir dissolved in dimethylsulfoxide (2.0 mM) were administered intraperitoneally (i.p) at an injection volume of 10.0  $\mu\text{L/g}$ , equaling a dose of 0.4  $\mu\text{mols}$  per gram animal. At least three animals were injected per timepoint per drug. Blood samples ( $\sim 250$   $\mu\text{L}$ ) were obtained via cardiac puncture at 0, 10, 30, 60, 180, 360, and 720 minutes after injection, collected in  $\text{K}_2\text{EDTA}$  microtainers, and immediately centrifuged at 3,706 rpm for 16 minutes to separate the plasma fraction from the cellular components. Each fraction was then processed immediately using the extraction procedure described below.

### **3.4.6 Determination of Inhibitor Concentrations in Plasma and Blood**

Both blood and plasma inhibitor levels were determined by using a modified version of a previously established and validated LC-MS method.<sup>50</sup> Briefly, 100  $\mu\text{L}$  of blood or plasma was added to a 1.5 mL polypropylene microcentrifuge tube, followed by protein precipitation with 100  $\mu\text{L}$  of a 0.1 M aqueous zinc sulfate and immediate vortexing for 30 s. Analytical grade acetonitrile (ACN) was then added (800  $\mu\text{L}$ ) and the sample was vortexed again for 30 s. Following high-speed centrifugation at 13,200 rpm for 10 minutes, the supernatant was transferred to a glass vial and subjected to LC-MS analysis. The LC-MS system used for these studies was a Shimadzu (Columbia, MD) series 2010EV instrument equipped with an APCI probe to minimize ion suppression. Quantification was performed using LCMSolution Version 2.05 and a set of

external standards.

### **3.4.7 Cell Culture**

Mouse embryonic fibroblast (MEF) cell lines were a gift from Kryn Stankunas (Stanford University, Palo Alto, CA). Briefly, these cells were derived from wild-type (WT) mice as well as mice in which both alleles of the FKBP12 gene were disrupted; these mutant MEFs fail to express FKBP12.<sup>48</sup> MEF cells were cultured in Dulbecco's modified essential medium (DMEM) with high glucose supplemented with 10% fetal bovine serum, 25 µg/mL Pen-Strep/Fungizone, and 55 µM β-mercaptoethanol. Cells were grown at 37°C in 5% CO<sub>2</sub> and 90% humidity.

### **3.4.8 Confocal Microscopy**

MEFs were seeded in 35-mm poly-*D*-lysine coated, glass-bottomed culture dishes at 100,000 cells per plate. Prior to microscopy, the media was replaced with Opti-MEM I reduced serum medium. The cells were then treated with Hoescht stain and either the mock-conjugated control probe, which lacks the SLF group, or Bodipy-SLF at a final concentration of 100 µM for 30 minutes and then washed with media. Confocal microscopy was performed on an Olympus laser-scanning confocal microscopy (FV500, Center Valley, PA) using single line excitation (488 nm). In the competition experiments, FK506 (LC Labs; 100 µM) was pre-incubated with the MEFs for 30 minutes.

### **3.4.9 HIV Infectivity Assay**

The HIV infectivity assays were performed by D. Horejsh (Commonwealth Biotechnologies, Richmond, VA). Briefly, the T-cell-tropic strain HIV-1LAI was used to infect CEM cells. CEM cells were grown in RPMI 1640 medium supplemented with 10% heat-inactivated fetal bovine serum, penicillin (100 units/mL), streptomycin (100 µg/mL), and polybrene (2 µg/mL) at 37°C with 5% CO<sub>2</sub>. The titered virus was added to duplicate wells, which were pre-treated with compounds for 1 hour, at a low multiplicity of infection (MOI=0.01) and incubated for 4 hr at 37 °C. The cells were washed three times with PBS (GIBCO/BRL), suspended in 2 mL of culture medium containing the same concentration of compound as the initial pre-incubation and further incubated at 37 °C in 5% CO<sub>2</sub>. After 4 days of culture, media containing infected cells (200 µL) was used to measure production of HIV-1 p24 by antigen capture ELISA. Each duplicate well in the infectivity assay is split into triplicate wells for the p24 ELISA, and IC<sub>50</sub> determined using GraphPad PRISM. Results are expressed in relation to a solvent vehicle control.

## Notes

Portions of this work have been published as “FK506-Binding Protein (FKBP) Partitions a Modified HIV Protease Inhibitor Into Blood Cells and Prolongs its Lifetime *in vivo*,” Marinec, P. S., Chen, L., Barr, K. J., Mutz, M. W., Crabtree, G. R., and Gestwicki, J. E., *Proceedings of the National Academy of Sciences*, 2009, 106: 1336-1341.

P. S. Marinec and J. E. Gestwicki designed the experiments and prepared the manuscript. P. S. Marinec performed the synthetic work, HIV-1 protease assays, confocal microscopy, LC-MS analysis, and *ex vivo* and *in vivo* experiments. L. Chen was responsible for the animal care. The HIV-1 infectivity assays were performed by D. Horejsh of Commonwealth Biosciences.



### 3.5 References

1. Broder, S.; Gallo, R.C. A pathogenic retrovirus (HTLV-III) linked to AIDS. *N. Engl. J. Med.*, **1984**, 311, 1292.
2. Briggs, J.A.G.; Wilk, T.; Welker, R.; Krausslich, H.G.; Fuller, S.D. Structural organization of authentic, mature HIV-1 virions and cores. *EMBO J.*, **2003**, 22, 1707.
3. Wyatt, R.; Kwong, P.D.; Desjardins, E.; Sweet, R.W.; Robinson, J.; Hendrickson, W.A.; Sodroski, J.G. The antigenic structure of the HIV gp120 envelope glycoprotein. *Nature*, **1998**, 393, 705.
4. Momany, C.; Kovari, L.C.; Prongay, A.J.; Keller, W.; Gitti, R.K.; Lee, B.M.; Gorbalenya, A.E.; Tong, L.; McClure, J.; Ehrlich, L.S.; Summers, M.F.; Carter, C.; Rossmann, M.G. Crystal structure of dimeric HIV-1 capsid protein. *Nat. Struct. Biol.*, **1996**, 3, 763.
5. Easterbrook, P.J.; Emami, J.; Moyle, G.; Gazzard, B.G. Progressive CD4 cell depletion and death in zidovudine-treated patients. *J. Acquir. Immune. Defic. Syndr.*, **1993**, 6, 927.
6. Markovic, I. Advances in HIV-1 entry inhibitors: strategies to interfere with receptor and coreceptor engagement. *Curr. Pharm. Des.*, **2006**, 12, 1105.
7. Steffens, C.M.; Hope, T.J. Localization of CD4 and CCR5 in living cells. *J. Virol.*, **2003**, 77, 4985.
8. Gallo, S.A.; Puri, A.; Blumenthal, R. HIV-1 gp41 six-helix bundle formation occurs rapidly after the engagement of gp120 by CXCR4 in the HIV-1 Env-mediated fusion process. *Biochemistry*, **2001**, 40, 12231.
9. Greene, W.C. The brightening future of HIV therapeutics. *Nat. Immunol.*, **2004**, 5, 867.
10. Craigie, R. HIV integrase: a brief overview from chemistry to therapeutics. *J. Biol. Chem.*, **2001**, 276, 23213.
11. Karn, J. Control of human immunodeficiency virus replication by the tat, rev, nef and protease genes. *Curr. Opin. Immunol.*, **1991**, 3, 526.
12. Adamson, C.S.; Freed, E.O. Novel approaches to inhibiting HIV-1 replication. *Antiviral Res.*, **2010**, 85, 119.
13. Freed, E.O. HIV-1 replication. *Somat. Cell. Mol. Genet.*, **2001**, 26, 13.

14. Flexner, C. HIV drug development: The next 25 years. *Nat. Rev. Drug Discov.*, **2007**, 6, 959.
15. Clavel, F.; Hance A.J. HIV drug resistance. *N. Engl. J. Med.*, **2004**, 350, 1023.
16. Barbaro, G.; Scozzafava, A; Mastrolorenzo, A; Supuran, C.T. Highly active antiretroviral therapy: Current state of the art, new agents and their pharmacological interactions useful for improving therapeutic outcome. *Curr. Pharm. Des.*, **2005**, 11, 1805.
17. Turner, S.R. HIV protease inhibitors - the next generation. *Curr. Med. Chem. Anti-Infective Agents*, **2002**, 1, 141.
18. Dresser, G.K.; Spence, J.D.; Bailey, D.G. Pharmacokinetic-pharmacodynamic consequences and clinical relevance of cytochrome P450 3A4 inhibition. *Clin. Pharmacokinet.*, **2000**, 38, 41.
19. Vierling, P.; Greiner, J. Prodrugs of HIV protease inhibitors. *Curr. Pharm. Des.*, **2003**, 9, 1755.
20. Agarwal, S.; Boddu, S.H.; Jain, R.; Samanta, S.; Pal, D.; Mitra, A.K. Peptide prodrugs: Improved oral absorption of lopinavir, a HIV protease inhibitor. *Int. J. Pharm.*, **2008**, 359, 7.
21. Rouquayrol, M.; Gaucher, B.; Roche, D.; Greiner, J.; Vierling, P. Transepithelial transport of prodrugs of the HIV protease inhibitors saquinavir, indinavir, and nelfinavir across Caco-2 cell monolayers. *Pharm. Res.*, **2002**, 19, 1704.
22. Hamada, Y.; Matsumoto, H.; Yamaguchi, S.; Kimura, T.; Hayashi, Y.; Kiso, Y. Water-soluble prodrugs of dipeptide HIV protease inhibitors based on O→N intramolecular acyl migration: Design, synthesis and kinetic study. *Bioorg. Med. Chem.*, **2004**, 12, 159.
23. Furfine, E.S.; Baker, C.T.; Hale, M.R.; Reynolds, D.J.; Salisbury, J.A.; Searle, A.D.; Studenberg, S.D.; Todd, D.; Tung, R.D.; Spaltenstein, A. Preclinical pharmacology and pharmacokinetics of GW433908, a water-soluble prodrug of the human immunodeficiency virus protease inhibitor amprenavir. *Antimicrob. Agents Chemother.*, **2004**, 48, 791.
24. Wire, M.B.; Shelton, M.J.; Studenberg, S. Fosamprenavir: Clinical pharmacokinetics and drug interactions of the amprenavir prodrug. *Clin. Pharmacokinet.*, **2006**, 45, 137.

25. Gunaseelan, S.; Debrah, O.; Wan, L.; Leibowitz, M.J.; Rabson, A.B.; Stein, S.; Sinko, P.J. Synthesis of poly(ethylene glycol)-based saquinavir prodrug conjugates and assessment of release and anti-HIV-1 bioactivity using a novel protease inhibition assay. *Bioconjug. Chem.*, **2004**, 15, 1322.
26. Matsumoto, H.; Kimura, T.; Hamawaki, T.; Kumagai, A.; Goto, T.; Sano, K.; Hayashi, Y.; Kiso, Y. Design, synthesis, and biological evaluation of anti-HIV double-drugs: Conjugates of HIV protease inhibitors with a reverse transcriptase inhibitor through spontaneously cleavable linkers. *Bioorg. Med. Chem.*, **2001**, 9, 1589.
27. Van Duyne, G.D.; Standaert, R.F.; Karplus, P.A.; Schreiber, S.L.; Clardy, J. Atomic structure of FKBP-FK506, an immunophilin-immunosuppressant complex. *Science*, **1991**, 252, 839.
28. Ho, S.; Clipstone, N.; Timmermann, L.; Northrop, J.; Graef, I.; Fiorentino, D.; Nourse, J.; Crabtree, G.R. The mechanism of action of cyclosporin A and FK506. *Clin. Immunol. Immunopathol.*, **1996**, 80, S40.
29. Liu, J.; Albers, M.W.; Wandless, T.J.; Luan, S.; Alberg, D.G.; Belshaw, P.J.; Cohen, P.; MacKintosh, C.; Klee, C.B.; Schreiber, S.L. Inhibition of T cell signaling by immunophilin-ligand complexes correlates with loss of calcineurin phosphatase activity. *Biochemistry*, **1992**, 31, 3896.
30. Griffith, J.P.; Kim, J.L.; Kim, E.E.; Sintchak, M.D.; Thomson, J.A.; Fitzgibbon, M.J.; Fleming, M.A.; Caron, P.R.; Hsiao, K.; Navia, M.A. X-ray structure of calcineurin inhibited by the immunophilin-immunosuppressant FKBP12-FK506 complex. *Cell*, **1995**, 82, 507.
31. Takahara, S. Efficacy of FK506 in renal transplantation. *Ann. N.Y. Acad. Sci.*, **1993**, 696, 235.
32. Fay, J.W.; Wingard, J.R.; Antin, J.H.; Collins, R.H.; Pineiro, L.A.; Blazar, B.R.; Saral, R.; Bierer, B.E.; Przepiorka, D.; Fitzsimmons, W.E.; Maher, R.M.; Weisdorf, D.J. FK506 (Tacrolimus) monotherapy for prevention of graft-versus host disease after histocompatible sibling allogeneic bone marrow transplantation. *Blood*, **1996**, 87, 3514.
33. Yura, H.; Yoshimura, N.; Hamashima, T.; Akamatsu, K.; Nishikawa, M.; Takakura, Y.; Hashida, M. Synthesis and pharmacokinetics of a novel macromolecular prodrug of Tacrolimus (FK506), FK506-dextran conjugate. *J. Control Release*, **1999**, 57, 87.
34. Galat, A. Peptidyl cis/trans isomerases (immunophilins): Biological diversity - targets - functions. *Curr. Topics Med. Chem.*, **2003**, 3, 1315.

35. Baughman, G.; Wiederrecht, G.J.; Chang, F.; Martin, M.M.; Bourgeois, S. Tissue distribution and abundance of human FKBP51, and FK506-binding protein that can mediate calcineurin inhibition. *Biochem. Biophys. Res. Commun.*, **1997**, 232, 437.
36. Nowakowski-Gashaw, I.; Mrozikiewicz, P.M.; Roots, I.; Brockmoller, J. Rapid quantification of CYP3A4 expression in human leukocytes by real-time reverse transcription-PCR. *Clin. Chem.*, **2002**, 48, 366.
37. Marinec, P.S.; Lancia, J.K.; Gestwicki, J.E. Bifunctional molecules evade cytochrome P450 metabolism by forming protective complexes with FK506-binding protein. *Mol. Biosystems*, **2008**, 4, 571.
38. Baker, C.T.; Salituro, F.G.; Court, J.J.; Deininger, D.D.; Kim, E.E.; Li, B.; Novak, P.M.; Rao, B.G.; Pazhanisamy, S.; Schairer, W.C.; Tung, R.D. Design, synthesis, and conformational analysis of a novel series of HIV protease inhibitors. *Bioorg. Med. Chem. Lett.*, **1998**, 8, 3631.
39. Surleraux, D.L.; Tahri, A.; Verschueren, W.G.; Pille, G.M.; de Kock, H.A.; Jonckers, T.H.; Peeters, A.; De Meyer, S.; Azijn, H.; Pauwels, R.; de Bethune, M.P.; King, N.M.; Prabu-Jeyabalan, M.; Schiffer, C.A.; Wigerinck, P.B. Discovery and selection of TMC114, a next generation HIV-1 protease inhibitor. *J. Med. Chem.*, **2005**, 48, 1813.
40. Maynard-Smith, L.A.; Chen, L.C.; Banaszynski, L.A.; Ooi, A.G.; Wandless, T.J. A directed approach for engineering conditional protein stability using biologically silent small molecules. *J. Biol. Chem.*, **2007**, 282, 24866.
41. Amara, J.F.; Clackson, T.; Rivera, V.M.; Guo, T.; Keenan, T.; Natesan, S.; Pollock, R.; Yang, W.; Courage, N.L.; Holt, D.A.; Gilman, M. A versatile synthetic dimerizer for the regulation of protein-protein interactions. *Proc. Natl. Acad. Sci. USA*, **1997**, 94, 10618.
42. Gestwicki, J.E.; Marinec, P.S. Chemical control over protein-protein interactions: Beyond inhibitors. *Comb. Chem. High Throughput Screen*, **2007**, 10, 667.
43. Clackson, T. *Controlling Protein-protein Interactions Using Chemical Inducers and Disruptors of Dimerization*, **2007**, Wiley, Weinham, Germany.

44. Koh, Y.; Nakata, H.; Maeda, K.; Ogata, H.; Bilcer, G.; Devasamudram, T.; Kincaid, J.F.; Boross, P.; Wang, Y.F.; Tie, Y.; Volarath, P.; Gaddis, L.; Harrison, R.W.; Weber, I.T.; Ghosh, A.K.; Mitsuya, H. Novel bis-tetrahydrofuranylurethane-containing nonpeptidic protease inhibitor (PI) UIC-94017 (TMC114) with potent activity against multi-PI resistant human immunodeficiency virus in vitro. *Antimicrob. Agents Chemother.*, **2003**, 47, 3123.
45. Gestwicki, J.E.; Crabtree, G.R.; Graef, I.A. Harnessing chaperones to generate small-molecule inhibitors of amyloid beta aggregation. *Science*, **2004**, 306, 865.
46. Briesewitz, R.; Ray, G.T.; Wandless, T.J.; Crabtree, G.R. Affinity modulation of small-molecule ligands by borrowing endogenous protein surfaces. *Proc. Natl. Acad. Sci. USA*, **1999**, 96, 1953.
47. Mathias, C.V.; Mathias, C.F.; Simões, M.J.; Amed, A.M.; Simões, R.S.; Oliveira-Filho, R.M.; Kulay, L. Jr. Safety of nelfinavir use during pregnancy: An experimental approach in rats. *Clin. Exp. Obstet. Gynecol.*, **2005**, 32, 163.
48. Stankunas, K.; Bayle, J.H.; Gestwicki, J.E.; Lin, Y.M.; Wandless, T.J.; Crabtree, G.R. Conditional protein alleles using knockin mice and a chemical inducer of dimerization. *Mol. Cell*, **2003**, 12, 1615.
49. Stankunas, K.; Bayle, J.H.; Havranek, J.J.; Wandless, T.J.; Baker, D.; Crabtree, G.R.; Gestwicki, J.E. Rescue of degradation-prone mutants of the FK506-rapamycin binding (FRB) protein with chemical ligands. *Chembiochem.*, **2007**, 8, 1162.

## Chapter IV

### Synthesis of Orthogonally Reactive FK506 Derivatives via Olefin Cross Metathesis

#### 4.1 Abstract

Chemical inducers of dimerization (CIDs) are employed in a wide range of biological applications to control protein localization, modulate protein–protein interactions and improve drug lifetimes. These bifunctional chemical probes are typically assembled from two synthetic modules, each providing affinity for a distinct protein target. FK506 and its derivatives are often employed as modules in the syntheses of these bifunctional constructs, owing to the abundance and favorable distribution of their target, FK506-binding protein (FKBP). However, the structural complexity of FK506 necessitates multi-step syntheses and/or multiple protection–deprotection schemes prior to installation into CIDs. In this work, we describe an efficient, one-step synthesis of FK506 derivatives through a selective, microwave-accelerated, cross metathesis diversification step of the C39 terminal alkene. Using this approach, FK506 is modified with an array of functional groups, including primary amines and carboxylic acids, making the resulting derivatives suitable for the modular assembly of CIDs. To illustrate this idea, we report the synthesis of a heterobifunctional HIV protease inhibitor. This approach is expected to allow rapid and modular synthesis of new bifunctional

compounds that are capable of binding FKBP.

#### 4.1.1 Selection of the FKBP Ligand in CID Systems

As introduced in Chapter 1, the natural product FK506 is a powerful immunosuppressant that functions through an intriguing mechanism in which it first interacts with the FK506-binding protein (FKBP), and then this complex binds tightly to the phosphatase calcineurin.<sup>2, 3</sup> This unusual binding property has been mirrored in synthetic tools termed chemical inducers of dimerization (CIDs).<sup>4-6</sup> CID systems have been employed in a broad range of applications, many focused on understanding signaling pathways, subcellular localization and protein-protein interactions.<sup>7-14</sup> Furthermore, as illustrated in Chapters 2 and 3, this platform has been used in drug discovery applications to modulate specificity, lifetime, and affinity.<sup>15-19</sup>

Despite this versatility, methods for the modular construction of CIDs have not been extensively explored. One notable exception is a study by the Verdine group that explored the systematic synthesis of compounds coupled to the synthetic ligand for FKBP (SLF).<sup>20</sup> SLF is an attractive chemical component because it is a non-immunosuppressive analog of FK506 that can be attached to other molecules via pendant anilines<sup>18</sup> or carboxylates.<sup>11, 21-23</sup> Although SLF has been used to synthesize many useful CIDs, there are limitations to this approach, including modest aqueous solubility and decreased affinity for FKBP (~10-fold compared to FK506).<sup>24</sup> In addition, SLF is challenging to use on a large scale

because its synthesis requires ~12 steps, with modest overall yield.<sup>21, 23, 24</sup> One alternative is to employ FK506 as a commercially available FKBP-binding ligand. In fact, this strategy was used to create the first CID, a homodimer of FK506 termed FK1012.<sup>7</sup> However, because of its structural complexity, manipulations of FK506 are challenging; for example, reported methods for preparing reactive intermediates require five steps with ~50% yield.<sup>7</sup>

#### **4.1.2 Cross Metathesis as a Synthetic Route to Functionalizing FK506**

We reasoned that an improved entry into reactive FK506 derivatives might involve selectively modifying the C39 alkene via cross metathesis (CM) using Grubbs' second generation ruthenium catalyst (GII).<sup>25</sup> The GII catalyst was chosen, in part, because it is tolerant of the many functional groups found in FK506, such as alcohols and ketones. In support of this idea, both the Wender and Schreiber groups have diversified complex natural products via CM at a terminal alkene.<sup>26, 27</sup> Another attractive feature of this approach is that the extracyclic C39 position of FK506 is crucial for binding calcineurin. Thus, modifications at this site would be expected to block immunosuppression without impacting the affinity for FKBP.<sup>28</sup> Consistent with this model, Clemons et al. used CM to selectively append bulky groups to the C39 position on FK506 to interrupt binding to calcineurin<sup>27</sup> and Diver and Schreiber used CM to produce FK1012-like homodimers, which are non-immunosuppressive but able to dimerize chimeric FKBP fusions.<sup>29</sup> Based on these studies, it was our goal to explore CM as a means to develop modular building blocks for rapidly creating



FKBP-binding CIDs.

## 4.2 Results

### 4.2.1 Optimization of Microwave Time and Temperature

Our initial efforts focused on optimizing the microwave-accelerated coupling between FK506 and a representative olefin, 3,4-epoxy-1-butene (Figure 4-1). Recently, Chapman et al. identified a surprisingly narrow window of conditions for efficient GII-mediated, microwave-accelerated, ring-closing metathesis on peptide substrates.<sup>30</sup> Guided by this effort, we systematically varied the reaction conditions and found that microwave irradiation for 5 min yielded good conversion rates (40–64%), while shorter (1–2 min) or longer (10–20 min) irradiation times reduced the yields (Figure 4-2A).

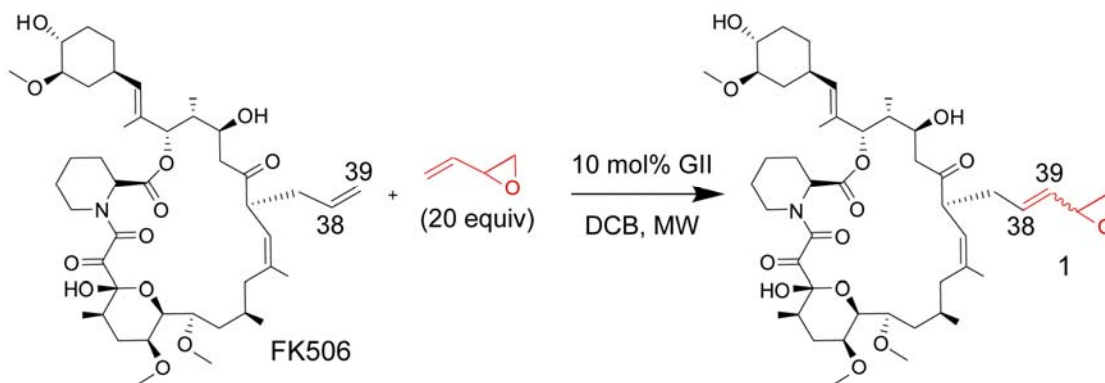


**Figure 4-1. Cross Metathesis of 3,4-epoxy-1-butene to FK506 Creates A Reactive Derivative (1).** Grubb's ruthenium catalyst (GII), FK506, and the epoxide-bearing olefin were irradiated in 1,2-dichlorobenzene (DCB).

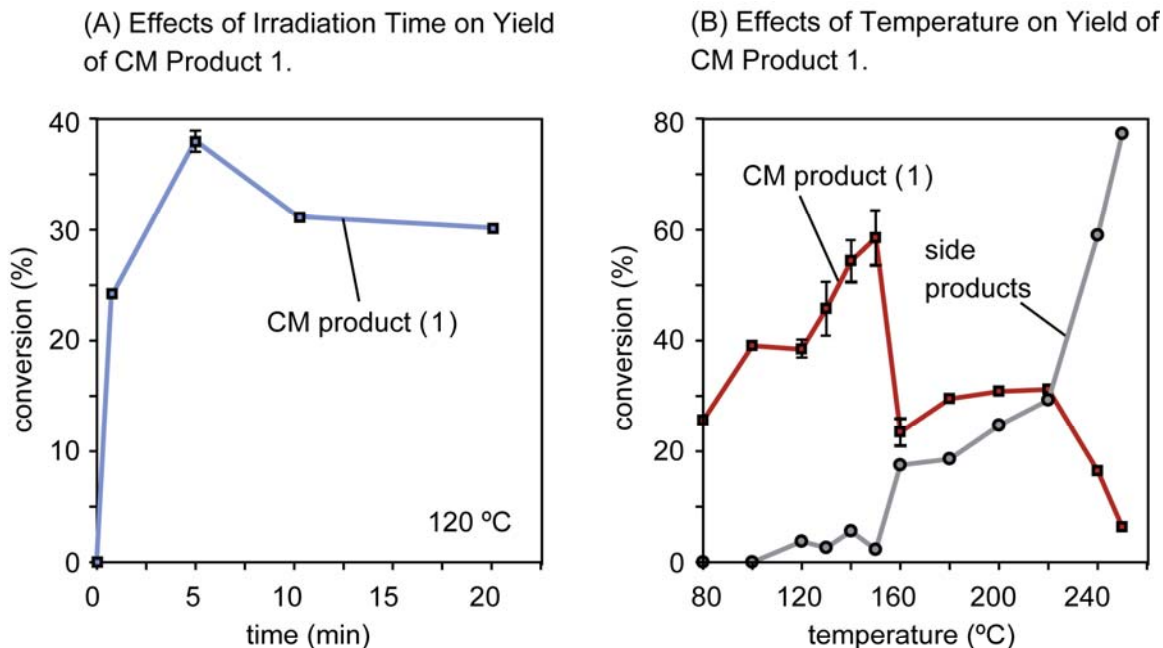


**Figure 4-2. Varying the Reaction Time and Temperature Reveals Optimal CM Conditions.** Results are the average of three independent reactions with the standard error shown. Yields were estimated from quantitative LC-MS profiles. DCB was used as the solvent in all the reactions.

Additionally, by varying temperature, we identified a clear peak of efficiency at 150°C. Higher temperatures resulted in lower yields and greater side-product formation, while reactions at lower temperatures consisted mostly of unreacted starting materials (Figure 4-2B). Importantly, when a 20-fold molar excess of the olefin was used, these reactions proceeded readily on unprotected FK506, while lower ratios favored formation of FK1012-like homodimers.

#### 4.2.2 Selection of Solvent

As the success of microwave-accelerated reactions is often dependent on absorption of microwave energy by the reaction medium, we examined a variety

of solvents and monitored production of the desired CM product (1) by liquid chromatography–mass spectrometry (LC–MS). Using this screening approach, we found that 1,2-dichlorobenzene (DCB) and 1,2-dichloroethane (DCE) resulted in the highest yielding reactions (61–64%; Table 4-1). Other solvents with strong dielectric constants, such as ethanol, were poor choices because of reagent insolubility.

**Table 4-1. Summary of Cross Metathesis Reactions Between FK506 and 3,4-epoxy-1-butene in Different Solvents (5 min, 150°C)**

Solvent	Yield (%)
1,2-DCB	64
1,2-DCE	61
DCM	Trace
DMF	20
ACN	3
Isopropanol	42
1-Butanol	18
EtOH	5
MeOH	4
DMSO	2

#### 4.2.3 Evaluation of Target Alkenes

With these results in hand, our next goal was to evaluate a series of target olefins. Structural and chemical diversity were key in our selection criteria, as we hoped to produce a range of FK506 intermediates containing orthogonally reactive electrophiles and nucleophiles for the “plug and play” synthesis of CIDs. Accordingly, we prepared a series of reactions using 21 different target olefins and 10% GII catalyst irradiated in a sealed tube at 150°C for 5 min in DCB

**Table 4-2. Summary of Cross Metathesis Reactions Between FK506 and Functionalized Olefins**

Olefin	Solvent	Yield (%)
None	DCB	4 (FK1012)
Acrylamide	DCB	99
Acrylic acid	DCB	99
Acrylic acid, succinimidyl ester	DCB	25
Acryloyl chloride	DCB	6
	Isopropanol	88
Allylamine	DCB	Trace
Allylbromide	DCB	11
Allylchloroformate	DCB	12
2-Allylchlorohexanone	DCB	44
Allylisothiocyanate	DCB	27
Allylisocyanate	DCB	22
N-Boc allylamine	DCB	50
3-Butene-1-ol	DCB	39
3-Butenylamine	DCB	5
	Isopropanol	2
3,4-Epoxy-1-butene	DCB	56
5-Hexenitrile	DCB	36
Methyl acrylate	DCB	97
5-Norbornene-2-carboxylic acid	DCB	8
	Isopropanol	7
4-Pentenoyl chloride	DCB	25
4-Pentynoic acid	DCB	Trace
	Isopropanol	Trace
4-Vinylaniline	DCB	5
4-Vinylbenzoic acid	DCB	79
	Isopropanol	9

(Table 4-2). Based on the work of Chatterjee et al., it was our hypothesis that target olefins bearing relatively bulky and electron-withdrawing groups might provide the highest yielding CM reactions.<sup>31</sup> In agreement with this concept, the compounds with carbonyls or carboxylates close to the reacting olefinic center had the highest conversion efficiency. For example, methyl acrylate gave an excellent yield (99%), as did olefins with acrylic or benzoic acids (79–99%).

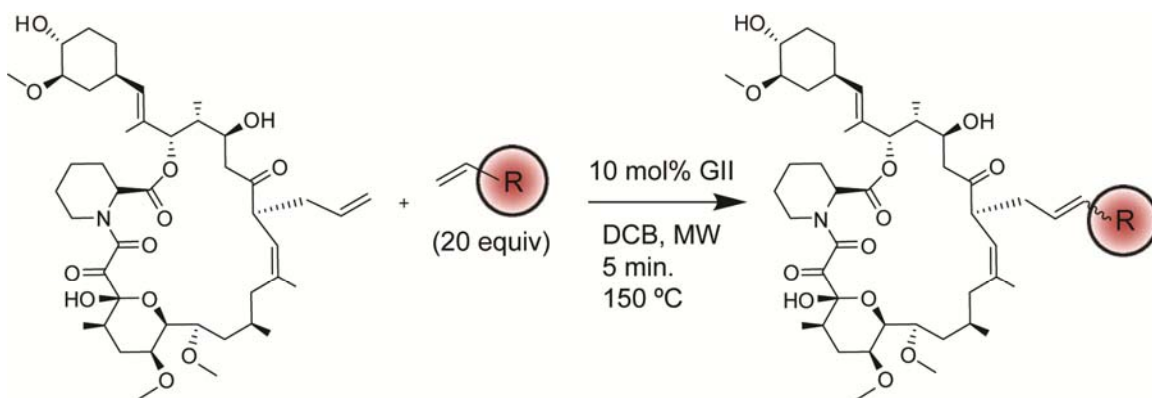
Some of the halogenated olefins, such as allyl bromide, had low yields, which MS experiments confirmed was due to the propensity of the unhindered allyl halide to undergo rapid, non-productive homodimerization. Poor yields were also observed for free amines, such as allylamine and 3-butenylamine (less than 5%), while protecting with Boc anhydride significantly improved reaction yield for the allylamine reaction (50%). Finally, for a subset of olefins that were only mildly soluble in DCB, we explored isopropanol as an alternative solvent. This strategy improved the solubility of all the chosen substrates and the yield of the CM reaction involving acryloyl chloride improved from 6% to 88%; however, this solvent did not significantly improve the reaction efficiency for the other olefins.

#### **4.2.4 Scaling the Synthesis of Reactive FK506 Derivatives**

From these studies, we selected FK506 derivatives with the most favorable combination of properties (e.g., yield, solubility, and reactive functionality) for re-synthesis and expanded studies. No effort was made to separate E and Z isomers, because these were found to be equally active in biological assays.<sup>29</sup> Following HPLC purification to remove trace amounts of unmodified FK506, a small collection of derivatives (**1–6**) suitable for the generation of CIDs was produced (Figure 4-3).

#### **4.2.5 A Novel Method for the Facile Removal of Ruthenium**

Because these molecules are intended for use in the exploration of biological systems, we were also interested in finding efficient ways to remove



compound	R=	yield	compound	R=	yield
1		55-60%	4		75-80%
2		>95%	5		35-40%
3		>95%	6*		45-50%

\*following Boc deprotection

**Figure 4-3. Synthesis of Reactive FK506 Derivatives.** From the screen of 21 olefins, these FK506 derivatives were chosen for re-synthesis, scale up and characterization. Yields are representative of at least two independent syntheses.

ruthenium byproducts. Even trace amounts of these organometallic complexes can lead to olefin isomerization, product decomposition, and cell toxicity. Several relevant purification methods have already been explored, including the use of tris(hydroxymethyl)phosphine, triphenylphosphine oxide, and dimethyl sulfoxide.<sup>32-34</sup> However, these procedures require multiple reagents, subsequent column chromatography, and relatively long exposure times for maximal efficacy. Here, we explored a quick and efficient strategy using silica-bonded equivalents

of the metal scavenger 1-propanethiol. We found that treatment of the crude reaction mixture with 5 equivalents of resin for 30 min reduced the levels of the ruthenium byproducts by greater than 50-fold (Figure 4-4). This simple method compared favorably to other approaches, especially in the minimal handling steps and short times required.

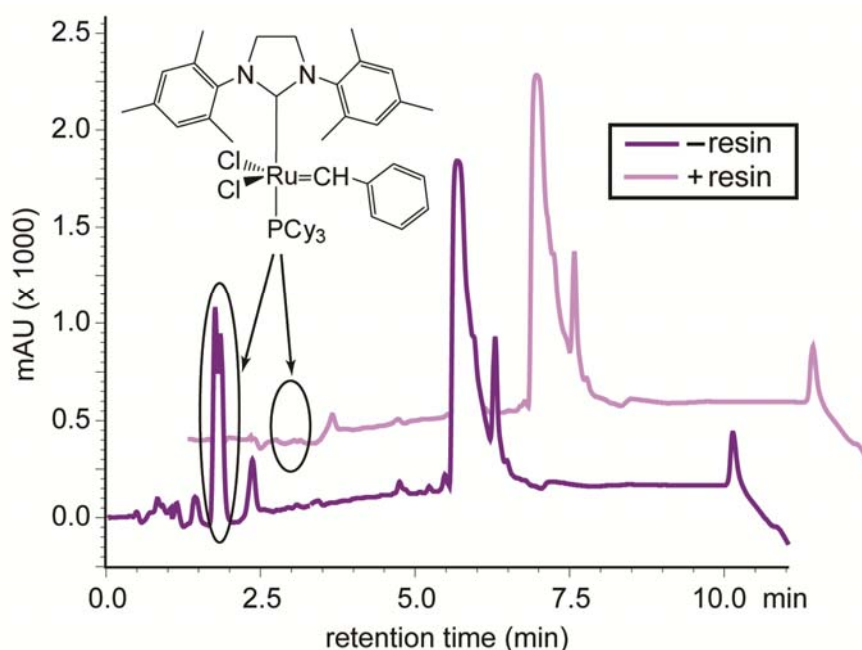


**Figure 4-4. Removal of Ruthenium Byproducts by Scavenger Resin.** LC-MS traces of a CM reaction between FK506 and 3,4-epoxy-1-butene is shown before and after treatment with 5 equiv of resin. The peak area of the ruthenium byproducts was reduced by greater than 50-fold, without any appreciable reductions in the product peak. Results are representative of the traces from other reactions.

#### 4.2.6 Design and Synthesis of an FK506-Bearing HIV Protease Inhibitor

One of the potential advantages of using FK506 as the protein-binding moiety in the synthesis of bifunctional molecules is its superior affinity for FKBP, especially when compared to SLF.<sup>24</sup> In Chapter 3, we reported that appending

SLF to an HIV protease inhibitor partitions the resulting molecule into blood cells and prolongs its lifetime >20-fold *in vivo*.<sup>35</sup> Evidence suggests that this improved persistence results from the modified compound being sequestered into the cytoplasm of the blood cells, an environment that contains high levels of FKBP but is nearly devoid of P450 enzymes that metabolize xenobiotics. Based on this model, we reasoned that cellular partitioning and drug lifetime might be sensitive to the affinity for FKBP.<sup>19</sup> Therefore, as a proof-of-concept for the present work, we sought to generate a fusion between FK506 and an HIV protease inhibitor, which would allow us to directly compare SLF- and FK506-conjugated molecules.

Based on these studies, we coupled the reactive FK506 derivative **2** in a single step to an Amprenavir-like core to yield the bifunctional molecule **7** (Figure 4-5). Coupling of the core to the FK506 derivative occurred through a pendant amine, which is known to be a well tolerated attachment point on the protease inhibitor (Figure 4-6).<sup>35, 36</sup>

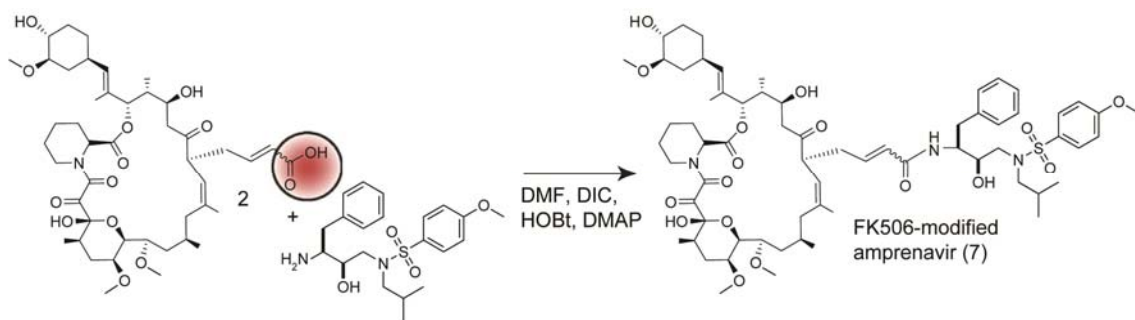


**Figure 4-5. Modular Synthesis of a Modified HIV Protease Inhibitor by Installation of FK506.** Reactive intermediate **2** was coupled to the known core of an HIV protease inhibitor to produce the bifunctional molecule **7** in good purified yield.



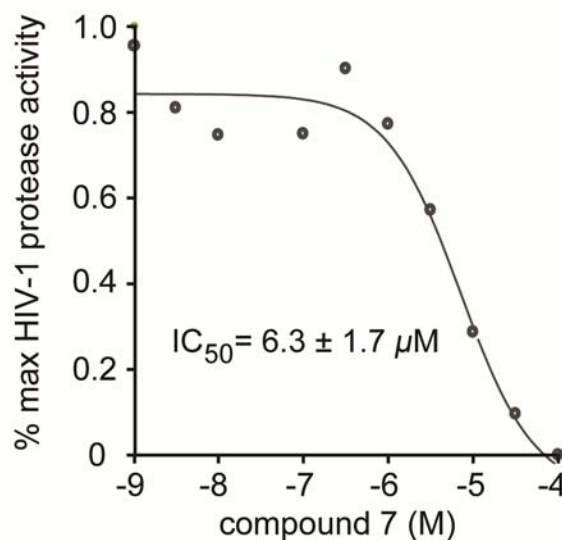


**Figure 4-6. An FK506-Modified Inhibitor Retains Anti-protease Activity *in vitro*.**  
Results are the average of triplicates.

#### 4.2.7 FK506-Functionalization Dramatically Alters Cellular Partitioning

To test the influence of FKBP binding on cellular partitioning, we first examined the distribution of 4-methoxy Amprenavir in whole blood and, consistent with the studies in Chapter 3, we found that it distributed evenly between the plasma and cellular compartments (Figure 4-7). Next, we confirmed that the corresponding SLF-modified derivative **8** showed a strong (~8-fold) preference for the cellular fraction (Figure 4-7).<sup>35</sup> Remarkably, the FK506-modified derivative **7** was concentrated by more than 22-fold in the FKBP-rich peripheral blood cells. Thus, replacing SLF with FK506 exaggerated cellular partitioning by almost three-fold, consistent with an important role for FKBP-binding affinity. These results clearly illustrate one advantage of using orthogonally reactive FK506 derivatives to synthesize new CIDs.

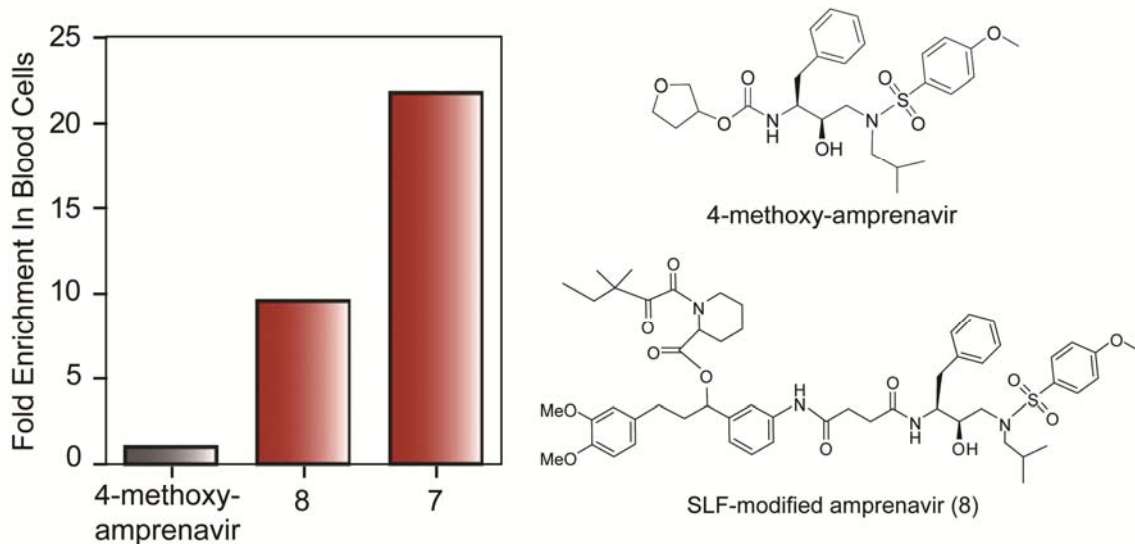


**Figure 4-7. An FK506-coupled HIV Protease Inhibitor is Partitioned into Blood Cells.** Fresh whole blood from male C57BL/6 mice was treated with either 4-methoxyamprenavir, SLF-conjugated amprenavir (8) or FK506-modified amprenavir (7) at 100  $\mu$ M. After 6 h at 37°C, whole blood was separated into plasma and cellular components by centrifugation and the compound in each fraction quantified by LC-MS. The fold partitioning was determined by dividing the cellular concentration by the concentration in the plasma. Error of triplicate experiments was approximately 10%.

#### 4.2.8. FKBP is Required for Partitioning *ex vivo*

As discussed in Chapter 3, binding to FKBP appears to be essential for effective partitioning of bifunctional molecules into cells. To further test this idea, we performed a competition experiment between the previously synthesized SLFavir and the FK506-derivatized protease inhibitor **7**. If FKBP is required, and cellular partitioning is indeed sensitive to the affinity of the ligand for FKBP, then the higher-affinity conjugate **7** should be able to dose-dependently displace the lower-affinity SLF-modified protease inhibitor in FKBP-rich cells. In agreement with this, when whole blood pre-treated with SLFavir for 30 minutes was challenged with a 10  $\mu$ M concentration of **7**, approximately 41% of the total SLFavir was found in the cellular component of blood (Figure 4-8A). However,

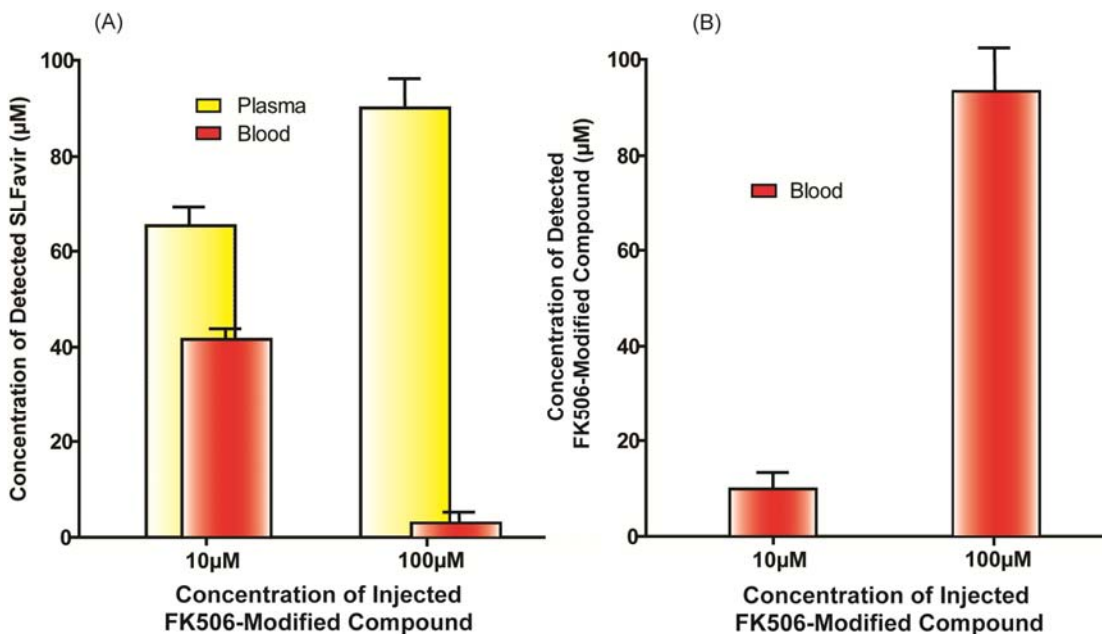


**Figure 4-8. SLFavir is Dose-Dependently Displaced by the Higher Affinity FK506-Modified Compound.** (A) Concentration of SLFavir in the plasma and in the blood. (B) Concentration of the FK506-modified compound in the cellular component of blood.

when the pre-treated blood was challenged with a 10-fold higher concentration of **7** (100 μM), only ~3% of the total SLFavir remained inside the cells, while the rest was displaced into the plasma (Figure 4-8A). The intracellular contents then consisted primarily of **7** (Figure 4-8B). This demonstrates that the affinity of the FKBP-binding group on bifunctional compounds determines the extent to which these molecules are sequestered into cells and seems to be one of the most critical structural design elements in our strategy.

#### 4.2.9 Appending Drugs to the C39 Position of FK506 Blocks Its Immunosuppressive Activity.

Another fundamental aspect of our design criteria is that bifunctional molecules are coupled through the C39 unsaturated terminal alkene on the

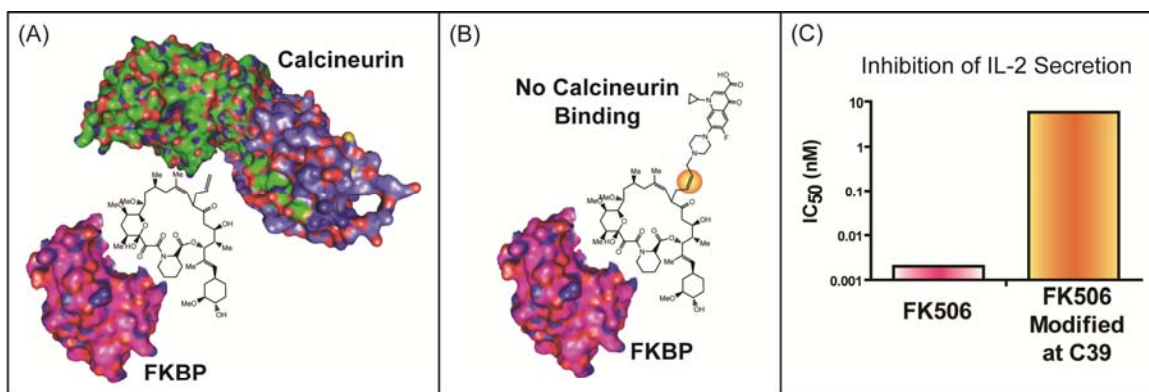


**Figure 4-9. Covalently Modifying the C39 Terminal Alkene of FK506 Disrupts Calcineurin Binding.** (A) The FKBP-FK506 complex can bind to calcineurin if the calcineurin-binding face is unobstructed. (B) Appending even small groups to the C39 terminal alkene of FK506 can disrupt its ability to bind to calcineurin. (C) Chemically modifying FK506 at this point severely impairs its immunosuppressive properties.

calcineurin-binding face of FK506 (Figure 4-9B). This area is critical to calcineurin's interaction with the FKBP-FK506 complex and results in downstream inhibition of IL-2 dependent T-cell activation. We imagined that appending bulky functional groups or other small molecules at this point would ablate FK506's immunosuppressive properties and assist the resulting bifunctional compound in avoiding off-target activities. To explicitly test this idea, we subjected FK506 and a few modified derivatives to immunosuppressive assays in collaboration with Amplyx Pharmaceuticals. These experiments revealed that appending relatively simple substituents at this terminal alkene resulted in a >3000-fold shift in immunosuppressive activity as measured by IL-2 secretion in Jurkat T cells (Figure 4-9C). The low, residual amount of IL-2 inhibitory activity seen in this assay is most likely due to an incomplete separation of the product from the parent FK506 during HPLC purification or product decomposition. Based on these findings, we conclude that conjugating small molecules through the C39 position of FK506 blocks its ability to bind

calcineurin, thereby effectively abolishing the immunosuppressive activity of the bifunctional compounds.

### **4.3 Discussion**

#### **4.3.1 Potential Implications of this Synthetic Route for the Rapid Creation of New CIDs**

The goal of this effort was to generate reactive building blocks for CID applications. Accordingly, we systematically investigated several reaction variables and identified conditions suitable for microwave-accelerated CM and diversification at the C39 position of FK506. Our efforts afforded reactive analogs (**1-6**), which display either electrophiles or nucleophiles. These derivatives are designed for facile installation into parent compounds bearing the corresponding functionality. One key feature of this strategy is that the reactive intermediates are accessed in a single step using unprotected FK506. During the course of these studies, we also explored a scavenger resin-based method for removing ruthenium byproducts, which may be particularly advantageous for parallel syntheses of CIDs. Finally, as demonstrated by the synthesis of the bifunctional protease inhibitor **7**, these methods are expected to provide a convenient and modular platform for creating FKBP-binding CIDs with exciting new properties.

### **4.4 Experimental Procedures**

#### **4.4.1 General Method for Cross Metathesis**

To a solution of FK506 (2.0 mg; 0.00249 mmol) in dichlorobenzene (2.0 mL)

was added the target olefin (20 equiv; 0.0498 mmol) followed by catalyst (0.1 equiv; 0.211 mg; 0.249  $\mu$ mol) in a microwave vial. The vial was then sparged with nitrogen, sealed, and placed in a Biotage Initiator EXP microwave reactor. The mixture was stirred for 30 s, followed by irradiation at the desired temperature and time. To achieve the desired temperature, the microwave power was typically ~20 W.

#### **4.4.2 Quantification of the Cross Metathesis Reaction**

To quantify reaction progress, crude mixtures were placed in 1.5 ml vials and analyzed with a Shimadzu (Columbia, MD) series 2010EV Liquid Chromatograph Mass Spectrometer equipped with an APCI probe to minimize ion suppression. Samples (5.0  $\mu$ L) were injected onto 1.8  $\mu$ m ZORBAX Eclipse XDB-C18 column (Agilent), and elution was performed with a stepwise 10–100% gradient of acetonitrile over 11 min. Products eluted between 5.5 and 6 min, while the peak for unreacted FK506 was found at 6.7 min. Quantification was performed using LCMSolution Version 2.05 using external standards.

#### **4.4.3 Synthetic Scale-Up of Select Reactions**

For the CM reactions that were selected for further analysis, the scale was increased 10-fold and the resulting crude reactions were treated with silica-immobilized, 1-propanethiol (5 equiv; Biotage; Isolute Si-Thiol) for 30 min, filtered and then the product was purified by preparative chromatography on a Waters Spherisorb S10 ODS2 column (10 - 250 mm). For compound 6, the crude

product was additionally treated with 5 equiv of 1:1 TFA:DCM, followed by dilution into DCM, neutralization with 5% sodium bicarbonate and concentration by rotoevaporation prior to HPLC.

#### **4.4.4 Synthesis of a Bifunctional Protease Inhibitor**

As a test of the modular assembly of bifunctional molecules, the reactive FK506 derivative **2** (1.0 equiv; 15.8 mg; 0.0186 mmol) was added to the advanced HIV protease inhibitor (1.2 equiv; 9.1 mg; 0.0224 mmol) in 3.0 mL of DMF with DIC (10.0 equiv; 29.2  $\mu$ L; 0.1863 mmol), HOBt (1.0 equiv; 2.5 mg; 0.1863 mmol) and DMAP (1.0 equiv; 2.3 mg; 0.1863 mmol). This reaction was stirred at room temperature overnight and the resulting product **7** purified in 75% yield by HPLC as described above. The blood partitioning experiments were performed as described.<sup>35</sup> The synthesis of the Amprenavir core structure and compound **8** have been reported.<sup>35</sup>

#### **4.4.5 *In vitro* Evaluation of Tacrolimavir**

To determine the inhibitory potency of compound **7**, a commercially available, FRET-based assay was used (Bachem, Torrance, CA), as previously reported.<sup>35</sup> Briefly, HIV-1 protease was preincubated with inhibitor for 60 min at 37 °C, followed by addition of 30 nM HIV-1 protease substrate **1** (Arg-Glu(EDANS)-Ser-Gln-Asn-Tyr-Pro-Ile-Val-Gln-Lys(dabcyl)-Arg; Molecular Probes, Eugene OR). Substrate cleavage was measured for 60 min. at 37°C by monitoring fluorescence at 490 nm on a SpectraMax M5 plate reader (Molecular

Devices, Mountain View, CA).

#### 4.4.6 *Ex vivo* Evaluation of Tacrolimavir

Stock solutions of **7** in dimethylsulfoxide (10 mM) were diluted into freshly collected mouse blood at a final concentration of 100  $\mu$ M. The samples were then incubated at 37°C for 1 hour with shaking. After centrifuging the samples at 3,706 rpm for 5 minutes, 100  $\mu$ L of blood or plasma was added to a 1.5 mL polypropylene microcentrifuge tube, followed by protein precipitation with 100  $\mu$ L of a 0.1 M aqueous zinc sulfate and immediate vortexing for 30 s. Analytical grade acetonitrile (ACN) was then added (800  $\mu$ L) and the sample was vortexed again for 30 s. Following high-speed centrifugation at 13,200 rpm for 10 minutes, the supernatant was transferred to a glass vial and subjected to LC-MS analysis.

#### 4.5 Appendix of Selected Spectra

##### 4.5.1 FK506 Coupled to 3,4-Epoxy-1-butene (**1**)

Molecular formula  $C_{46}H_{71}NO_{13}$ ;  $^1H$  NMR (dDMSO; ppm):  $\delta$  7.6(s),  $\delta$  7.2(s),  $\delta$  6.6-6.68(bs),  $\delta$  5.7(m),  $\delta$  5.65(t),  $\delta$  5.6(m),  $\delta$  5.55(t),  $\delta$  5.46-5.52(dd),  $\delta$  5.4-5.46(m),  $\delta$  5.26-5.3(m),  $\delta$  5.2-5.26(dd),  $\delta$  5.12-5.2(m),  $\delta$  5.0-5.1(m),  $\delta$  4.84-4.9(m),  $\delta$  4.74-4.8(t),  $\delta$  4.64-4.74(m),  $\delta$  4.5-4.58(m),  $\delta$  4.2-4.3(d),  $\delta$  3.9(s),  $\delta$  3.6(d),  $\delta$  3.5-3.55(m),  $\delta$  3.4(m),  $\delta$  3.35-3.4(s),  $\delta$  3.35(m),  $\delta$  3.3-3.5(m),  $\delta$  3.3(d),  $\delta$  3.25-3.3(dd),  $\delta$  3.2-3.25(s),  $\delta$  2.9-3.0(m),  $\delta$  2.2-2.3(d),  $\delta$  2.0-2.1(m),  $\delta$  1.8-1.95(m),  $\delta$  1.7-1.8(d),  $\delta$  1.65-1.7(t),  $\delta$  1.65(d),  $\delta$  1.6(d),  $\delta$  1.5(d),  $\delta$  1.2-1.3(m),  $\delta$  1(m),  $\delta$  0.7-0.9(m),  $\delta$  0.1(s).



#### 4.5.2 FK506 Coupled to Acrylic Acid (2)

Molecular formula  $C_{45}H_{69}NO_{14}$ ;  $^1H$  NMR (dDMSO; ppm):  $\delta$  6.9-7.1(bm),  $\delta$  6.7(m),  $\delta$  5.7-5.8(dd),  $\delta$  5.4(m),  $\delta$  5.26(d),  $\delta$  5.1-5.16(d),  $\delta$  5.04-5.1(d),  $\delta$  4.8(d),  $\delta$  4.7(d),  $\delta$  4.44(s),  $\delta$  4.24-4.4(bs),  $\delta$  4.2-4.24(d),  $\delta$  3.9(m),  $\delta$  3.72(d),  $\delta$  3.6(d),  $\delta$  3.52(m),  $\delta$  3.3-3.36(m),  $\delta$  3.26-3.3(m),  $\delta$  3.2-3.24(d),  $\delta$  3.18(s),  $\delta$  2.94(m),  $\delta$  2.6-2.7(m),  $\delta$  2.58(d),  $\delta$  2.2-2.3(m),  $\delta$  2.1(d),  $\delta$  1.9(d),  $\delta$  1.8(m),  $\delta$  1.72(d),  $\delta$  1.7(s),  $\delta$  1.64-1.66(d),  $\delta$  1.6-1.62(d),  $\delta$  1.57(s),  $\delta$  1.55(s),  $\delta$  1.26-1.54(m),  $\delta$  1.0-1.06(m),  $\delta$  0.8-0.9(m),  $\delta$  0,74(d).

#### 4.5.3 FK506 Coupled to Acrylamide (3)

Molecular formula  $C_{45}H_{70}N_2O_{13}$ ;  $^1H$  NMR (dDMSO; ppm):  $\delta$  7.3(d),  $\delta$  6.9(d),  $\delta$  6.5(m),  $\delta$  5.8-5.9(m),  $\delta$  5.25(d),  $\delta$  5.15(d),  $\delta$  5.1(d),  $\delta$  5.05(d),  $\delta$  4.8(d),  $\delta$  4.7(d),  $\delta$  4.45(s),  $\delta$  4.25(d),  $\delta$  3.96-4.2(bs),  $\delta$  3.9(m),  $\delta$  3.7(dd),  $\delta$  3.6(d),  $\delta$  3.55(d),  $\delta$  3.45(m),  $\delta$  3.3(d),  $\delta$  3.27(d),  $\delta$  3.21(s),  $\delta$  2.9-2.96(m),  $\delta$  2.6-2.8(m),  $\delta$  2.58(s),  $\delta$  2.42-2.5(m),  $\delta$  2.4(m),  $\delta$  2.2-2.3(m),  $\delta$  2.15-2.2(m),  $\delta$  2.06-2.1(m),  $\delta$  1.85-1.96(m),  $\delta$  1.8(m),  $\delta$  1.7(s),  $\delta$  1.64(s),  $\delta$  1.6(s),  $\delta$  1.54(s),  $\delta$  1.46-1.5(m),  $\delta$  1.24-1.36(m),  $\delta$  1.2(t),  $\delta$  1.03(t),  $\delta$  0.87(d),  $\delta$  0.78-0.84(m), 0.76(d).

#### 4.5.4 FK506 Coupled to 4-Vinylbenzoic Acid (4)

Molecular formula  $C_{51}H_{73}NO_{14}$ ;  $^1H$  NMR (dDMSO; ppm):  $\delta$  12.7- 13.0(bs),  $\delta$  7.87-7.9(d),  $\delta$  7.3-7.5(t),  $\delta$  7.0-7.1(d),  $\delta$  6.6(s),  $\delta$  6.4(d),  $\delta$  6.25-6.3(m),  $\delta$  5.2(d),  $\delta$  5.0-5.1(m),  $\delta$  4.8(d),  $\delta$  4.7(d),  $\delta$  4.4(s),  $\delta$  4.2(d),  $\delta$  3.8-3.9(bs),  $\delta$  3.25-3.3(d),  $\delta$  3.2-3.24(s),  $\delta$  3.15-3.2(s),  $\delta$  2.8-2.9(bm),  $\delta$  2.4-2.5(s),  $\delta$  2.3(s),  $\delta$  1.8-2.2(m),  $\delta$

2.0-2.05(m), δ 1.75-1.90(m), δ 1.55-1.65(d), δ 1.5(s), δ 1.48(s), δ 1.05-1.3(m), δ 0.7-0.85(m).

#### 4.5.5 FK506 Coupled to 4-Hexenitrile (5)

Molecular formula  $C_{48}H_{74}N_2O_{12}$ ;  $^1H$  NMR (dDMSO; ppm): δ 7.12(s), 7.05(d), δ 6.64(s), δ 5.64-5.74(m), δ 5.3-5.9(m), δ 5.25(d), δ 5.14(d), δ 5.09(d), δ 5.06(m), δ 5.03(m), δ 5.0(m), δ 4.96(d), δ 4.8(t), δ 4.7(d), δ 4.47(s), δ 4.24(d), δ 3.88(bs), δ 3.6(d), δ 3.54(d), δ 3.45(m), δ 3.33(m), δ 3.28(d), δ 3.22(s), δ 2.9-2.97(m), δ 2.8(t), δ 2.67(d), δ 2.48(m), δ 2.44(t), δ 2.38(s), δ 2.32(s), δ 2.22-2.3(m), δ 2.17(d), δ 2.04-2.12(m), δ 2.02(d), δ 1.84-1.94(m), δ 1.8(d), δ 1.78(d), δ 1.76(d), δ 1.7(d), δ 1.68(d), δ 1.65(d), δ 1.6(s), δ 1.54(s), δ 1.46-1.5(m), δ 1.24-1.4(m), δ 1.1(d), δ 1.04(d), δ 0.9(s), δ 0.78-0.9(m), δ 0.76(d).

#### 4.5.6 FK506 Coupled to N-Boc Allyl Amine (6)

Molecular formula  $C_{45}H_{72}N_2O_{12}$ ;  $^1H$  NMR (dDMSO; ppm): δ 7.301(s), δ 7.216(s), δ 7.13(s), δ 5.685(m), δ 5.525(d), δ 5.48(m), δ 5.432-5.440(d), δ 5.418(bs), δ 5.38(d), δ 5.247(d), δ 5.245(d), δ 5.11-5.14(dd), δ 5.07(d), δ 5.036-5.051(d), δ 4.944(t), δ 4.835-4.895(m), δ 4.785(t), δ 4.695(d), δ 4.506(d), δ 4.461(d), δ 4.442(s), δ 4.430(s), δ 4.415(s), δ 4.40(s), δ 4.236-4.256(d), δ 4.187-4.211(t), δ 4.12(t), δ 3.931(m), δ 3.84-3.90(m), δ 3.595-3.612(d), δ 3.471-3.532(dd), 3.458-3.471(d), δ 3.323(s), δ 3.272-3.288(dd), δ 3.227(d), δ 2.921-2.953(m), δ 2.82(t), δ 2.75(bm), 2.625-2.68(dd), δ 2.42(t), δ 2.374(s), δ 2.359(d), δ 2.266(m), δ 2.162-2.185(d), δ 2.105(m), δ 1.882(dd), δ 1.785(m), δ 1.705(s), δ

1.656(s),  $\delta$  1.541-1.606(dd),  $\delta$  1.458-1.49(m), 1.397(d),  $\delta$  1.263-1.324(m),  $\delta$  1.08-1.12(m),  $\delta$  1.025(m), 0.892(d),  $\delta$  0.864(m),  $\delta$  0.815-0.837(dd),  $\delta$  0.795(d),  $\delta$  0.782-0.793(t),  $\delta$  0.765(d).

#### 4.5.7 FK506 Coupled to an HIV Protease Inhibitor (7)

Molecular formula  $C_{66}H_{97}N_3O_{17}S$ ; expected mass (m/z) = 1236.55; actual mass (m/z) = 1235.95.  $^1H$  NMR (dDMSO; ppm):  $\delta$  7.74(d),  $\delta$  7.63(s),  $\delta$  7.57(d),  $\delta$  7.51(s),  $\delta$  7.44(d),  $\delta$  7.36(s),  $\delta$  7.28(t),  $\delta$  7.19(s),  $\delta$  7.11(t),  $\delta$  6.9(d),  $\delta$  6.86(d),  $\delta$  5.42(s),  $\delta$  5.36(s),  $\delta$  5.27(s),  $\delta$  5.125(dd),  $\delta$  5.04(d),  $\delta$  4.8(m),  $\delta$  4.7(d),  $\delta$  4.6(s),  $\delta$  4.48(s),  $\delta$  4.24(d),  $\delta$  3.9(s),  $\delta$  3.87(d),  $\delta$  3.81(s),  $\delta$  3.78(s),  $\delta$  3.71(s),  $\delta$  3.62(d),  $\delta$  3.54(d),  $\delta$  3.41(dd),  $\delta$  3.33(d),  $\delta$  3.28(d),  $\delta$  3.22(s),  $\delta$  2.9–3.08(m),  $\delta$  2.91(d),  $\delta$  2.78(m),  $\delta$  2.72(m),  $\delta$  2.27(s),  $\delta$  2.1(s),  $\delta$  2.0(m),  $\delta$  1.92(s),  $\delta$  1.86(m),  $\delta$  1.8(d),  $\delta$  1.72(d),  $\delta$  1.65(d),  $\delta$  1.62(s),  $\delta$  1.55(s),  $\delta$  1.48(m),  $\delta$  1.39(s),  $\delta$  1.26(t),  $\delta$  1.21(t),  $\delta$  1.14(t),  $\delta$  1.03(m),  $\delta$  0.86(d),  $\delta$  0.81(d),  $\delta$  0.79(d),  $\delta$  0.73(d).

## Notes

Portions of this work have been published as “Microwave-Assisted Organic Synthesis of Orthogonally Reactive FK506-Derivatives via Olefin Cross Metathesis,” Marinec, P. S., Evans, C. G., Gibbons, G. S., Tarnowski, M. A., Overbeek, D. L., and Gestwicki, J. E., *Bioorganic Medicinal Chemistry*, 2009, 17: 5763-5768.

P. S. Marinec and J. E. Gestwicki designed the experiments and prepared the manuscript. P. S. Marinec and G. S. Gibbons performed the synthetic work and *ex vivo* experiments. P. S. Marinec, G. S. Gibbons, M. A. Tarnowski, and D. L. Overbeek performed the LC-MS analysis. C. G. Evans was responsible for the NMR characterization of all the compounds.

## 4.6 References

1. Dumont, F. J. FK506, an immunosuppressant targeting calcineurin function. *Curr. Med. Chem.*, **2000**, 7, 731.
2. Liu, J.; Albers, M. W.; Wandless, T. J.; Luan, S.; Alberg, D. G.; Belshaw, P. J.; Cohen, P.; MacKintosh, C.; Klee, C. B.; Schreiber, S. L. Inhibition of T cell signaling by immunophilin-ligand complexes correlates with loss of calcineurin phosphatase activity. *Biochemistry*, **1992**, 31, 3896.
3. Griffith, J. P.; Kim, J. L.; Kim, E. E.; Sintchak, M. D.; Thomson, J. A.; Fitzgibbon, M. J.; Fleming, M. A.; Caron, P. R.; Hsiao, K.; Navia, M. A. X-ray structure of calcineurin inhibited by the immunophilin-immunosuppressant FKBP12-FK506 complex. *Cell*, **1995**, 82, 507.
4. Lin, H.; Cornish, V. W. In Vivo Protein-Protein Interaction Assays: Beyond Proteins. *Angew. Chem. Int. Ed.*, **2001**, 40, 871.
5. Clackson, T. Dissecting the functions of proteins and pathways using chemically induced dimerization. *Chem. Biol. Drug Des.*, **2006**, 67, 440.
6. Gestwicki, J. E.; Marinec, P. S. Chemical control over protein-protein interactions: beyond inhibitors. *Comb. Chem. High Throughput Screen.*, **2007**, 10, 667.
7. Spencer, D. M.; Wandless, T. J.; Schreiber, S. L.; Crabtree, G. R. Controlling signal transduction with synthetic ligands. *Science*, **1993**, 262, 1019.
8. Belshaw, P.J.; Ho, S.N.; Crabtree, G. R.; Schreiber, S.L. Controlling protein association and subcellular localization with a synthetic ligand that induces heterodimerization of proteins. *Proc. Natl. Acad. Sci. USA*, **1996**, 93, 4604.
9. Pownall, M. E.; Welm, B. E.; Freeman, K. W.; Spencer, D. M.; Rosen, J. M.; Isaacs, H. V. An inducible system for the study of FGF signalling in early amphibian development. *Dev. Biol.*, **2003**, 256, 89.
10. de Graffenried, C. L.; Laughlin, S. T.; Kohler, J. J.; Bertozzi, C. R. A small-molecule switch for Golgi sulfotransferases. *Proc. Natl. Acad. Sci. U.S.A.*, **2004**, 101, 16715.
11. Gestwicki, J.E.; Crabtree, G.R.; Graef, I.A. Harnessing chaperones to generate small-molecule inhibitors of amyloid beta aggregation. *Science*, **2004**, 306, 865.

12. Karpova, A.Y.; Tervo, D.G.; Gray, N.W.; Svoboda, K. Rapid and reversible chemical inactivation of synaptic transmission in genetically targeted neurons. *Neuron*, **2005**, *48*, 727.
13. Haruki, H.; Nishikawa, J.; Laemmli, U.K. The anchor-away technique: rapid, conditional establishment of yeast mutant phenotypes. *Mol. Cell.*, **2008**, *31*, 925.
14. Geda, P.; Patury, S.; Ma, J.; Bharucha, N.; Dobry, C.J.; Lawson, S.K.; Gestwicki, J.E.; Kumar, A. A small molecule-directed approach to control protein localization and function. *Yeast*, **2008**, *25*, 577.
15. Briesewitz, R.; Ray, G.T.; Wandless, T.J.; Crabtree, G.R. Affinity modulation of small-molecule ligands by borrowing endogenous protein surfaces. *Proc. Natl. Acad. Sci. USA*, **1999**, *96*, 1953.
16. Pollock, R.; Giel, M.; Linher, K.; Clackson, T. Regulation of endogenous gene expression with a small-molecule dimerizer. *Nat. Biotechnol.*, **2002**, *20*, 729.
17. Baker, K.; Bleczinski, C.; Lin, H.; Salazar-Jimenez, G.; Sengupta, D.; Krane, S.; Cornish, V. W. Chemical complementation: a reaction-independent genetic assay for enzyme catalysis. *Proc. Natl. Acad. Sci. U.S.A.*, **2002**, *99*, 16537.
18. Braun, P.D.; Barglow, K.T.; Lin, Y.M.; Akompong, T.; Briesewitz, R.; Ray, G.T.; Haldar, K.; Wandless, T.J. A bifunctional molecule that displays context-dependent cellular activity. *J. Am. Chem. Soc.*, **2003**, *125*, 7575.
19. Marinec, P. S.; Lancia, J. K.; Gestwicki, J. E. Bifunctional molecules evade cytochrome P(450) metabolism by forming protective complexes with FK506-binding protein. *Mol. Biosyst.*, **2008**, *4*, 571.
20. Koide, K.; Finkelstein, J. M.; Ball, Z.; Verdine, G. L. A synthetic library of cell-permeable molecules. *J. Am. Chem. Soc.*, **2001**, *123*, 398.
21. Amara, J.F.; Clackson, T.; Rivera, V.M.; Guo, T.; Keenan, T.; Natesan, S.; Pollock, R.; Yang, W.; Courage, N.L.; Holt, D.A.; Gilman, M. A versatile synthetic dimerizer for the regulation of protein-protein interactions. *Proc. Natl. Acad. Sci. USA*, **1997**, *94*, 10618.
22. Keenan, T.; Yaeger, D. R.; Courage, N. L.; Rollins, C. T.; Pavone, M. E.; Rivera, V.M.; Yang, W.; Guo, T.; Amara, J. F.; Clackson, T.; Gilman, M.; Holt, D. A. Synthesis and activity of bivalent FKBP12 ligands for the regulated dimerization of proteins. *Bioorg. Med. Chem.*, **1998**, *6*, 1309.

23. Clackson, T.; Yang, W.; Rozamus, L.W.; Hatada, M.; Amara, J.F.; Rollins, C.T.; Stevenson, L.F.; Magari, S.R.; Wood, S.A.; Courage, N.L.; Lu, X.; Cerasoli, F. Jr.; Gilman, M.; Holt, D.A. Redesigning an FKBP-ligand interface to generate chemical dimerizers with novel specificity. *Proc. Natl. Acad. Sci. USA*, **1998**, 95, 10437.
24. Holt, D. A.; Luengo, J. I.; Yamashita, D. S.; Oh, H.-J.; Konialian, A. L.; Yen, H.-K.; Rozamus, L. W.; Brandt, M.; Bossard, M. J.; Levy, M. A.; Eggelston, D. S.; Liang, J.; Schultz, L. W.; Stout, T. J.; Clardy, J. Design, synthesis, and kinetic evaluation of high-affinity FKBP ligands and the X-ray crystal structures of their complexes with FKBP12. *J. Am. Chem. Soc.*, **1993**, 115, 9925.
25. Hoveyda, A. H.; Zhugralin, A. R. The remarkable metal-catalysed olefin metathesis reaction. *Nature*, **2007**, 450, 243.
26. Wender, P. A.; Hilinski, M. K.; Skaanderup, P. R.; Soldermann, N. G.; Mooberry, S. L. Pharmacophore mapping in the laulimalide series: total synthesis of a vinylogue for a late-stage metathesis diversification strategy. *Org. Lett.*, **2006**, 8, 4105.
27. Clemons, P. A.; Gladstone, B. G.; Seth, A.; Chao, E. D.; Foley, M. A.; Schreiber, S. L. Synthesis of calcineurin-resistant derivatives of FK506 and selection of compensatory receptors. *Chem. Biol.*, **2002**, 9, 49.
28. Dumont, F. J.; Staruch, M. J.; Koprak, S. L.; Siekierka, J. J.; Lin, C. S.; Harrison, R.; Sewell, T.; Kindt, V. M.; Beattie, T. R.; Wyvratt, M. The immunosuppressive and toxic effects of FK-506 are mechanistically related: pharmacology of a novel antagonist of FK-506 and rapamycin. *J. Exp. Med.*, **1992**, 176, 751.
29. Diver, S. T.; Schreiber, S. L. Single-Step Synthesis of Cell-Permeable Protein Dimerizers That Activate Signal Transduction and Gene Expression. *J. Am. Chem. Soc.*, **1997**, 119, 5106.
30. Chapman, R. N.; Arora, P. S. Optimized synthesis of hydrogen-bond surrogate helices: surprising effects of microwave heating on the activity of Grubbs catalysts. *Org. Lett.*, **2006**, 8, 5825.
31. Chatterjee, A. K.; Choi, T. L.; Sanders, D. P.; Grubbs, R. H. A general model for selectivity in olefin cross metathesis. *J. Am. Chem. Soc.*, **2003**, 125, 11360.

32. Ahn, Y. M.; Yang, K.; Georg, G. I. A convenient method for the efficient removal of ruthenium byproducts generated during olefin metathesis reactions. *Org. Lett.*, **2001**, 3, 1411.
33. Hong, S. H.; Grubbs, R. H. Efficient removal of ruthenium byproducts from olefin metathesis products by simple aqueous extraction. *Org. Lett.*, **2007**, 9, 1955.
34. Haack, K.; Ahn, Y. M.; Georg, G. I. A convenient method to remove ruthenium byproducts from olefin metathesis reactions using polymer-bound triphenylphosphine oxide (TPPO). *Mol. Divers.*, **2005**, 9, 301.
35. Marinec, P. S.; Chen, L.; Barr, K. J.; Mutz, M. W.; Crabtree, G. R.; Gestwicki, J.E. FK506-binding protein (FKBP) partitions a modified HIV protease inhibitor into blood cells and prolongs its lifetime in vivo. *Proc. Natl. Acad. Sci. U.S.A.*, **2009**, 106, 1336.
36. Surleraux, D. L.; Tahri, A.; Verschueren, W. G.; Pille, G. M.; de Kock, H. A.; Jonckers, T. H.; Peeters, A.; De Meyer, S.; Azijn, H.; Pauwels, R.; de Bethune, M.P.; King, N. M.; Prabu-Jeyabalan, M.; Schiffer, C. A.; Wigerinck, P. B. Discovery and selection of TMC114, a next generation HIV-1 protease inhibitor. *J. Med. Chem.*, **2005**, 48, 1813.



## Chapter V

### Conclusions & Future Directions

#### 5.1 Conclusions

Despite the extraordinary advances in drug development over the last three decades, the acquired immunodeficiency syndrome is now a pandemic of staggering proportions. The World Health Organization estimates that over 35.8 million people worldwide are currently living with the virus that causes AIDS, including 3.0 million people newly infected in 2008. Perhaps even more unnerving is the fact that AIDS has killed over 29 million people since it was first recognized just over 29 years ago, making it one of the deadliest epidemics in human history. Unfortunately, the current generation of antiretroviral therapeutics is only partially and temporarily effective in suppressing viral replication and is plagued by poor pharmacokinetics, debilitating side effects, severe liver toxicity, and drug resistance. While combination therapies such as HAART have somewhat curbed the mortality rate from opportunistic infections due to AIDS, a new person is infected with the HIV retrovirus every six seconds. This last staggering statistic just reemphasizes the fact that there is a real burden on us as scientists and more importantly, as innovators, to develop novel approaches for both treating and preventing the spread of this malignant disease.

### 5.1.1 A Look Back

Five years ago, we began exploring the intriguing mechanism of action behind the most unusual pharmacology of FK506. How can it be that this molecule defies each and every rule of drug-likeness, yet still exhibits such a pervasive pharmacokinetic profile? These studies proved to be illuminating with respect to understanding an elaborate, molecular mechanism for avoiding hepatic extraction and metabolic interrogation: hiding within cells. Our research then led to the discovery that it's possible to synthetically endow other xenobiotics with a mercurial propensity for degradation with this same cloaking technology through covalent appendage to an FKBP-binding group. As demonstrated in Chapter 3 with SLFavir, synthetically attaching an FKBP-binding moiety onto an existing, clinically used HIV-1 protease inhibitor improved its plasma lifetime >20-fold in a mouse model. This drastic shift in pharmacokinetics is roughly equivalent to a half-life of over 50 hours in humans, a value unheard of in even the most promising of current generation antivirals. What also makes this strategy particularly attractive is that, unlike most prodrug approaches that require enzymatic processing to release the active form of the drug, SLFavir retains nanomolar potency against HIV-1 protease without any prior modification.

In an effort to expand the repertoire of chemical functionalities amenable to our “nature-inspired” bifunctional strategy, we systematically investigated a number of synthetic variables and reaction parameters in order to identify an ideal set of conditions suitable for microwave-accelerated cross metathesis. This

led to the synthesis of a library of reactive FK506 analogs designed for facile installation onto a variety of target compounds. We demonstrated the effectiveness of this platform technology in the rapid assembly of Tacrolimavir, an FK506-bearing HIV-1 protease inhibitor that exhibited an even higher degree of cellular partitioning than the prototypical SLFavir. We expect the technology that was developed over the course of my doctoral research to result in an arsenal of new and exciting compounds in the fight against HIV.

In conclusion, chemical inducers of dimerization are of tremendous utility in modern chemical biology. Inspired by the natural products rapamycin and FK506, these CID systems have played integral roles in manipulating vast networks of protein-protein interactions, both inhibiting these physical connections as well as promoting them. During my thesis, however, we explored a conceptually different use for CIDs: enhancing the pharmacology of small molecules. Our work has uncovered an entirely new property inherent in the already fascinating chemical structure of FK506, and greatly expands the utility of chemical inducers of dimerization in biological systems. We consider these results critical to the development of next generation therapeutics for the treatment of HIV, and it is our hope that the basic principles and novel technologies described within this dissertation will lead to profoundly innovative solutions for curbing the spread of infectious diseases worldwide.

## 5.2 Future Directions

### 5.2.1 The Promise of FKBP-Binding Antibiotics

Given the modularity of the chemical platform developed in Chapter 4, we suspect that our bifunctional approach to enhancing pharmacokinetics may be a general strategy applicable to myriad compounds across diverse drug classes. Importantly, this strategy might be exploited with antibiotics, as the therapeutic treatment of infectious disease remains a critical, worldwide problem. Analogous to antivirals, the fundamental concern with antibiotics is rapid metabolism, as most of the currently prescribed drugs are good substrates for metabolic enzymes and exhibit lifetimes drastically shorter than even HIV-1 protease inhibitors. For example, the broad-spectrum antimicrobial ampicillin has a half-life of only 60 minutes and is fully cleared from the human body within 5 to 6 hours. To maintain adequate therapeutic concentrations, this and other beta-lactams are often dosed multiple times per day; however the high pill burdens are known to reduce patient compliance, and importantly, provide the opportunity for resistance to emerge. Novel approaches for prolonging the lifetimes of these antimicrobial agents would be expected to directly impact this problem.

Based on the promising results obtained with SLFavir, it is our hypothesis that adding FKBP-binding groups to other anti-infective agents, such as beta-lactam antibiotics, might enhance their lifetimes as well. This property could be exploited to elevate circulating drug concentrations, improve dosing schedules, and possibly, reduce the incidence of mutations.

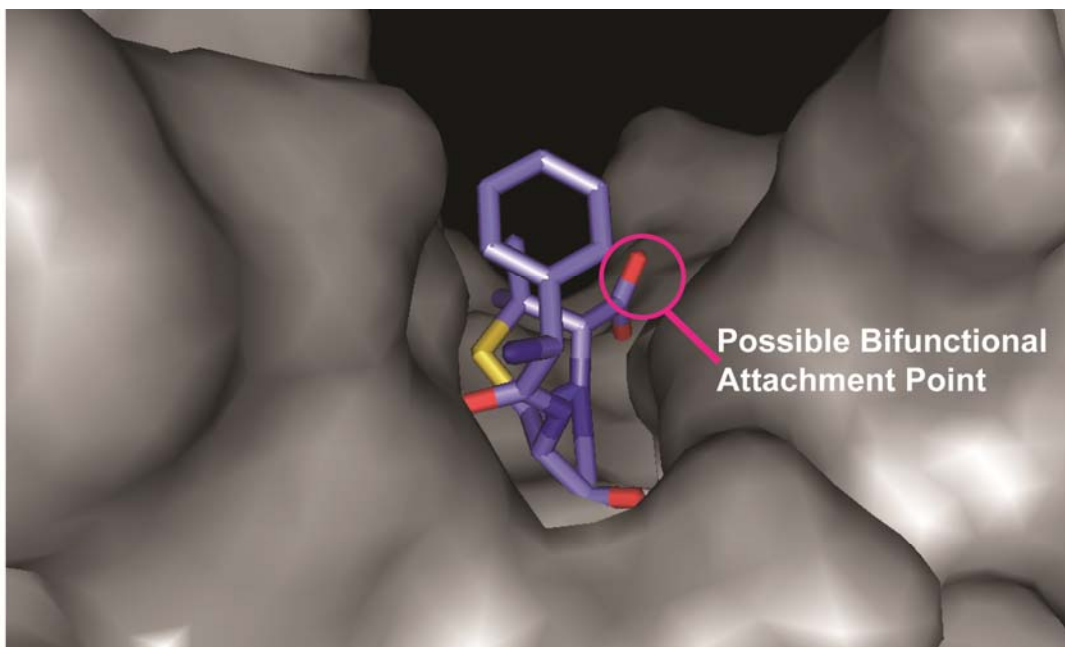


**Figure 5-1. Crystal Structure of Ampicillin Bound to Penicillin Binding Protein.** The crystal structure reveals that the carboxylate of the antibiotic sticks out of the well-defined cleft, and might therefore be amenable to chemical modification with an FKBP-binding group.

Towards this goal, we have initiated several lines of inquiry into the chemical modification of these antibiotics such that they acquire an affinity for FKBP. For example, we recently synthesized bifunctional, FKBP-binding variants of both the beta-lactam Ampicillin and the fluoroquinolone Ciprofloxacin. These hybrid compounds were designed using information gleaned from the co-crystal structures of the antibiotics in complex with their protein targets. For instance, the crystal structure of Ampicillin reveals that its carboxyl group points out of the well-defined cleft when bound to a Penicillin Binding Protein (Figure 5-1). Moreover, as this carboxylate is not implicated in Ampicillin's mechanism of action at the bacterial cell wall, this site may tolerate conjugation to other molecules. As such, we installed a flexible, 4-carbon diamine at this site to serve

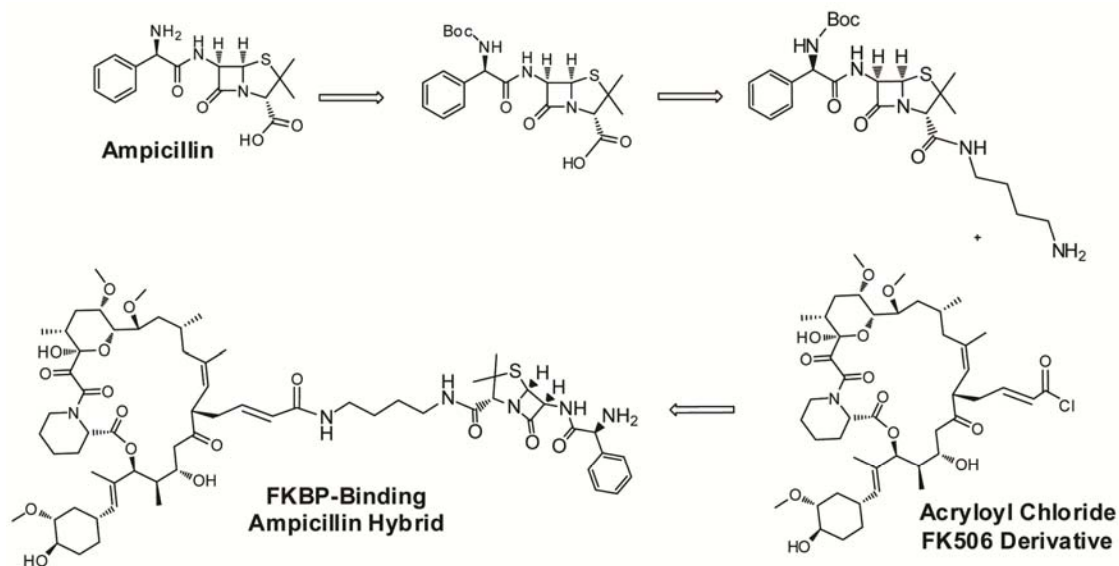
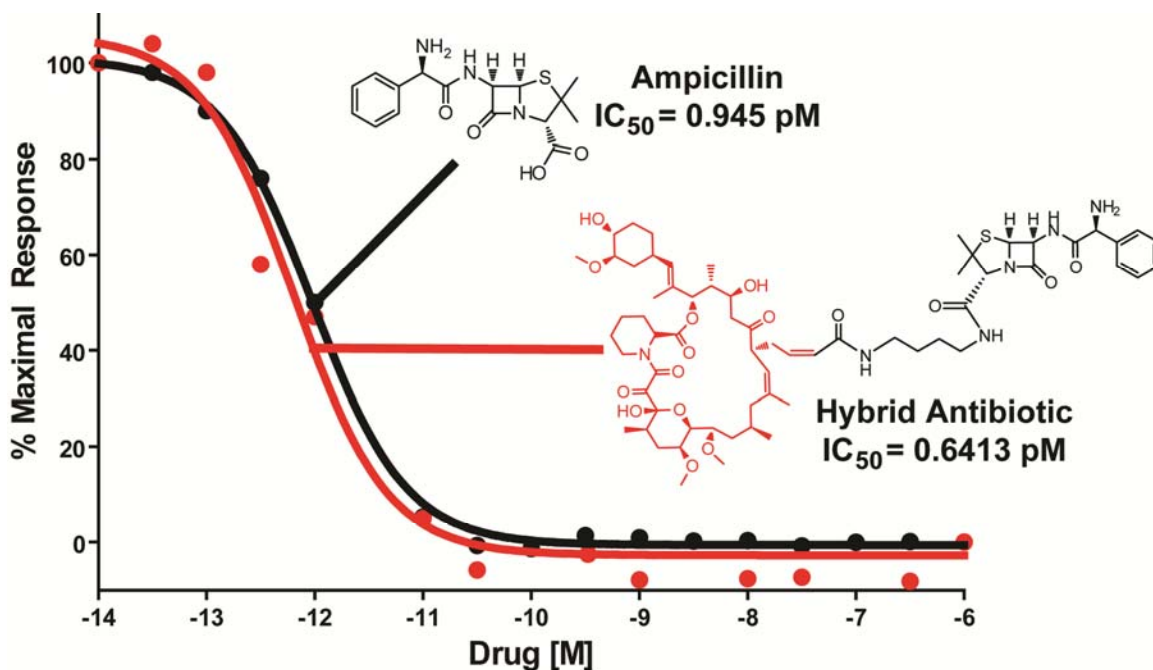


Figure 5-2. The Synthesis of a Bifunctional Antibiotic

as a molecular linker (Figure 5-2). Employing the rapid microwave-assisted platform discussed in Chapter 4, we were then able to use the acryloyl chloride derivative of FK506 to synthesize an FKBP-binding surrogate of Ampicillin quickly and in high-yield (>95%).

A critical test of this method's therapeutic potential and choice in modification site is the ability of the bifunctional antibiotic to maintain bactericidal activity in proliferation assays. As illustrated in Figure 5-3, the FKBP-binding Ampicillin hybrid exhibits sub-picomolar potency against laboratory strains of *Staphylococcus aureus*, similar to that of the parent compound. Thus, it is reasonable to conclude that modifying Ampicillin at this distal carboxylate does not affect its ability to bind the Penicillin Binding Protein, and furthermore, has no deleterious effects on its antimicrobial efficacy.



**Figure 5-3. An FKBP-Binding Beta Lactam Retains Picomolar Activity Against *S. Aureus*.**

In collaboration with the Nunez Laboratory in the Department of Pathology, we will soon begin a more comprehensive evaluation of the antimicrobial potential of such bifunctional antibiotics against a panel of bacterial strains including *Listeria monocytogenes*, *Legionella pneumophila*, and *Salmonella*. Initial experiments will be performed in the context of cell-based infectivity assays, where macrophages extracted from the bone marrows of mice will be plated and exposed to the bacteria for 30 minutes. This will be followed by the addition of gentamicin to kill any remaining extracellular pathogens, a washout, and treatment with the bifunctional antibiotic of interest. Since FKBP expression is abundant in macrophages, we expect the bifunctional antibiotics to readily partition into these cellular compartments while exhibiting high levels of bactericidal activity. With these compelling results in hand, it will be an exciting

prospect to begin exploring the new pharmacokinetic profiles of these hybrid antibiotics *in vivo* with LD<sub>50</sub> experiments in mice.

### 5.2.2 Diversifying the Chemistry of the Synthetic Linker

The linker that bridges the two chemical domains is thought to be one of the most important features in bifunctional molecules.<sup>1, 2, 3</sup> In one key example, Briesewitz *et al.* found that very short linkers give rise to compounds that no longer bind both targets simultaneously, likely due to steric clashes between the protein surfaces.<sup>4</sup> In our work, we discovered that linkers exploiting favorable, secondary contacts on the protein surface can improve potency by ~100-fold.<sup>5, 1</sup> Moreover, the Wandless group recently found that the linker can control cellular partitioning in the context of ternary complexes.<sup>6</sup> Guided by these efforts, it would be interesting to explore the critical design criteria for FKBP-binding Amprenavir derivatives. In the general synthetic route, an amide is formed between the linker and the Amprenavir core, followed by deprotection and installation of the SLF- or FK506-moiety (Figure 5-4A).<sup>7</sup> Using this established approach, a series of SLF- (**1a-g**) or FK506-bearing compounds (**2a-g**) could readily be generated. By using the linkers in compounds **1a-b** and **2a-b**, we could specifically test whether replacing the tetrahydrofuran ring of Amprenavir, which is removed during the creation of SLFavir and Tacrolimavir, restores the lost affinity for HIV protease, as might be suggested by the published SAR studies.<sup>8</sup> Other linkers (*e.g.* compounds **1c-e**) can specifically explore strategic placement of hydrophobic and polar groups, based on the presence of



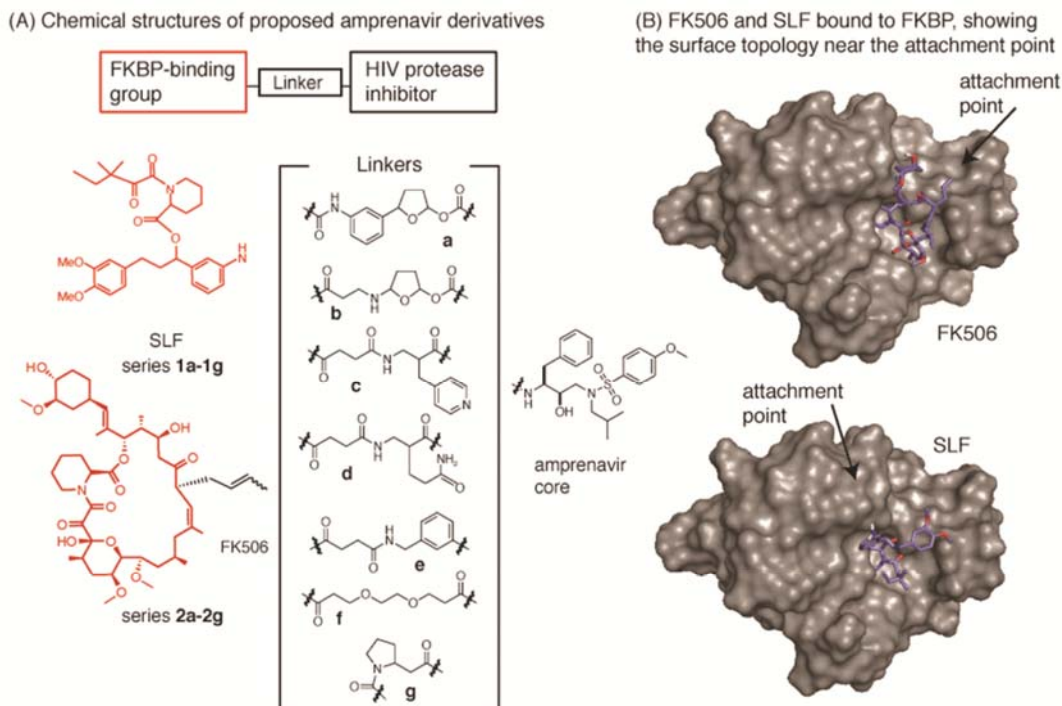


**Figure 5-4. Designing a Library of Amprenavir Conjugates.** (A) Installing a series of linkers will produce a variety of derivatives, using either FK506 or SLF as the FKBP-binding group. (B) Models of FK506 and SLF bound to FKBP. These models were generated in PyMol, using the available crystal structures to display initial configurations and DOCK to refine the pose. Based on these models, a relatively short linker (~10 to 15 Å) would be sufficient to link FKBP to HIV protease.

complementary regions on the surface of FKBP that are predicted by co-crystal structures and DOCK-based simulations.<sup>5,6</sup> Interestingly, SLF and FKBP appear to project from different sites on the FKBP surface, thus their optimal linkers might be different (Figure 5-4B). Finally, the roles of flexibility and orientation, which can control the likelihood of forming the ternary complex by dictating how the two proteins come together, might be explored using compounds such as **1f-g**. Consistent with this idea, adding purified FKBP12 did not inhibit the activity of SLFavir in my HIV protease assays.<sup>9</sup> Together, this library of bifunctional molecules is expected to contain compounds that vary in their affinities and their

ability to form a ternary complex. Based on our modeling results, we predict that bifunctional molecules might simultaneously bind to both FKBP and HIV protease. It is therefore critical to understand these interactions as the formation of the ternary complex should significantly enhance the apparent avidity and decrease the apparent off-rate of the hybrid antivirals. Future work in the Gestwicki lab will address these questions.

### **5.2.3 Dual-Targeting of HIV-1 Infected Lymphocytes**

A central aspect of our model is that bifunctional compounds might be selectively targeted to FKBP-expressing, HIV-infected cells by the slow off-rates expected from the ternary complex between HIV protease, the drug, and FKBP.<sup>10</sup> A primary goal, then, would be to understand how physical interactions between a bifunctional protease inhibitor and its two protein targets give rise to cellular partitioning decisions.

To directly test this idea, we could express HIV protease in FKBP-rich, Jurkat cells. The partitioning of compounds into these “dual expressor” cells will then be compared to control cells expressing only FKBP or HIV protease. In a second set of experiments, we could label the “dual expressor” cells with DAPI, mix them into whole blood and study how they compete for bifunctional compounds. Finally, we could determine the functional consequences of these partitioning behaviors by measuring the compound’s antiviral activity against live HIV-1 virus, in collaboration with Dr. Steve King and Prof. David Markovitz (UM

Internal Medicine).<sup>11</sup> In these infectivity experiments, we could test relative potency in two scenarios: (i) in the presence of free, unconjugated SLF to compete for FKBP-binding sites and (ii) in the presence of the “dual-expressor” Jurkat cells. These studies will reveal how the relative availability of FKBP and HIV protease control partitioning and compound potency. We expect that, if the expression levels are known and the affinities can be tuned, then we might be able to uncover design criteria and find compounds that target HIV-infected blood cells.

In an analogous fashion, it may be possible to exploit such targeting strategies with bifunctional antibiotics as well. Intracellular pathogens are notoriously difficult to treat, owing to the poor penetration of many antimicrobials into the infected cells. For example, staphylococci inside of neutrophils can survive incubation even with extremely high concentrations of  $\beta$ -lactam antibiotics, as these agents cannot enter the neutrophils due to polar nature of their functional groups. This is true for macrophage infection with listeria as well. While the mechanisms of their entry and pathogenesis certainly differ, these seemingly disparate conditions do share a single commonality: their host cells are replete with FKBP. This makes the prospect of bifunctional  $\beta$ -lactams even more enticing, as the pharmacokinetic enhancements seen with the addition of FKBP-binding groups would undoubtedly be synergistic to the targeting aspects of this strategy. It is exciting to consider what other targets might be amenable to this “nature-inspired” strategy and all the endless bifunctional possibilities.

### 5.3 References

1. Gestwicki, J. E.; Crabtree, G. R.; Graef, I. A., Harnessing chaperones to generate small-molecule inhibitors of amyloid beta aggregation. *Science* **2004**, *306* (5697), 865-9.
2. Amara, J. F.; Clackson, T.; Rivera, V. M.; Guo, T.; Keenan, T.; Natesan, S.; Pollock, R.; Yang, W.; Courage, N. L.; Holt, D. A.; Gilman, M., A versatile synthetic dimerizer for the regulation of protein-protein interactions. *Proc Natl Acad Sci U S A* **1997**, *94* (20), 10618-23.
3. Abida, W. M.; Carter, B. T.; Althoff, E. A.; Lin, H.; Cornish, V. W., Receptor-dependence of the transcription read-out in a small-molecule three-hybrid system. *ChemBiochem* **2002**, *3* (9), 887-95.
4. Briesewitz, R.; Ray, G. T.; Wandless, T. J.; Crabtree, G. R., Affinity modulation of small-molecule ligands by borrowing endogenous protein surfaces. *Proc Natl Acad Sci U S A* **1999**, *96* (5), 1953-8.
5. Marinec, P. S.; Lancia, J. K.; Gestwicki, J. E., Bifunctional molecules evade cytochrome P450 metabolism by forming protective complexes with FK506-binding protein. *Mol. Biosystems* **2008**, *4*, 571-578.
6. Braun, P. D.; Barglow, K. T.; Lin, Y. M.; Akompong, T.; Briesewitz, R.; Ray, G. T.; Haldar, K.; Wandless, T. J., A bifunctional molecule that displays context-dependent cellular activity. *J Am Chem Soc* **2003**, *125* (25), 7575-80.
7. Marinec, P. S.; Evans, C. G.; Gibbons, G. S.; Tarnowski, M. A.; Overbeek, D. L.; Gestwicki, J. E., Synthesis of orthogonally reactive FK506 derivatives via olefin cross metathesis. *Bioorg Med Chem* **2009**, *17* (16), 5763-8.
8. Rocheblave, L.; Bihel, F.; De Michelis, C.; Priem, G.; Courcambeck, J.; Bonnet, B.; Chermann, J. C.; Kraus, J. L., Synthesis and antiviral activity of new anti-HIV amprenavir bioisosteres. *J Med Chem* **2002**, *45* (15), 3321-4.
9. Marinec, P. S.; Chen, L.; Barr, K. J.; Mutz, M. W.; Crabtree, G. R.; Gestwicki, J. E., FK506-binding protein (FKBP) partitions a modified HIV protease inhibitor into blood cells and prolongs its lifetime in vivo. *Proc Natl Acad Sci U S A* **2009**, *106* (5), 1336-41.
10. Kiessling, L. L.; Gestwicki, J. E.; Strong, L. E., Synthetic multivalent ligands as probes of signal transduction. *Angew Chem Int Ed Engl* **2006**, *45* (15), 2348-68.
11. Swanson, M. D.; Winter, H. C.; Goldstein, I. J.; Markovitz, D. M., A lectin isolated from bananas is a potent inhibitor of HIV replication. *J Biol Chem* **285** (12), 8646-55.